Elsevier Editorial System(tm) for Geomorphology

Manuscript Draft

Manuscript Number: GEOMOR-9246R1

Title: Controls on jökulhlaup-transported buried ice melt-out at Skeiðarársandur, Iceland: implications for the evolution of ice-marginal environments

Article Type: Research Paper

Keywords: Jökulhlaup; buried ice melt-out; Skeiðarársandur Iceland; ice-marginal environments

Corresponding Author: Professor Andy Russell,

Corresponding Author's Institution:

First Author: David J Blauvelt, PhD

Order of Authors: David J Blauvelt, PhD; Andy Russell; Andrew R Large, PhD; Fiona S Tweed, PhD; John F Hiemstra, PhD; Bernd Kulessa, PhD; David J Evans, PhD; Richard I Waller, PhD

Abstract: High-magnitude jökulhlaups, glacier margin position and ice-thickness have been identified as key controls on sandur evolution. Existing models however have focused primarily on observations made during short windows of time and often do not account for the subsequent modification of proglacial landsystems by repeated jökulhlaups or post-depositional modification due to melt out over decadal time-scales. Digital Elevation Models (DEMs) were used to reconstruct the development of large depressions on Skeiðarársandur, an outwash plain in southeast Iceland. These depressions measure up to 1 km in width and up to 13 m in depth and are associated with ice bodies up to 1 km in length and up to 150 m in height emplaced during a high-magnitude jökulhlaup in 1903 and subsequently buried by jökulhlaups in 1913 and 1922. The continued melting of the Harðaskriða ice bodies over a century following their emplacement, together with subsequent repeated burial, by high-magnitude jökulhlaups demonstrates that jökulhlaups may continue to serve as important controls on sandur evolution on a decadal to centennial timescale (101 - 102 years). The Harðaskriða depressions developed only following the retreat of the glacier margin after 1945, which highlights the controls of margin position on the evolution of the sandur. Margin position and thickness of the glacier profile was seen to affect not only the distribution and thickness of sediment emplaced during jökulhaups but also the rate and pattern of melt in the decades following the decoupling of the margin from the sandur. The jökulhlaup landsystem model signatures identified at this site may provide a useful analogue for interpreting landforms and strata emplaced by glacier margin fluctuations, jökulhlaups and melt out generated by retreating continental Pleistocene ice sheets.

Research Data Related to this Submission

There are no linked research data sets for this submission. The following reason is given:
Data will be made available on request

9th March 2020

Dear Achim,

Thanks you for editing our paper and for expediting two very swift reviews. I have listed our response (highlighted in yellow) to each of the reviewers comments below. I have also provided an annotated copy of the revised manuscript highlighting the changes we've made and a 'clean' copy of the revised manuscript.

Best regards,

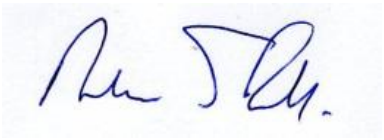

Andy Russell

Response to Reviewer #1 General comments:

'The manuscript looks like it has been "in the pipeline" for many years.'

'The elevation data stop in 2007 but could easily have been updated to the present, using ArcticDEM. I recommend that this is done.'

We have addressed this comment – see below

'Furthermore, the methods used for DEM production are not well-described (see comments in text). Again, this might have to do with the time that has elapsed since the work was done and submission.'

We have added further explanation of the DEM production methods (see below).

'Almost all the figures need to be finalized before potential publication - see specific comments in the pdf.'

All of the figures have been revised according to the reviewers comments (see below).

'The depositional model gives a good overview of processes, sediments and landforms. However, it could be significantly improved in terms of graphic quality.'

I don't really understand the comments on the manuscript regarding 'white spacing' but we have tidied-up the diagram.

Response to Reviewer #1 Comments on manuscript:

P1 Abstract *'Wrong letter, use ð.'*
Amended

P2 1. Introduction and aims *'I prefer just "Introduction" as headline. The introduction commonly end with the aims of the paper'*

Amended

P2 Evans and Twig, 2002 *'The model in Evans & Twigg (2002; Fig. 18) is essentially copied from Krüger (1994; Fig. 92, p. 109) even though they don't cite his work as source for the figure. Please cite the original work in addition or only. Contact me if you need a pdf of Krüger (1994).'*

We have added the citation to Krüger (1994). David Evans acknowledges the oversight on the original Evans and Twigg paper but has since rectified this in the Evans (2003) Landsystems book. As this is not the first time that Anders Schomaker has raised this issue it should be noted that one should only have to make an apology for an oversight once!

P2 *'by definition, many studies of contemporary...'* Not all though. See e.g. Korsgaard et al. (2015): https://doi.org/10.1016/j.geomorph.2015.09.010 + many other papers from Brúarjökull, Iceland.

There is no disagreement here. We state 'many' (not all) studies of contemporary ice-marginal processes provide only a snapshot of geomorphological and sedimentological evolution of an ice-marginal zone. Later (line 55), we acknowledge a range of literature regarding palimpsest landscapes and have added reference to Schomacker and Kjær (2007) and Korsgaard et al. (2015).

P5 '*It's not really clear to me how the DEMS were produced. Stereophotogrammetry on digital aerial imagery? The methods section needs to be more accurate on how this was done. See for example Korsgaard et al. 2015 in Geomorphology (they also used SocetSet).'*

We have added the following additional text to provide more detail of the methodology used.

'DEM's were produced using stereophotogrammetry on digital aerial imagery. Vertical aerial photographs collected for DEM creation were obtained from the National Land Survey of Iceland, Landmælingar Íslands. Images were scanned by Landmælingar Íslands with an Eversmart Jazz+ Scitex scanner, at a resolution of 2000 dpi and delivered as tagged image format (tif) files. Camera calibration documentation and flight lines drawn on 1:100,000 topographic maps were provided for all photographs taken after 1954. Photographs from 1945, taken by the U.S. Air Force, were purchased from Landmælingar Íslands, who provided known flight elevations and camera focal lengths. Colour digital images acquired in 2007 by NERC ARSF (IPY07/13) were also used in this study.'

and

'BAE's SocetSet 5.5 (Ngate) software was used to generate the DEMs. Triangulation (interior and exterior orientation) was accomplished for all photosets. Once an internal coordinate system was established within the photographs, the control points measured in the field could be used to relate the image to the ground (absolute orientation). The ISN93 coordinates of the GCPs were used to identify points on the images. Once the x, y and z values of GCPs were identified on both (or more) images, SocetSet then performed point measurement automatically, using digital image matching (Baily et al., 2003).'

P5 2007 *'This is 12 years ago and a lot could potentially have happened since then. It would be relatively easy to use ArcticDEM and update the study to the present instead of ending it in 2007. I recommend that the authors do so.'*

The first image below compares the 03 and 97 DEMs to the 2018 ArcticDEM. While the stagnation feature is large, relatively, in horizontal extent (2 km), in vertical extend they're relatively small features, often under 10 m, depending on post spacing (20 m vs 10 m) and scale of the being used.

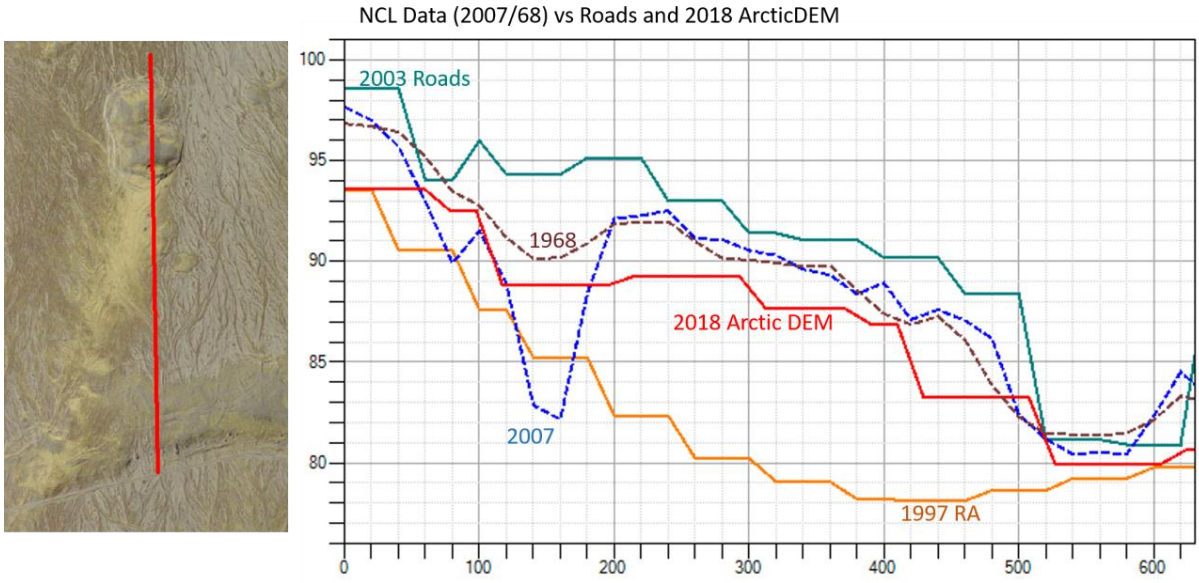

The second comparison shows the same three profiles (1997, 2003 and 2018 ArcticDEM) as in the above figure compared with our 1968 and 2007 DEMs. Based on this visual comparison, we have not included the 2018 ArcticDEM in any of the stagnation figures in this paper. However we have added it to figure 3 (glacier margin recession/lowering) with a disclaimer.

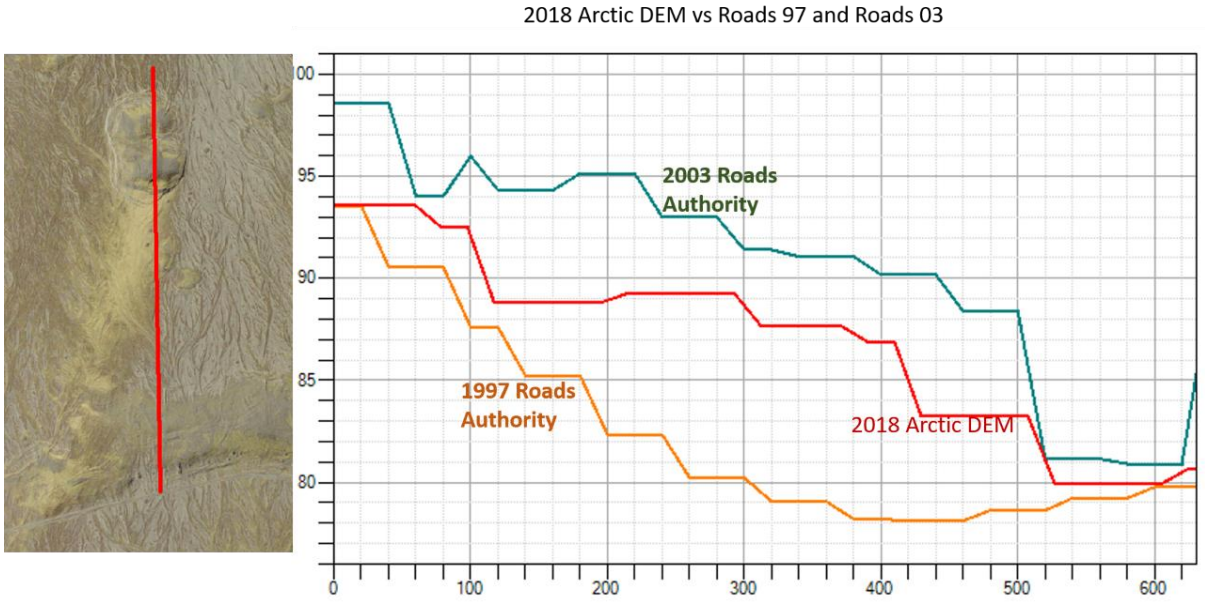

We have therefore added the following two sentences to the methods to articulate our limited use of ArcticDEM.

'Although the 2018 ArcticDEM was used to provide a general comparison of glacier recession and proglacial fluvial system incision (Porter et al., 2018) (Fig. 3). Offsets between the 2018 ArcticDEM and photogrammetrically-derived DEMs precluded it's use for quantification of rates of lowering of the Harðaskriða depressions.'

P5 ring road. *'(Fig. 1)'*

Added: '(Fig. 1)'

P6 historical images *'Do you mean aerial photographs or oblique ground photographs? Please clarify.'*

Changed to: 'historical aerial photographs'

Line 156 – aerial photographs (not sure of the dtes off the top of my head?)

"historical images" has been changed to "historical aerial photographs"

P6 Leica's *'Check methods. SocetSet is produced by BAE Systems, not Leica.'*

"Leica" has been changed to "BAE"

P6 *(Figs 5 & 6)*

Changed to 'Figs. 5 and 6'

P7 Most recent satellite imagery. *'Please specify what imagery and from what date.'* add imagery source/date

We have added '(DigitalGlobe, 2016)' to the manuscript.

P11 *'See also Krüger and Kjær papers from Kötlujökull, Iceland on this topic.'*

We have added references to Krüger and Kjær, 2000; Kjær and Krüger, 2001;

P13 *'dug down in deep sand channel…bank that…were…many human stories" (Thórarinsson, 1974).' 'Doesn't really make sense to me. Please check the Icelandic translation once more, it does not look right.'*

We revisited the original source and re-translated this as: "dug into the sand a deep, 'many persons high', steep-sided channel"

Table 1 Caption. *'Starts AD 1598. Not sure what 1929 refers to.'*

Caption text changed to: 'Chronology of glacier margin fluctuations and jökulhlaups (1598-1954)….'

Figure 1 *'The text in the lower right side of the image is impossible to read.'*

Figure revised to Remove "showing the three major lobes" and add "Imagery: ESRI and Digital Globe, 2016."

Figure 2 *'Move the scale bar to the lower left corner and make it less apparent. It takes too much attention now.'*

Figure revised to Remove "on top of 2003 photomosaic (1997 photomosaic underlain to fill gaps)" add "Imagery: ESRI and Digital Globe, 2016."

Figure 3 *'The coordinate labels at the lower and right side of the aerial photograph are too small to read.' 'Delete purple and blue lines on top of the x-axis.' 'At the y-axis label: m a.s.l. (and not m asl).'*

Figure revised to Remove "Vertical lines indicate limit of DEMs" add "Imagery: ESRI and Digital Globe, 2016."

Figure 4 *'The coordinate labels are too small to read.'*

Figure revised

Figure 5 *'I'm not convinced. (a) is missing something for scale, and I simply don't see any indications of normal faulted blocks. Please point them out using arrows on the photograph.*
(b) Same here, I don't see any evidence of normal faulting. The "rings" appear to be caused by the patchy moss cover. Please point out using arrows on the photograph.'

Both photos have been cropped to show the features more clearly. The old gravel road which shows subsidence and ground deformation has been marked on. We have also indicated the tops of the normally faulted blocks.

Figure 6 *'Appears to have the potential to be a nice figure. But I can't read it on the background of the olive-colored aerial photograph. Please modyfy so the map symbols can be read. It might help to use a B/W photograph with 50% transparency as background.'*

Figure revised. Note, per reviewer's request, we used a grey background with 50% transparency.

Figure 7 *'Smoothen the elevation contour lines! Make box with scale bar less apparent.' 'm a.s.l. in axis legends.'*

Figure revised to smooth contours and add 'm a.s.l.'

Figure 8 *'Smoothen elevation contours.'*

Figure revised to smooth contours and add 'm a.s.l.'

Figure 9 *'Sorry but I don't see any drumlin shaped or drumlinised landforms on A. Please provide better data. The landforms also don't appear to be located in a subglacial landscape.'*

Figure revised We added contour lines to hopefully show the drumlin shapes better.

Figure 11 *'Please provide raw radargrams above each annotated radargram. It will double the amount of radargrams but as of now, it's not possible too see the raw data. The reader can't evaluate the data and the interpretation as they are presented here. However the data appear good, so the deserve a better presentation.'*

Figure revised to include raw radargrams alongside annotated ones.

Figure 12 *'Is there some way this figure can be redrawn and made tidier? It looks like a sketch. Also the white spacing (bot horisontal and vertical) should be of the same size and justified.*
That said, I think the scientific content is OK and justified.'

We've evened-up the spacing between each of the panels and have tidied-up the diagram.

Response to Reviewer #2' Comments:

'...a merger between the two first chapters that would it make easier for readers unfamiliar with Iceland to understand the aims of the manuscript'

We have merged these two sections

'Abstract: Line 16 ff.: The first sentence is a bit long and complicated. I suggest cutting it

in 2 sentences and re-writing it. Otherwise, the abstract is well written and informative.'

We have split this sentence in two.

'1. Introduction: I recommend that the two chapters are merged and the contents of chapter 2 are placed at the end of the current introduction and followed by the section on their research aims (line 75 ff.)'

This has been done.

'Line 67 ff.: The authors may additionally want to point out that buried ice in proglacial settings (i.e. distal to the ice margin), for example in sandurs/outwash plains, is hardly discussed in most related studies as they often focus on the narrower marginal zones.'

We have added the following sentence: 'Studies of buried ice melt out also tend to have focussed on the immediate ice proximal areas of proglacial outwash plains.'

'Line 84: Add space following ";" or alternatively split sentence in two.'

Sentence has been split.

3. Field area

'General comment: In their introduction, the authors correctly point out a climatic impact on the timing/pattern of burial ice melting. They also highlight the potential palaeoclimatic importance of their studied features. It would, therefore, be helpful if any information about the current climate (regional meteorological data) would be provided. I assume that for the detailed site no information may be available, but giving an estimate would be helpful (also to be able to judge if any permafrost is involved - what supposedly is not the case). This and some information about the altitude would help the reader unfamiliar with the site.'

We have added the following sentence and references to the Study area section: 'Skeiðarársandur has a strong maritime climate, where the maximum depth of winter freezing is only of the order of centimetres (Douglas and Harrison, 1996; Thórhallsdóttir, 1996) making the presence of permafrost impossible.'

'Line 116: Why not "study area"?'

We have changed this heading to 'Study area'

'5. Results section 5.2 is a bit lengthy and it should be assessed whether some shortening can be applied.'

We feel we cannot shorten this section without detriment to the manuscript.

'6. Discussion I am not sure whether a shortening would be possible without losing viable information, but if possible, the authors may decide in favour of it.'

We have tried to make discussion as concise as possible but feel that it is a reasonable length considering the structure and content of the paper.

'Line 417 ff.: Is it possible that acceleration of the buried ice has not just been influenced by retreat of the glacier margin and the rise in ambient temperature but also by regional air temperature rise in the late mid-20th century? May an unknown threshold exist that, once passed, may lead to faster melt of the buried ice? Would be something that possibly could be explored further.'

We acknowledge the role of increased ambient temperatures and agree with the reviewer that this is a topic which requires further exploration. We feel that the investigation of potential thresholds for buried glacier ice melt is a topic for a future project.

'I wonder whether "wider implications" is necessary in the chapter heading.'

We have removed 'wider implications from the section heading.

'Table 2: I would prefer giving the unit also in the table (head line) rather than only in the caption.'

We have added units to each of the column headers of this table.

Highlights

- New model for the origin of large (<1 km wide, <13 m deep) depressions on Skeiðarársandur, southeast Iceland.
- 1 km long, 150 m high piece of glacier margin detached and transported during the 1903 high-magnitude jökulhlaup.
- Large jökulhlaup-transported ice blocks subsequently buried by jökulhlaups in 1913 and 1922.
- Digital Elevation Models (DEMs) and Ground Penetrating Radar (GPR) used to reconstruct the development of depressions.
- Jökulhlaup-transported ice bodies continue to melt over a century following their emplacement at an average rate of 19.4 ± 2.6 cm per year.

Graphical Abstract

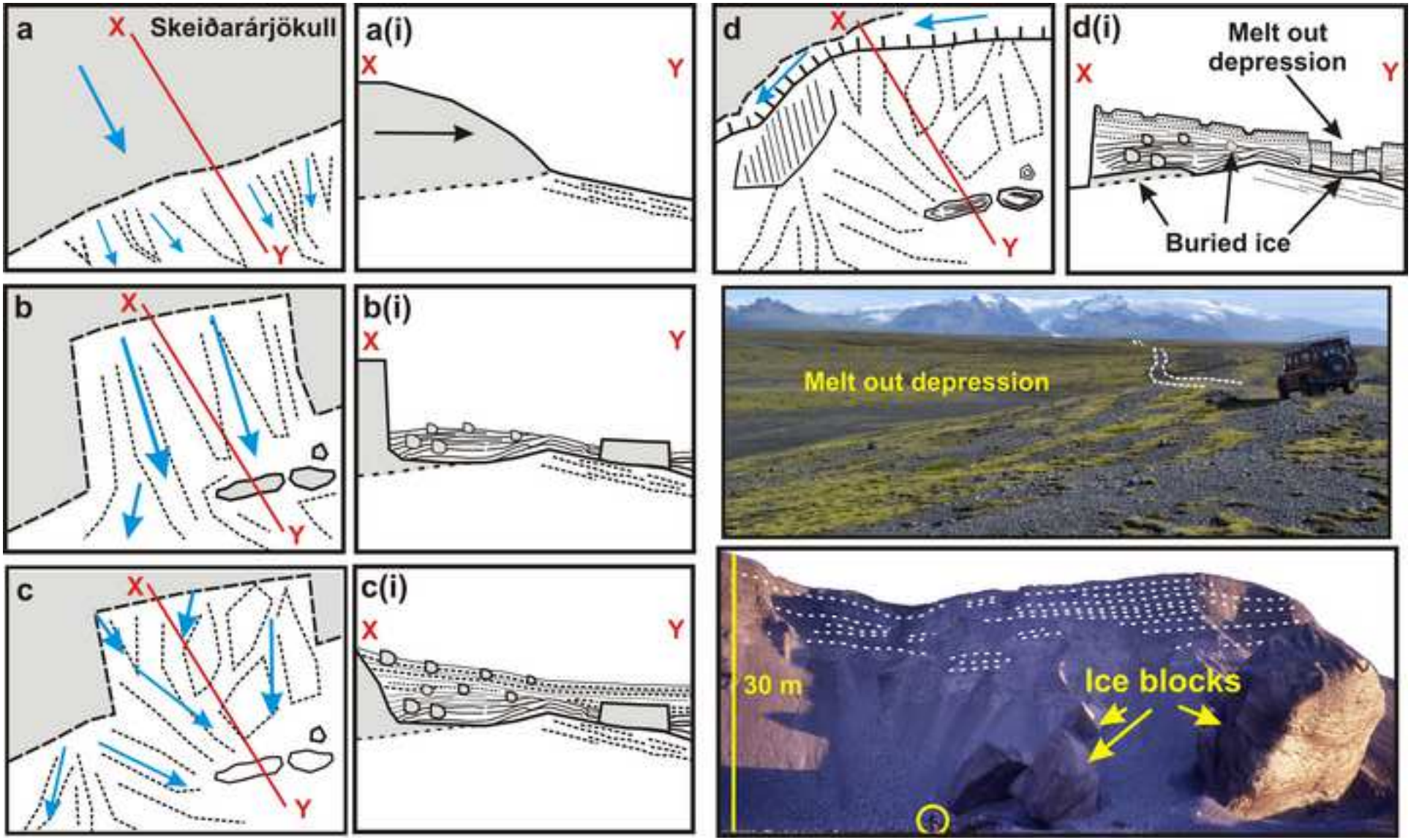

Controls on jökulhlaup-transported buried ice melt-out at Skeiðarársandur, Iceland: implications for the evolution of ice-marginal environments

David J. Blauvelt[1], Andrew J. Russell[1*], Andrew R.G. Large[2], Fiona S. Tweed[3], John F. Hiemstra[4], Bernd Kulessa[4,5], David J.A. Evans[6] and Richard I. Waller[7]

[1] 116 East Glebe Rd, Alexandria VA, 22305, USA
[2] Newcastle University, School of Geography Politics and Sociology, NE1 7RU, UK
[3]Geography, Staffordshire University, College Road, Stoke-on-Trent, ST4 2DE, UK
[4]College of Science, Swansea University, Singleton Park, SA2 8PP, Wales, UK
[5]School of Technology, Environments and Design, University of Tasmania, Hobart, Tasmania 7001, Australia
[6]Department of Geography, Durham University, Lower Mountjoy, South Road, Durham, DH1 3LE, UK
[7]School of Geography, Geology and the Environment, Keele University, Staffordshire, ST5 5BG, UK

[*]*Corresponding Author*: andy.russell@ncl.ac.uk

Abstract

High-magnitude jökulhlaups, glacier margin position and ice-thickness have been identified as key controls on sandur evolution. Existing models however have focused primarily on observations made during short windows of time and often do not account for the subsequent modification of proglacial landsystems by repeated jökulhlaups or post-depositional modification due to melt out over decadal time-scales. Digital Elevation Models (DEMs) were used to reconstruct the development of large depressions on Skeiðarársandur, an outwash plain in southeast Iceland. These depressions measure up to 1 km in width and up to 13 m in depth and are associated with ice bodies up to 1 km in length and up to 150 m in height emplaced during a high-magnitude jökulhlaup in 1903 and subsequently buried by jökulhlaups in 1913 and 1922. The continued melting of the Harðaskriða ice bodies over a century following their emplacement, together with subsequent repeated burial, by high-magnitude jökulhlaups demonstrates that jökulhlaups may continue to serve as important controls on sandur evolution on a decadal to centennial timescale (10^1 – 10^2 years). The Harðaskriða depressions developed only following the retreat of the glacier margin after 1945, which highlights the controls of margin position on the evolution of the sandur. Margin position and thickness of the glacier profile was seen to affect not only the distribution and thickness of sediment emplaced during jökulhaups but also the rate and pattern of melt in the decades following the decoupling of the margin from the sandur. The jökulhlaup landsystem model signatures identified at this site may provide a useful analogue for interpreting landforms and strata emplaced by glacier margin fluctuations, jökulhlaups and melt out generated by retreating continental Pleistocene ice sheets.

Controls on jökulhlaup-transported buried ice melt-out at Skeiðarársandur, Iceland: implications for the evolution of ice-marginal environments

David J. Blauvelt[1], Andrew J. Russell[1*], Andrew R.G. Large[2], Fiona S. Tweed[3], John F. Hiemstra[4], Bernd Kulessa[4,5], David J.A. Evans[6] and Richard I. Waller[7]

[1] 116 East Glebe Rd, Alexandria VA, 22305, USA
[2] Newcastle University, School of Geography Politics and Sociology, NE1 7RU, UK
[3]Geography, Staffordshire University, College Road, Stoke-on-Trent, ST4 2DE, UK
[4]College of Science, Swansea University, Singleton Park, SA2 8PP, Wales, UK
[5]School of Technology, Environments and Design, University of Tasmania, Hobart, Tasmania 7001, Australia
[6]Department of Geography, Durham University, Lower Mountjoy, South Road, Durham, DH1 3LE, UK
[7]School of Geography, Geology and the Environment, Keele University, Staffordshire, ST5 5BG, UK

[*]*Corresponding Author*: andy.russell@ncl.ac.uk

Abstract

High-magnitude jökulhlaups, glacier margin position and ice-thickness have been identified as key controls on sandur evolution. Existing models however have focused primarily on observations made during short windows of time and often do not account for the subsequent modification of proglacial landsystems by repeated jökulhlaups or post-depositional modification due to melt out over decadal time-scales. Digital Elevation Models (DEMs) were used to reconstruct the development of large depressions on Skeiðarársandur, an outwash plain in southeast Iceland. These depressions measure up to 1 km in width and up to 13 m in depth and are associated with ice bodies up to 1 km in length and up to 150 m in height emplaced during a high-magnitude jökulhlaup in 1903 and subsequently buried by jökulhlaups in 1913 and 1922. The continued melting of the Harðaskriða ice bodies over a century following their emplacement, together with subsequent repeated burial, by high-magnitude jökulhlaups demonstrates that jökulhlaups may continue to serve as important controls on sandur evolution on a decadal to centennial timescale (10^1 – 10^2 years). The Harðaskriða depressions developed only following the retreat of the glacier margin after 1945, which highlights the controls of margin position on the evolution of the sandur. Margin position and thickness of the glacier profile was seen to affect not only the distribution and thickness of sediment emplaced during jökulhaups but also the rate and pattern of melt in the decades following the decoupling of the margin from the sandur. The jökulhlaup landsystem model signatures identified at this site may provide a useful analogue for interpreting landforms and strata emplaced by glacier margin fluctuations, jökulhlaups and melt out generated by retreating continental Pleistocene ice sheets.

1. Introduction ~~and aims~~

Glaciers are frequently used as indicators of climate change as they respond dynamically to changes in the climate driven components of their mass balance. Knowledge of the former extent of glaciers can be used to reconstruct palaeo-climate and to define the former position of contemporary glaciers. Distinctive assemblages of landforms and deposits at modern glacier-margins have stimulated the development of models which can be used to reconstruct ice-marginal processes. Models such as the ice-marginal landsystem (e.g. Krüger, 1994; Evans and Twigg, 2002; Evans et al., 2019) were developed from the detailed investigation of contemporary glacier margins and have been used to reconstruct palaeo-glacier margins in the Quaternary record (e.g. Evans et al., 1999). By definition, many studies of contemporary ice-marginal processes provide only a snapshot of the geomorphological and sedimentological evolution of an ice-marginal zone, as they do not take account of post-depositional landscape modification processes and are not always able to constrain the influences of previous landsystems on landscape evolution. Palimpsest landscapes comprising a number of superimposed landsystems allow landform overprinting and the potential for landsystem legacy to persist for periods of 10^1-10^2 yr^{-1} modifying subsequent landsystems (Kleman, 1992; Kleman and Stroeven, 1997; Schomacker and Kjær, 2007; Korsgaard et al., 2015).

Ice-marginal and proglacial geomorphology can be modified by a number of post-depositional processes such as aeolian deflation and deposition, fluvial erosion and deposition, periglacial and paraglacial slope processes (e.g. Ballantyne, 2002; Mountney and Russell, 2006, 2009). Melt-out of buried glacier ice has been well-documented from modern ice-margins (Price, 1969; Schomacker and Kjær, 2007; Tonkin et al., 2016) as well as being interpreted from the Quaternary record (Eyles et al., 1999; Fard, 2003). Buried ice melt-out has been invoked to account for a number of distinctive landforms such as ‘kame and kettle’ topography and ‘hummocky moraine’, both of which result from topographic inversion as buried ice melts, causing slow collapse of overlying sediment (e.g. Everest and Bradwell, 2003; Lukas et al. 2005; Bennett and Glasser, 2009).

Despite widespread acknowledgement of the importance of buried ice within former glacier margins, relatively little attention has been paid to the process of ice emplacement and how this may determine buried ice distribution and melt-out styles. Studies of buried ice melt out also tend to have focussed on the immediate ice proximal areas of proglacial outwash plains. Similarly, there are scant data on the rates of ice melting beneath thick debris mantles; exceptions include McKenzie (1969) and Schomacker (2008). Buried ice is known to have survived for decades to centuries (e.g. French and Harry, 1990; Evans and England, 1992; Everest and Bradwell, 2003; Schomacker, 2008) however there have been few detailed studies of melt-out rates over these timescales.

Processes occurring in the ice-marginal zones of glaciers and ice sheets are complex. Subaerial processes re-work glacially-deposited debris and the melt-out of buried ice leads to collapse structures and topographic inversion (Price, 1969; Bennett and Glasser, 2009). Even a thin (> 0.01 m) layer of debris covering glacier ice can provide sufficient insulation to retard ablation (e.g. Lister, 1953; Østrem, 1959; Nakawo and Young, 1981, 1982; Nicholson and Benn, 2006) and ablation can be very slow under thick debris mantles. Very slow melt rates can therefore permit the survival of buried glacier ice for long periods of time. The sustained collapse of overlying sediment due to buried ice melt-out is a significant post-depositional modification process in deglaciated landscapes with ice-cored topography (Ballantyne, 2002). The correlation between climatic parameters and melt rates of buried ice bodies is weak however, suggesting that both burial processes and topography play a key role in the rates of ice melting (Nicholson and Benn, 2006; Schomacker, 2008).

Glacier ice can also be buried '*in situ*' by supraglacial sediment deposition on top of an active or stagnant glacier margin (e.g. Russell and Knudsen, 2002; Schomacker and Kjær, 2007; Schomacker et al., 2006). During jökulhlaups, ice blocks become detached by englacial hydrofracturing, meltwater conduit collapse and ice cliff collapse (Roberts et al. 2000; Roberts, 2005). Ice-blocks up to 10^2 m in diameter are known to have been washed from glacier margins by jökulhlaups on to outwash plains (sandar) and subsequently either partially or completely buried by sandur aggradation (Tómasson, 1996; Russell and Knudsen, 1999; Roberts et al., 2000; Fay 2001, 2002a,b; Roberts, 2005;

Russell et al., 2006). Melt out of ice blocks transported by the 2010 Eyjafjallajökull eruption generated jökulhlaups is thought to have played a major role in post depositional landscape evolution (Harrison et al., 2019).

Comment [AR1]: New relevant publication added.

During the November 1996 jökulhlaup, ~8.3 x 10^6 m^3 of ice was removed from Skeiðarárjökull (Fay, 2002; Russell et al., 2001a, 2005). Sections of the snout of Skeiðarárjökull were fractured *in situ* into blocks up to 200 m x 400 m in size (Roberts et al., 2000). Ice blocks as large as 45 m in diameter were transported from the glacier margin (Fay, 2002; Russell et al., 2005). Some of these ice blocks were deposited as a linear jökulhlaup flow-parallel cluster, resulting in a single coalesced kettle hole approximately 130 m wide and 40 m long (Fay, 2002a; Russell and Knudsen, 1999, 2002). The largest accumulation of ice blocks was over 1 km in length with a width of up to 300 m (Fay, 2002a; Russell and Knudsen, 2002). Ice blocks transported and buried by such single high-magnitude jökulhlaups are known to persist for 10^1-10^2 yr^{-1} (e.g. Fay, 2002; Everest and Bradwell, 2003; Russell et al., 2005).

The aims of this paper are to: (1) determine the origin of a series of actively developing depressions within the proglacial area of Skeiðarársandur, southeast Iceland; (2) evaluate the mode and significance of buried ice emplacement and subsequent melt for depression development; and (3) explain their significance for sandur evolution. To fulfil these aims we quantify the decadal evolution of the depressions and characterise their sub-surface sedimentary architecture and relate to the wider record of jökulhlaups on Skeiðarársandur.

2~~3~~. Study~~Field~~ area

Harðaskriða is located 3.6 km from the current margin of Skeiðarárjökull within the central zone of Skeiðarársandur, a 1300 km^2 outwash plain fed by Skeiðarárjökull in southeast Iceland (Fig. 1). Skeiðarárjökull is a temperate, surge-type, outlet glacier of Vatnajökull ice cap with a 23 km wide piedmont snout (Björnsson, 1998). Skeiðarársandur has a strong maritime climate, where the maximum depth of winter freezing is only of the order of centimetres (Douglas and Harrison, 1996; Thórhallsdóttir, 1996) making the presence of permafrost impossible. Skeiðarárjökull and Skeiðarársandur have been subject to repeated high-magnitude jökulhlaups generated

both by subglacial volcanic eruptions and the drainage of subglacial and ice-marginal lakes (Thórarinsson et al., 1974; Björnsson, 1992; 1997). The Harðaskriða area of Skeiðarársandur last experienced meltwater flow during the 1922 jökulhlaup, after which glacier margin recession created incised proglacial channels at the Háöldukvísl and Gígjukvísl; subsequently a proglacial trench developed, allowing all subsequent meltwater to be routed westward (Galon, 1973) (Figs 2, 3 and 4; Table 1). The Harðaskriða area is now part of an elevated sandur surface which was unaffected by the large November 1996 jökulhlaup (Snorrason et al., 2002). The Harðaskriða area was however inundated by eleven large jökulhlaups between 1861 and 1938 when Skeiðarárjökull was at its Little Ice Age maximum extent (Thórarinsson, 1974; Björnsson, 1997; Glaciorisk, 2005) (Table 1). These high frequency high-magnitude jökulhlaups resulted in significant aggradation on the eastern and central proximal areas of Skeiðarársandur with accumulated elevations of up to ~125 m above sea level (a.s.l.) compared with elevations of below 90 m a.s.l. for equivalent-aged sandur surfaces to the west (Blauvelt, 2013). Historic accounts indicate a number of large jökulhlaups associated with glacier margin disruption and ice block release in the Harðaskriða area between 1861 and 1938 (Thórarinsson, 1974; Glaciorisk, 2005) (Fig. 2; Table 1). The 1897 and 1903 jökulhlaups can also be specifically linked to the Harðaskriða area (Thórarinsson, 1974). A 1 km long, 150 m high piece of the glacier margin was washed out on to the sandur during the 1903 jökulhlaup possibly associated with detachment along a large, ice flow transverse, hydrofracture generating a large 'embayment' (Roberts et al., 2000, Roberts, 2005).

The Harðaskriða comprises outwash surfaces characterised by a well-developed channel and bar pattern supporting numerous ice block obstacle marks up to 10 m in diameter (Fig. 4). These outwash surfaces are however disrupted by four large depressions the largest of which has maximum dimensions of 604 x 108 m and a depth of ~13 m (Figs 5, 6 and 7). Although there are historic accounts of high magnitude jökulhlaup processes and immediate impacts at Harðaskriða there has been no detailed examination of the development of the resulting landforms and deposits.

3. Methods

3.1. Topographic survey and DEM generation

DEMs for 1968 and 2007 were produced using stereophotogrammetry on digital aerial imagery. Vertical aerial photographs collected for DEM creation were obtained from the National Land Survey of Iceland, Landmælingar Íslands. Images were scanned by Landmælingar Íslands with an Eversmart Jazz+ Scitex scanner, at a resolution of 2000 dpi and delivered as tagged image format (tif) files. Camera calibration documentation and flight lines drawn on 1:100,000 topographic maps were provided for all photographs taken after 1954. Photographs from 1945, taken by the U.S. Air Force, were purchased from Landmælingar Íslands, who provided known flight elevations and camera focal lengths. Colour digital images acquired in 2007 by NERC ARSF (IPY07/13) were also used in this study. Digital elevation models (20 m resolution) and photo mosaics were purchased from Loftmyndir HF for 1997 and 2003 datasets.

A differential GPS (dGPS) survey was conducted in 2007 between the glacier margin and Iceland's ring road (Fig. 1). Transects of four of the Harðaskriða depressions were surveyed (Fig. 7). Additionally, large-scale, persistent features across Skeiðarársandur including kettle holes, boulders and ridges that were visible on all historical aerial photographs ~~historical images~~ were utilised for ground control points (GCPs). Survey points were collected using a Thales ProMark III unit, corrected to Icelandic Roads Authority survey sites.

BAE's *SocetSet* 5.5 (*Ngate*) software was used to generate ~~the~~ ~~and~~ DEMs ~~generated using Leica's *SocetSet* 5.5 (*Ngate*) software~~. Triangulation (interior and exterior orientation) was accomplished for all photosets. Once an internal coordinate system was established within the photographs, the control points measured in the field could be used to relate the image to the ground (absolute orientation). The ISN93 coordinates of the GCPs were used to identify points on the images. Once the x, y and z values of GCPs were identified on both (or more) images, SocetSet then performed point measurement automatically, using digital image matching (Baily et al., 2003).

Systematic errors and random errors were evaluated by comparing apparent elevation differences between the DEMs and ground control points measured with the dGPS. The location of the check points and ground control points are summarised in Table 2. Systematic errors are given as root-mean-square error (RMS) measures and the

95th percentile limit is given for random errors a technique commonly used in DEM quality analysis (Schiefer and Gilbert, 2007). All units are in metres above sea level (m a.s.l.). Following manual clean up ('post pushing') of the study area, all check points fell under 1 m. Due to the comparatively small scale and dynamic terrain of the study area, no additional registration was applied.

Elevation differences were used to provide an approximate estimate of the volumetric loss for four of the major Harðaskriða depressions (Fig. 8) and the elevation loss of the adjoining glacier (Fig. 3). Whilst the poor quality of the 1945 images precluded the production of a 1945 DEM surface to quantify subsidence over the last sixty-two years, an attempt was made to provide as close an approximation as possible. Comparing surfaces constructed from two subsequent time periods (before and after) is often utilised as a cost-effective method to quickly quantify large-scale volumetric changes due to melt out, subsidence, flooding, human interference or other causes (Schiefer and Gilbert, 2007). By removing elevation points that lay within the depressions on the 2007 imagery and generating a triangular irregular network, or TIN, across the missing data points, a 1945 DEM surface could be simulated.

Although the 2018 ArcticDEM was used to provide a general comparison of glacier recession and proglacial fluvial system incision (Porter et al., 2018) (Fig. 3), offsets between the 2018 ArcticDEM and photogrammetrically-derived DEMs, as well as the difficulty in removing bias in this type of terrain, precluded its use for quantification of rates of lowering of the Harðaskriða depressions.

3.2. Ground Penetrating Radar survey

Ground-Penetrating Radar (GPR) profiles were collected from depression 4 (Figs. 5 and 6) using the MALÅ ProEx system with a 13 m long (distance Tx – Rx = 6 m), low-frequency (30 MHz) Rough Terrain Antenna (RTA). GPR-lines (all corrected for topography), both outside and across the depression, were collected in 2013 (i.e. 6 years after the GPS surveys). The objectives were to gain insight in the subsurface sediment architecture, deformation or collapse structures, and to investigate the possibility of the presence of remnants of buried ice.

The basic principles of GPR surveying are that electromagnetic waves travel at different velocities dependent on the electrical and magnetic properties of the earth materials, and that incident waves are refracted or reflected on interfaces between materials with contrasting dielectric permittivities. The nature of the signal that is returned to the surface (i.e. its intensity, polarity and propagation velocity) can then be analysed using processing software (ReflexW; cf. Sandmeier, 2012) which allows the reconstruction and modelling of the architecture of the subsurface.

Figure 6 shows the survey plan with a single E-W profile capturing the length of the depression, and three shorter N-S profiles across the depression. Data were collected as a continuous array with additional transects surveyed to connect the long and cross profiles (the radar profiles outside the depression were used for reference only). Assuming an average propagation velocity of c. 0.07 m ns^{-1} (cf. Cassidy et al., 2003), depth penetration in the sandur sediments was c. 30 m. This is a value typical for velocities in wet, sandy to gravelly materials and may be an underestimation in case of significant quantities of buried ice present in the subsurface.

4. Results

4.1. Morphology of Harðaskriða depressions

All depression measurements are based on their 2007 dimensions. Depression 1 is approximately oval in shape and ranges in width from 164 m (north-south) to 108 m (east-west) (Figs. 7 and 8). The northern and southern rims are characterised by outwardly dipping arcuate and concentric normal faults. Along the southern rim, normal faulting has resulted in the rotation of two large blocks (up to 60 m in length and 15 m wide). The base of this depression is characterised by sagging, uneven terrain, and is divided into two portions of unequal depth. The northernmost part of the depression measured 10 ± 1.64 m in depth, while the southern part of the depression measured 12 ± 1.64 m in depth. R~~Most r~~ecent satellite imagery (DigitalGlobe, 2016) indicates further depression widening attributed to continued melt-out.

Depression 2 is approximately circular in shape and ranges in width from 89 m (north-south) to 104 m (east-west) and 13 ± 1.64 m deep (Fig. 7). The northern portion contains

concentric normal faults and two extensional faults that trend north-south (40 m and 50 m in length). Along the southernmost rim of this depression, normal faulting has resulted in the rotation of two blocks, the largest 60 m long and 13 m wide.

Depression 3 possesses an irregular, elongate morphology that trends east-west. The depression ranges in width from 342 m (east-west) and 116 m (north-south) and is 12 ±1.64 m deep (Fig. 7). The margin, while not circular in shape, contains numerous normal faults and recesses that surround the depression. The southern margin is marked by several rotated blocks and steep walls. The margin appears to slump in rotational blocks towards the centre, resulting in 'steps' that dip outwards from the depression. A dirt road observed on the 1945 aerial photographs remains visible on the 2007 aerial photographs. Its original surface, although now undulating, remains discernible as it traverses depression 3, suggesting that subsidence has been gradual in nature.

Depression 4, the widest of the depressions, is similar in shape to depression 3, possessing an irregular shape and trending east-west (Fig. 7). The depression ranges in width from 604 m (east-west) to 148 m (north-south). Similar to the other depressions, the walls are steepest along the southern margin, and the margin is characterised by horst and graben blocks and concentric extensional fractures (Figs 5a, b and 6). Numerous recesses have developed along the northern, eastern and western margin and possess a relatively gentle, stepped slope, compared to those along the steeper southern margin.

Directly 800 m north of these depressions and visible on the 1965 photographs are three drumlinised, elongate ridges that lead to the elevated sandur (Fig. 9a). These ridges trend north-south and, from east to west, are 176 m, 79 m and 151 m in length and 30, 37, and 34 ±1.64 m in height respectively. Elevation profiles were extracted of the area immediately adjacent to these ridges (Profile 1) and the prominent ridges (Profiles 2-4) that rose towards the elevated sandur surface (Fig. 9b). While varying in height, the ridges all span an average of 33 m from the base of the depression to the sandur. Later photo series (1965 - 1997) indicate that these ridges ~~have been~~were largely removed by the fluvial erosion of shifting proglacial drainage channels and by the November 1996 jökulhlaup. The sedimentary section revealed by erosion during the November 1996 jökulhlaup shows a number of large ice blocks up to 30 m in diameter contained within stratified coarse grained jökulhlaup deposits (Fig. 10). Vertical lowering of 12 ± 1.64 m over the 62 years since 1947 was calculated from the height difference

between the 1945 and 2007 sandur surfaces, representing an average rate of 19.4 ± 2.6 cm of lowering per year (Figs 7 and 8).

4.2. Sub-surface structure of Harðaskriða depressions

Using a relatively low radar frequency, and assuming that the subsurface sediment mostly comprises sand and small to medium gravel (with no outsized boulders to cause 'disruptive' hyperbolae) it may be expected that the signal-to-noise ratio is adequate for resolving metre-scale sandur sedimentology down to a depth of c. 30 m.

There are two main sub horizontal reflectors in the GPR cross-profiles: one at an estimated depth of 6 m and one at c. 20 m below the surface (white solid lines in Fig. 11). A third discontinuous reflector is visible just above the noise which starts at 30 m. As it is right at the detection limit, interpreting this reflector will not be attempted below. The 6 m reflector tends to mirror the surface topography and the 20 m reflector is generally less undulating and continuous across the depression. All three profiles also show shorter sub horizontal reflectors that are thought to represent prominent bedding surfaces. Northward dipping reflectors, a single one in the central cross-profile and two parallel features in the east cross-profile (white dashed lines in Fig. 11), appear to extend down from the 6 m reflector, cross and deflect the 20 m reflector and then connect in a stepped fashion with the reflector at 30 m depth.

In all three cross-profiles, high-angle linear or curvilinear structures (indicated in red in Fig. 11) intersect, or terminate onto the aforementioned reflectors. They are interpreted as joints or normal faults. Particularly near the margins of the depression, they can be seen to disrupt or offset reflectors. Most structures are outward dipping, but there are also less common, apparently younger, inward-dipping faults. All such fractures seem to have developed to accommodate the flexure in the depression and are attributed to progressive subsidence due to gradual melt-out of buried ice. At the surface around the periphery of the depression, the structures present as stepped ring-structures (Figs 5a, b and 6), which are very similar to the 'concentric' ring-fractures described for collapsing calderas and other ice-melt phenomena by Branney (1995) and Branney and Gilbert (1995).

Whilst confident about the interpretation of the joint and fault structures, the characterisation of the subsurface materials from the radargrams is more challenging, particularly without the possibility of direct ground truthing. There are good exposures

near the Gígjukvísl, 5 km kilometres to the west (see Russell et al., 2001), but they are developed into proglacial surfaces which lack the 'pitted' surfaces diagnostic of jökulhlaup deposits. Fortuitously, the 1996 jökulhlaup cut a 30 m high section into sandur sediments 1.3 km north of the Harðaskriða depressions (Fig. 10) so there is at least some information available on textural heterogeneity of the sandur sediments and the distribution and dimensions of buried ice.

Apart from the aforementioned reflectors, the most conspicuous zones in the GPR profiles are those that seem to be devoid of energy returns. Such zones (indicated in blue in Fig. 11), can be observed mostly away from the centre of the depression and below the 6 m reflector, but there are also a few at greater depths. Assuming that these features are not processing artefacts, they must represent homogeneous materials with a low relative dielectric permittivity ε_r. Where a reflector - mostly that at 6 m depth, forms the upper surface of such zones - the polarity is opposite to that of the air wave (phase change of 180°) which would suggest that the overlying sediment has a relatively high ε_r. Since ice has an ε_r of 3-4 (Brandt et al., 2007) and overlying materials, which can logically assumed to be relatively (wet) jökulhlaup sediments may be expected to have an ε_r in the order of 10-30 - and drawing analogies with nearby exposures - the zones are tentatively interpreted as remnants of buried ice.

The observation that the interpreted blocks of buried ice are ubiquitous at the north and south sides of the cross-profiles, but less common in the central parts is compatible with the idea that subsidence has been greatest in the centre of the depression. The inward dipping reflector on the south side in the central and east cross-profiles (Fig. 11, middle and lower panels) may delineate the upper surface of relatively intact buried ice. The deeper parts of this surface may have served as a slip-plane extending into one of the deeper identified normal faults.

Although its strength is variable, it is clear that the reflector at 20 m is more continuous than the 6 m reflector. Interestingly, its polarity is the same as the air wave which suggests that it represents a contact between a lower permittivity (above) to a higher permittivity material below. The fact that it does not show significant offsets where intersected by high angle faults is taken as evidence that the reflector is not a sedimentary surface. Instead it is proposed that it represents the local groundwater table (wet/saturated sand: ε_r = 10-30; Brandt et al., 2007), although it is noted that

365 other studies on the sandur (cf. Cassidy et al., 2003; Burke et al., 2010) have found the
366 groundwater table to be significantly shallower.
367
368 **5~~6~~. Discussion**
369 The average rate of 19.4 ± 2.6 cm of lowering per year between 1945 and 2007
370 determined from this study is an order of magnitude lower than the 1.88 ma^{-1} reported
371 for immediate post jökulhlaup ice-melt out within the Gígjökull basin between 2010 and
372 2016 (Harrison et al., 2019). Higher buried ice melt rate at Gígjökull can be attributed to
373 the simultaneous deposition of smaller ice fragments with jökulhlaup deposits rather
374 than the melt of large isolated blocks.
375
376 Combined DEMs, dGPS measurements and GPR surveys reveal that the Harðaskriða
377 depressions experienced the greatest vertical loss within their centres, due to slump in
378 rotational blocks towards the centres, characteristic of 'horst and graben' structures.
379 This process has resulted in 'steps' that have developed along the side of each of the
380 features into the centre. The concentric rings of normal faulting, horst and graben and
381 normal and extensional faults described at the Harðaskriða depressions 1 - 4 are
382 consistent with observations made at other field sites involving the melt-out of smaller
383 bodies of ice that have been transported by lahars and jökulhlaups (Maizels, 1992;
384 Branney, 1995; Branney and Gilbert, 1995; Olszewski and Weckwerth, 1998). Such
385 features have also been used as indirect evidence of buried bodies of ice at other
386 locations (e.g. Boulton, 1972; Hambrey, 1984; Krüger and Kjær, 2000; Kjær and Krüger,
387 2001; Dickson and Head, 2006).
388 As the ice bodies buried at Harðaskriða began to melt, the loss of volume and drainage
389 of subsurface water may have resulted in the subsidence of the overlying sediment
390 (McDonald and Shilts, 1975, Maizels, 1992). This sort of subsidence can produce
391 outwardly-dipping arcuate hairline fractures that can elongate into a ring, causing the
392 subsidence of a coherent block of sediment as seen in depressions 1 and 2 (Branney,
393 1995; Branney and Gilbert, 1995). These overhanging scarps become unstable and
394 collapse along new arcuate faults, resulting in the development of extensional crevasses
395 that may continue to expand along small vertical and normal faults causing some walls
396 to collapse, resulting in keystone graben (Sanford, 1959; McDonald and Shilts, 1975).
397 Continued collapse leads to intersection of arcuate fractures resulting in blocks that tilt

and subside into the pit, while mass movements and slumping may accelerate the melting rate of a buried ice body (Johnson, 1992).

At larger collapse pits, such as depressions 3 and 4, irregular topographic margins with embayments also developed (Branney, 1995; Branney and Gilbert, 1995). These features, combined with the steep walls of the depressions and undisturbed nature of the surrounding outwash plain are consistent with bodies of ice that have been surrounded by sediment (Maizels, 1991). The gentle slopes of the northern walls and the steeper slopes of the southern walls are consistent with the development of a 'normal' kettle hole (Maizels, 1992; Olszewski and Weckwerth, 1998), as proglacial outwash would have resulted in the development of gravitational flow on the northern side, while block displacement and subsidence developed on the southern side following melt out.

The existence of large bodies of buried ice greater than 30 m in thickness on Skeiðarársandur have been identified and documented using resistivity studies (Everest and Bradwell, 2003) and confirmed at exposures (Klimek, 1972; Bogacki, 1973; Churski, 1973; Jewtuchowicz, 1973; Russell and Knudsen, 1999; Molewski, 2000). Ridges and detached slabs of dead ice in the eastern and western parts of Skeiðarársandur have also been identified and described and are attributed to deposition by the retreating ice margin (Galon, 1973; Jewtuchowicz, 1973; Wojcik, 1973). Unlike ice-cored ridges, plains or moraines elsewhere on the sandur, the geometry, orientation and size of the bodies of ice that resulted in the Harðaskriða depressions are consistent with other descriptions of isolated blocks of ice emplaced during high-magnitude jökulhlaups (Maizels, 1992; Maizels and Russell, 1992; Branney, 1995; Branney and Gilbert, 1995; Harrison et al., 2019).

A topographic map published in 1904 (Danish Staff Map) depicts several elongated, east-west trending ridges extending across central Skeiðarársandur that appear to be continuations of the 19th century moraines that persist today in the western region of the sandur (Fig. 2). By 1945, aerial photographs reveal that these moraines are no longer visible on the central sandur, and reportedly buried or removed by jökulhlaups (Galon, 1973; Jewtuchowicz, 1973; Wojcik, 1973; Wisniewski, 1997; Knudsen et al., 2001). While some of the depressions and landforms correspond to the approximate positions of the

19th century moraines, largest Harðaskriða depressions are developed approximately 400 m south of this limit, suggesting that they are not related to buried ice bodies contained within the pre-existing 19th century moraines (Fig. 4).

According to Thórarinsson (1974), a large piece of the glacier margin detached during the 1903 jökulhlaup approximately 1 km in length and up to 150 m in height; it was also documented that a fracture of similar size and length developed up glacier located where the floodwaters burst from the glacier margin. During this same flood, house-size ice blocks were emplaced on the sandur and the flood waters *"dug into the sand a deep, 'many persons high', steep-sided channel"* (Thórarinsson, 1974). Ice blocks, regardless of their original shapes, result in circular depressions, such as Depression 2, however dumbbell-shaped pits may form where circular collapse pits from two closely adjacent buried blocks of ice overlap, such as Depression 1 (Branney and Gilbert, 1995). The geometry and orientation of the largest elongated depressions (Depressions 3 and 4) may therefore correspond to the 1 km wide portion of the margin that was detached during the 1903 jökulhlaup described by Thórarinsson (1974). In the absence of evidence of a disrupted glacier snout or ice blocks on the topographic map published in 1904, it is presumed that the field survey that formed the basis for this map pre-dated the 1903 jökulhlaup.

Thórarinsson (1974) stated that jökulhlaups in 1913 and 1922 inundated the central sandur with floodwaters and sediment. During later periods of glacier stillstand, meltwater runoff was concentrated in the central part of the sandur, resulting in the formation of wide outwash channels (Galon, 1973). In common with glacier termini elsewhere in Iceland, the margin of Skeiðarárjökull experienced climate-forced recession from their Little Ice Age maximum extents (Thórarinsson, 1943; Sigurðsson, 2005). Recession of Skeiðarárjökull resulted in meltwater drainage from the glacier margin at progressively lower elevations leading to sandur incision (Galon, 1973). As such, subsequent jökulhlaups in 1934 and 1938 did not affect Harðaskriða, as the floodwaters were routed through other channels such as the Háöldukvísl, 1.5 km to the east (Fig. 1). Aerial photographs taken in 1945 show the formation of a proglacial trench and meltwater flow in a westerly direction towards the Gígjukvísl (Figs 1 and 3).

While the jökulhlaup-transported ice bodies may have been emplaced as early as 1897 and as late as 1922, any melting that occurred during that time is not captured due to a lack of available imagery. The rate of melt of a buried ice body may be affected by a variety of factors, including the amount of sediment within the ice, depth of burial and geothermal heat flux (Nakawo and Young, 1981; Nicholson and Benn, 2006), making it difficult to estimate the initial size of the buried ice body. Ice blocks emplaced and completely buried by the 1903 jökulhlaup would have been further insulated by additional sediment aggradation during the 1913 and 1922 jökulhlaups (Thórarinsson, 1974). That glacier ice buried by November 1996 jökulhlaup deposits has survived for 23 years illustrates the feasibility of buried ice preservation between the 1903 and 1913 jökulhlaups.

It is noticeable that the Harðaskriða depressions are not visible on the 1945 photographs, suggesting that the buried ice has not exhibited high melting rates. It is not until the 1965 photographs, following the retreat of the central lobe of the glacier margin and the subsequent formation of the proglacial trench post-1945, that subsidence is visible. This observation and the sequence of events presented in this study suggests that the melt rate of the buried ice bodies may have been accelerated as a result of the retreat and decoupling of the glacier margin and the associated rise in ambient temperatures and lowering of local groundwater table. This demonstrates the control that glacier margin stability has on post-depositional modification processes, as buried ice bodies may be capable of persisting for much longer periods at a stable or advancing margin, characterised by proglacial aggradation, rather than at a retreating or stagnating margin characterised by proglacial incision.

According to Björnsson et al. (1999) profiles of the surface of Skeiðarárjökull in 1904 were ~100 m higher than in 1945, which would have resulted in a steeper ice surface gradient and therefore increased hydraulic gradient during high-magnitude jökulhlaups (Roberts et al., 2000, 2001; Roberts, 2005). This would have increased the capacity of jökulhlaups to excavate and transport sediment. The elongate, drumlinised ridges observed on the 1965 images on the down-glacier side of the proglacial trench generated by the retreat of the glacier margin are interpreted as conduit-fill eskers

created by sediment deposition as meltwater ascended by at least 30 m over a distance of ~200 m from the proglacial depression to innundate Harðaskriða (Fig. 9).

The landform and sediment assemblage at Harðaskriða reflect the role of multiple jökulhlaups just after the Little Ice Age maximum extent of Skeiðarárjökull. Initial glacier position before the 1903 jökulhlaup is associated with unconfined proglacial drainage (Russell and Knudsen, 1999, 2002; Russell et al., 2005, 2006) (Figures 11a and 11a(i)). Erosion of a 1 km wide ice-walled re-entrant into the snout of Skeiðarárjökull by the 1903 jökulhlaup liberated large ice blocks which were transported by the jökulhlaup onto the sandur for distances of up to 0.5 – 0.8 km (Fig. 11b). The largest 1903 jökulhlaup-transported ice blocks were probably partially buried as was the case with the largest ice blocks during the 1996 jökulhlaup (Russell and Knudsen, 1999; Fay, 2001, 2002a) (Fig. 11b(i)). Sediment aggradation during the 1913 and 1922 jökulhlaups buried the ice blocks emplaced in 1903 (Fig. 11c(i)). It is likely that the ice blocks had reduced in size by ablation between 1903 and 1913. Continued glacier recession resulted in the abandonment of the Harðaskriða sandur surface between 1933 and 1945 (Fig. 11d). Melt of buried ice results in depressions which have deepened and expanded in surface area between 1968 and 2007 (Fig. 11d(i)). The GPR survey undertaken in 2013 of the largest depression indicates the presence of buried glacier ice which together with the recent satellite observations of depression widening, suggests that the melt out processes are ongoing.

6. Conclusions ~~and wider implications~~

Continued melting of the Harðaskriða ice bodies nearly a century following their emplacement and burial demonstrates that jökulhlaups may continue to be an important control on sandur evolution over decadal to centennial timescales (10^1 – 10^2 years). Buried ice meltout associated with the development of the Harðaskriða depressions was enhanced by the lowering of the groundwater table following abandonment of the sandur brought about by glacier margin recession during the second half of the twentieth century. The occurrence of three high magnitude jökulhlaups within an 18-year period following the Little Ice Age glacier maximum extent resulted in significant sandur aggradation and ice block burial, assisting the long term preservation of ice. By contrast, a similar succession of jökulhlaups during a period of

glacier margin recession will reduce the potential for jökulhlaup-transported ice blocks to be buried as ~~due to~~ repeated 'decoupling' of the glacier margin from the its sandur reduces the potential for stacking of jökulhlaup deposits~~decoupling of the sandur from its glacier margin~~.

Our model of the jökulhlaup landsystem at Harðaskriða and the ability to identify them at other warm-based sediment-rich glaciers that may be subject to some or all the large-scale processes including margin fluctuations, jökulhlaup dynamics and secondary modification may provide a useful analogue for interpreting landforms and strata emplaced by margin fluctuations, jökulhlaups and melt out generated by the retreating continental Pleistocene ice sheets.

Acknowledgements

AJR, DJB, ARGL and FST acknowledge the Earthwatch Institute for fieldwork funding. AJR and ARGL thank the NERC ARSF (IPY07/13) for acquisition of 2007 aerial photography and AJR's fieldwork in 1996-97 was funded by (GR3/10960). We thank Ragnar Frank Kristjánsson and Regína Hreinsdóttir for valuable support for jökulhlaup-related research within Skaftafell/Vatnajökull National Park. We thank Marek Ewertowski for acquiring the 2013 GPS data and Chris Williams for conducting the topographic corrections of the GPR data. We thank Anders Schomacker and an anonymous reviewer for their constructive comments on this paper. Achim Belich is thanked for editorial oversight. Thanks to Salvatore G. Candela for assistance with digital elevation models.

551 **References**

552

553 Ballantyne, C.K., 2002. Paraglacial Geomorphology. Quaternary Science Reviews 21, 18-
554 19, 1935-2017.
555 Baily, B., Collier, P., Farres, P., Inkpen, R. and Pearson, A. 2003. Comparative assessment
556 of analytical and digital photogrammetric methods in the construction of DEMS
557 and geomorphological forms, Earth Surface Processes and Landforms 28, 307-
558 320.
559 Bennett, M.R., Glasser, N.F. 2009. Glacial geology: ice sheets and landforms. Second
560 edition. Oxford, Wiley-Blackwell. 385pp.
561 Brandt, O., Langley, K., Kohler, J., Hamran, S.E., 2007. Detection of buried ice and
562 sediment layers in permafrost using multi-frequency Ground Penetrating Radar:
563 a case examination on Svalbard. Remote Sensing in the Environment 111, 212-
564 227.
565 Björnsson, H., 1974 Explanation of jökulhlaups from Grímsvötn, Vatnajökull, Iceland,
566 Jökull 24, 1-26.
567 Björnsson, H., 1992 Jökulhlaups in Iceland: prediction, characteristics and simulation.
568 Annals of Glaciology 16, 95-106.
569 Björnsson, H., 1997. Grímsvatnahlaup Fyrr og Nu. In Haraldsson, H. (ed.) Vatnajökull:
570 Gos og hlaup 1996. Reykjavík: Vegagerðin, 61-77.
571 Björnsson, H., 1998. Hydrological characteristics of the drainage system beneath a
572 surging glacier. Nature 395, 771-774.
573 Björnsson, H., Pálsson, F., Magnússon, E., 1999. Skeiðarárjökull: Landslag og
574 rennslisleiður vatns undir sporði. Raunvísindastofnun Háslólans. RH-11-1999.
575 Blauvelt, D., 2013. Evolution of a Sandur: sixty years of change, Skeiðarársandur, Iceland.
576 PhD Thesis, Newcastle University, 301pp.
577 Bogacki, M., 1973 Geomorphological and geological analysis of the proglacial area of
578 Skeiðarárjökull. Central, western and eastern sections, Geographia Polonica 26,
579 57-88.
580 Boulton, G.S., 1972. Modern Arctic glaciers as depositional models for former ice sheets.
581 Journal of the Geological Society of London 128, 361-393.

582 Branney, M.J., 1995. Downsag and extension at calderas: new perspectives on collapse
583 geometries from ice-melt, mining and volcanic subsidence. Bulletin of
584 Volcanology 57, 303-318.
585 Branney, M.J., Gilbert, J.S. 1995. Ice-melt collapse pits and associated features in the
586 1991 lahar deposits of Volcan Hudson, Chile: criteria to distinguish eruption-
587 induced glacier melt. Bulletin of Volcanology 57, 293-302.
588 Burke, M.J., Woodward, J., Russell, A.J., Fleisher, P.J., Bailey, P.K. 2010. The sedimentary
589 architecture of outburst flood eskers: a comparison of ground-penetrating radar
590 from Bering Glacier, Alaska and Skeiðarárjökull, Iceland. GSA Bulletin 122, 9-10,
591 1637-1645.
592 Cassidy, N.J., Russell, A.J., Marren, P.M., Fay, H., Rushmer, E.L., Van Dijk, T.A.G.P.,
593 Knudsen Ó., 2003. GPR-derived architecture of November 1996 jökulhlaup
594 deposits, Skeiðarársandur, Iceland. in: Bristow, C.S., Jol, H.M., (Eds.) Ground
595 Penetrating Radar in Sedimentation, Spec. Publ. Geol. Soc. 211, pp. 153-166.
596 Churski, Z., 1973. Hydrographic features of the proglacial area of Skeiðarárjökull.
597 Geographia Polonica 26, 209-254.
598 Dickson, J., Head, J.W., 2006. Evidence for an Hesperian-aged South circum-Polar lake
599 margin environment on Mars. Planetary and Space Science 54, 251-272.
600 Douglas, T.D., Harrison, S. 1996. Turf-banked terraces in Öræfi, southeast Iceland:
601 morphology, rates of movement, and environmental controls. Arctic and Alpine
602 Research 28, 228-236.
603 Evans, D.J.A., England, J., 1992. Geomorphological evidence of Holocene climate change
604 from northwest Ellesmere Island, Canadian High Arctic. Holocene 2, 148-158.
605 Evans, D.J.A., Twigg, D.R., 2002. The active temperate glacial landsystem: A model based
606 on Breiðamerkurjökull and Fjallsjökull, Iceland. Quaternary Science Reviews 21,
607 20-22, 2143-2177.
608 Evans, D.J.A., Lemmen, D.S., Rea, B.R., 1999. Glacial landsystems of the southwest
609 Laurentide Ice Sheet: modern Icelandic analogues. Geomorphology 14, 673-691.
610 Evans D.J.A., Ewertowski, M.W. & Orton, C. 2019. The glacial landsystem of
611 Hoffellsjökull, SE Iceland: contrasting geomorphological signatures of active
612 temperate glacier recession driven by ice lobe and bed morphology. Geografiska
613 Annaler 101A, 249–276.

614 Everest, J., Bradwell, T., 2003. Buried glacier ice in southern Iceland and its wider
615 significance, Geomorphology 52, 347-358.
616 Eyles. N., Boyce, J.I., Barendregt, R.W. 1999. Hummocky moraine: sedimentary record of
617 stagnant Laurentide Ice Sheet lobes resting on soft beds. Sedimentary Geology
618 123, 3–4, 163-174.
619 Fay, H., 2001. The role of ice blocks in the creation of distinctive proglacial landscapes
620 during and following glacier outburst floods (jökulhlaups). PhD thesis, Keele
621 University.
622 Fay, H., 2002a. Formation of ice-block obstacle marks during the November 1996 glacier-
623 outburst flood (jökulhlaup), Skeiðarársandur, southern Iceland. in Martini, I.P.,
624 Baker, V.R. and Garzon, G. (eds) Flood and Megaflood Processes and Deposits:
625 Recent and Ancient Examples. International Association of Sedimentologists
626 Special Publication *32,* pp. 85-97.
627 Fay, H., 2002b. Formation of kettle holes following a glacial outburst flood (jökulhlaup),
628 Skeiðarársandur, southern Iceland. in: Snorasson, A., Finnsdóttir, H.P., Moss, M.,
629 (Eds.) The Extremes of the Extremes: Extraordinary Floods. Proceedings of a
630 symposium held at Reykjavik, Iceland, July 2000. IAHS Publication Number 271,
631 pp. 205-210.
632 Fard, A.M., 2003. Large dead-ice depressions in flat-topped eskers: evidence of a
633 Preboreal jökulhlaup in the Stockholm area, Sweden. Global and Planetary
634 Change 35, 3–4, 273-295.
635 French, H.M., Harry, D.G. 1990. Observations on buried ice and massive segregated ice,
636 western arctic coast, Canada. Permafrost and Periglacial Processes 1, 31-43.
637 Galon, R., 1973. Geomorphological and geological analysis of the proglacial area of
638 Skeiðarárjökull: central section. Geographica Polonica 26, 15-57.
639 Glacier risks database ~~(~~2005~~.)~~ http://www.nimbus.it/glaciorisk/gridabasemainmenu.asp
640 Accessed 25/04/2019.
641 Hambrey, M.J., 1984. Sedimentary processes and buried ice phenomena in the
642 proglacial areas of Spitsbergen glaciers. Journal of Glaciology 30, 104,116-119.
643 Harrison, D., Ross, N., Russell, A.J., Dunning, S.A. 2019. Post-jökulhlaup geomorphic
644 evolution of the Gígjökull Basin, Iceland. Annals of Glaciology 60(80), 1-11.
645 Hjulström, F., 1952. The geomorphology of the alluvial outwash plains (sandurs) of
646 Iceland and the mechanics of braided rivers. Proceedings of the XVIIth

International Congress of the International Geographical Union, Washington, pp. 337-342.

Hooke, R.L., Jennings, C.E., 2006. On the formation of tunnel valleys of the southern Laurentide ice sheet. Quaternary Science Reviews 25, 1364-1372.

Ives, J.D., 2007. Skaftafell in Iceland: a thousand years of change. Ormstunga: Reykjavik, 256pp.

Jewtuchowicz, S., 1973. The present-day marginal zone of Skeiðarárjökull. Geographia Polonica 26, 115-138.

Johnson, P.G., 1992. Stagnant glacier ice, St. Elias Mountains, Yukon. Geografiska Annaler 74A, 1, 13-19.

Kleman, J., 1992. The palimpsest glacial landscape in northwestern Sweden. Late Weichselian deglaciation landforms and traces of older west-centered ice sheets. Geografiska Annaler 74A, 4, 305-325.

Kleman, J., Stroeven, A.P., 1997. Preglacial surface remnants and Quaternary glacial regimes in northwestern Sweden. Geomorphology 19, 1–2, 35–54.

Klimek, K., 1972. Present-day fluvial processes and relief of Skeiðarársandur plain (Iceland). Polska Academia Nauk Institut Geografi 94, 129-139.

Knudsen, Ó., Jóhannesson, H., Russell, A.J., Haraldsson, H., 2001. Changes in the Gígjukvísl river channel during the November 1996 jökulhlaup, Skeiðarársandur, Iceland, Jökull 50, 19-32.

Korsgaard, N.J., Schomacker, A., Benediktsson, Í.Ö., Larsen,N.K., Ingólfsson,Ó., Kjær, K.H. 2015. Spatial distribution of erosion and deposition during a glacier surge: Brúarjökull, Iceland. Geomorphology 250, 258-270

Krüger, J. 1994. Glacial processes, sediments, landforms and stratigraphy in the terminus region of Mýrdalsjökull, Iceland. Folia Geographica Danica 21, 1–233.

Krüger, J. and Kjær, K.H. 2000. De-icing progression of ice-cored moraine in a humid, subpolar climate, Kötlujökull, Iceland. Holocene 10, 721-731.

Kjær, K.H. and Krüger, J. 2001. The final phase of dead-ice moraine development: processes and sediment architecture, Kötlujökull, Iceland. Sedimentology 48, 935-952.

Levy, A., Robinson, Z. Krause, S., Waller, R., Weatherill, J. 2015. Long-term variability of proglacial groundwater-fed hydrological systems in an area of glacier retreat, Skeiðarársandur, Iceland. Earth Surface Processes and Landforms 40, 981–994.

Formatted: Font: Not Bold

Formatted: Font: Not Bold

Lister, H., 1953. Report on glaciology at Breiðamerkurjökull, 1951. Jökull 1, 23-31.

Lukas, S., Nicholson, L.I., Ross, F.H., Humlum, O., 2005. Formation, meltout processes and landscape alteration of High-Arctic ice-cored moraines-examples from Nordenskiold Land, Central Spitsbergen. Polar Geography 29, 157-187.

Maizels, J.K., 1977. Experiments on the origin of kettle-holes. Journal of Glaciology 18, 291-303.

Maizels, J.K., 1991. Origin and evolution of Holocene sandurs in areas of jökulhlaup drainage, South Iceland. in: Maizels, J.K. and Caseldine, C. (eds) Environmental change in Iceland: past and present. Dordrecht: Kluwer, pp. 267-300.

Maizels, J.K., 1992. Boulder ring structures produced during jökulhlaup flows-origin and hydraulic significance. Geografiska Annaler 74A, 21-33.

Maizels, J.K., 1997. Jökulhlaup deposits in proglacial areas. Quaternary Science Reviews 16, 7, 93-819.

Maizels, J.K., Russell, A.J., 1992. Quaternary perspectives on jökulhlaup prediction. In Gray, J.M. (ed.) Applications of Quaternary Research. Quaternary Proceedings 2, 133-153.

McDonald, B.C., Shilts, W.W., 1975. Interpretation of faults in glaciofluvial sediments. in Jopling, A. V. and McDonald, B. C. (eds), Glaciofluvial and glaciolacustrine sedimentation. SEPM Special Publication 23, pp. 123-131.

McKenzie, G.D., 1969. Observations on a collapsing kame terrace in Glacier Bay National Monument, southeast Alaska. Journal of Glaciology 8, 413-414.

Nakawo, M., Young, G.J., 1981. Field experiments to determine the effect of a debris layer on ablation of glacier ice. Annals of Glaciology 2, 85-91.

Nakawo, M., Young, G.J., 1982. Estimate of glacier ablation under debris layer from surface temperature and meteorological variables. Journal of Glaciology 28, 29-34.

Nicholson, L., Benn, D.I., 2006. Calculating ice melt beneath a debris layer using meteorological data. Journal of Glaciology 52, 178, 463-470.

Nye, J.F., 1976. Water flow in glaciers: jökulhlaups, tunnels and veins. Journal of Glaciology 17, 181-207.

Olszewski, A., Weckwerth, P., 1999. The morphogenesis of kettles in the Höfðabrekkujökull forefield, Mýrdalssandur, Iceland. Jökull 47, 71-88.

Østrem, G., 1959. Ice melting under a thin layer of moraine and the existence of ice cores in moraine ridges. Geografiska Annaler 41A, 228-230.

Porter C and 28 others. 2018. ArcticDEM. doi: 10.7910/DVN/OHHUKH.

Price, R.J., 1969. Moraines, sandar, kames and eskers near Breiðamerkurjökull, Iceland. Transactions of the Institute of British Geographers 46, 17-43.

Price, R.J., Howarth, P.J., 1970. The evolution of the drainage system (1904 - 1965) in front of Breiðamerkurjökull, Iceland. Jökull 20, 27-37.

Roberts, M.J., 2005. Jökulhlaups: a reassessment of floodwater flow through glaciers. Reviews of Geophysics 43, RG1002, doi:10.1029/2003RG000147.

Roberts, M.J., Russell, A.J., Tweed, F.S., Knudsen, Ó. 2000. Ice fracturing during jökulhlaups; implications for englacial floodwater routing and outlet development. Earth Surface Processes and Landforms 25, 1429-1446.

Roberts, M.J., Russell, A.J., Tweed, F.S., Knudsen, Ó., 2001. Controls on englacial sediment deposition during the November 1996 jökulhlaup, Skeiðarárjökull, Iceland. Earth Surface Processes and Landforms 26, 935-952.

Roberts, M.J., Tweed, F.S., Russell, A.J., Knudsen, Ó., Lawson, D.E., Larson, G.J., Evenson, E.B., Björnsson, H., 2002. Glaciohydraulic supercooling in Iceland. Geology 30, 439-442.

Robinson, Z.P., Fairchild, I.J., Russell, A.J., 2008. Hydrogeological implications of glacial landscape evolution at Skeiðarársandur, SE Iceland. Geomorphology 97, 218-236.

Russell, A.J., Knudsen, Ó., 1999. Controls on the sedimentology of November 1996 jökulhlaup deposits, Skeiðarársandur, Iceland. in: Fluvial Sedimentology VI (ed. by N. D. Smith, & J. Rogers), I.A.S. Spec., Publ. 28, pp. 315-329.

Russell, A.J., Knudsen, Ó., 2002. The effects of glacier-outburst flood flow dynamics on ice-contact deposits: November 1996 jökulhlaup, Skeiðarársandur, Iceland. in: Martini, I.P., Baker, V.R., Garzon, G. (eds) Flood and megaflood deposits: recent and ancient examples. Oxford: Blackwell Science, pp. 67-83.

Russell, A.J., Knudsen, Ó., Fay, H., Marren, P.M., Heinz, J., Tronicke, J., 2001a. Morphology and sedimentology of a giant supraglacial, ice-walled, jökulhlaup channel, Skeiðarársandur, Iceland. Global Planetary Change 28, 203-226.

Russell, A.J., Knight, P.G., van Dijk, T.A.G.P., 2001b. Glacier surging as a control on the development of proglacial, fluvial landforms and deposits, Skeiðarársandur, Iceland. Global and Planetary Change 28, 163-174.

745 Russell, A.J. Fay, H., Marren, P.M., Tweed, F.S., Knudsen Ó., 2005. Icelandic jökulhlaup
746 impacts. in: Caseldine, C.J., Russell, A.J., Knudsen, Ó., & Harðardóttir, (eds.)
747 Iceland: Modern Processes and Past Environments. Elsevier Book. pp. 153-204.
748 Russell, A.J., Roberts, M.J., Fay, H., Marren, P.M., Cassidy, N.J., Tweed, F.S. and Harris, T.
749 2006. Icelandic jökulhlaup impacts: implications for ice-sheet hydrology,
750 sediment transfer and geomorphology. Geomorphology 75, 33-64.
751 Sanford, A.R., 1959. Analytical and experimental study of simple geologic structures.
752 Geological Society of America Bulletin 70, 19-52.
753 Schiefer, R., Gilbert, R., 2007. Reconstructing morphometric change in a proglacial
754 landscape using historical aerial photography and automated DEM generation.
755 Geomorphology 88, 167-178.
756 Sandmeier, K.J., 2012. ReflexW 8.1, Program for the Processing of Seismic, Acoustic or
757 Electromagnetic Reflection, Refraction and Transmission Data; Software Manual:
758 Karlsruhe, Germany.
759 Schomacker, A., 2008. What controls dead-ice melting under different climate
760 conditions? A discussion. Earth Science Reviews 90, 3–4, 103-113.
761 Schomacker, A., Kjær, K.H., 2007. Origin and de-icing of multiple generations of
762 ice-cored moraines at Brúarjökull, Iceland. Boreas 36, 4, 411-425.
763 Sigurðsson, O., 2005. Variations of termini of glaciers in Iceland in recent centuries and
764 their connection with climate. Developments in Quaternary Sciences 5, 241-255.
765 Smith, L.C., Sheng, Y., Magilligan, F.J., Smith, N.D., Gomez, B., Mertes, L.A.K., Krabill,
766 W.B., Garvin, J.B., 2006. Geomorphic impact and rapid subsequent recovery from
767 the 1996 Skeiðarársandur jökulhlaup, Iceland, measured with multi-year airborne
768 lidar. Geomorphology 75, 65-75.
769 Snorrason, Á., Jónsson, P., Pálsson, S., Árnason, S., Víkingsson, S., Kaldal, I., 2002.
770 November 1996 jökulhlaup on Skeiðarársandur outwash plain, Iceland. in:
771 Martini, I.P., Baker, V.R., Garzón, G., (Eds.), Flood and megaflood processes and
772 deposits: recent and ancient examples. Special Publication of the International
773 Association of Sedimentologists 32, pp. 55-65.
774 Thórarinsson, S., 1943. Oscillations of the Iceland Glaciers in the last 250 years.
775 Geografiska Annaler 25A, 1-54.
776 Thórarinsson, S. 1974. Vötnin Strið: Saga Skeiðarárhlaupa og Grimsvatnagosa.
777 Bókaútgáfa Menningarsjods, Reykjavik, 254p.

778 Thórarinsson, S., Sæmundsson, K., Williams, S.W.J., 1951. ERTS-1 image of Vatnajökull:
779 analysis of glaciological, structural and volcanic features. Jökull 23, 7-17.
780 Thórhallsdóttir, T.E. 1996. Seasonal and annual dynamics of frozen ground in the central
781 highland of Iceland. Arctic and Alpine Research 28, 237-243.
782 Tonkin, N., Midgley, N.G., Cook, S.J., Graham, D.J. 2016. Ice-cored moraine degradation
783 mapped and quantified using an unmanned aerial vehicle: A case study from a
784 polythermal glacier in Svalbard. Geomorphology 258, 1-10.
785 Wisniewski, E., Andrzejewski, L., Molewski, P., 1997. Fluctuations of the snout of
786 Skeiðarárjökull in Iceland in the last 100 years and some of their consequences in
787 the central part of its forefield. Landform Analysis 1, 73-78.
788 Wojcik, G., 1973. Glaciological studies on the Skeiðarárjökull. Geographia Polonica 26,
789 185-208.

790 **Tables**

791

Year	Eruption	Glacier margin advance/recession	Jökulhlaup impacts *(Impacts on the Harðaskriða area)*
1598	Yes	Advance	No detailed information available.
1629	Yes	Advance	Huge jökulhlaup with at least five enormous flood paths across Skeiðarársandur. Fertile land flooded, one family died and at least one man isolated 5 days on a high hill in the flood area.
1816	?	Little Ice Age Maximum	No detailed information available.
1838	?	Little Ice Age Maximum	No detailed information available.
1851	Yes	Little Ice Age Maximum	No detailed information available.
1861	Yes?	Little Ice Age Maximum	Large jökulhlaup (Stórahlaup) which destroyed much land close to the farms Svínafell, Hof and Hofsnes. Icebergs and large quicksand areas (kettle holes) formed in the flood path.
1867	Yes	Little Ice Age Maximum	Large jökulhlaup, 13 days duration, waning on the 4th day. Icebergs washed out onto Skeiðarársandur, which was completely covered by water.
1873	Yes	Little Ice Age Maximum	Fairly small jökulhlaup The discharge in the river Súla increased right after the beginning of the jökulhlaup in river Skeiðará.
1883	yes	Little Ice Age Maximum	No detailed information available.
1892	Yes?	Little Ice Age Maximum	One of the largest jökulhlaups in river Skeiðará with a duration of four days. Peak discharge reached after two days accompanied by tremendous noise. The next day ice blocks were covering the sandur all the way to the ocean. Ice blocks were up to 20 m in diameter and very tightly packed. South of the main flood outlet, icebergs, up to 20 m high, covered a 7 km wide region. Mud was spread over the flooded area and was unusually thick. Melting icebergs and quicksand made it difficult to cross the Skeiðarársandur for several months after the flood.
1897	Yes	Little Ice Age Maximum	This jökulhlaup was smaller than the one in 1892 and had a duration of 10 days with a 6 day rising stage. It burst from Skeiðarárjökull near Harðaskriða, a steep moraine south of central Skeiðarárjökull. Ice blocks up to 20m in diameter were spread over a 6 km wide area between Harðaskriða and the Skeiðará. ***(Potential source of jökulhlaup transported ice blocks to the Harðaskriða area).***
1903	Yes		Large jökulhlaup with a duration of 4 days reaching discharge peak very quickly and covering more of the western outwash plain than usual. Ice blocks were carried all the way to the ocean. A large piece of the glacier margin detached during the 1903 jökulhlaup approximately 1 km in length and up to 150 m in height; it was also documented that a fracture of similar size and length developed up glacier located where the floodwaters burst from the glacier margin. ***(Potential source of jökulhlaup transported ice blocks to the Harðaskriða area).***
1913	No	Recession	Large jökulhlaup of 12 days duration. The flood was focussed on the eastern part of Skeiðarársandur. Large amounts of ice detached from snout of Skeiðarárjökull with ice blocks described as being the size of houses.
1922	Yes	Recession	This large jökulhlaup had a duration of 14 days and had its main outlet on the eastern side of Skeiðarársandur. Rising stage

			discharge increased slowly for 6 days before any ice blocks were observed being transported downstream. Followed by 8 days of recession. The jökulhlaup waned within one day. ***(Potential for aggradation in the Harðaskriða area).***
1934	Yes	Recession	A large jökulhlaup with a volume of 4.5 km^3 with a 16 day duration and a peak discharge of 25,000 to 30,000 m^3s^{-1}. The eastern most outlet was 2.5 km wide and ice blocks carried to ocean. ***(Potential for aggradation in the Harðaskriða area).***
1938	Yes	Recession	A large jökulhlaup with a volume of 4.7 km^3, a peak discharge of 25,000 to 30,000 m^3s^{-1} and a 16 day duration. Almost all Skeiðarársandur was flooded with ice blocks covering the sandur, although they were smaller than those generated by the 1934 jökulhlaup. ***(Potential for aggradation in the Harðaskriða area).***
1941	No	Recession	A small jökulhlaup with a duration of 17 days and a volume of 1.4 km^3. Relatively small ice blocks released from the glacier snout. ***(No impact on the Harðaskriða area due to the formation of a proglacial trench diverting flow in a westward direction).***
1945	No	Recession	A jökulhlaup with a duration of 12 days, a volume of 2.6 km^3 and a peak discharge of 10,000 m^3s^{-1}. Jökulhlaup flowed in the Skeiðará, Sandgígjukvísl and Núpsá river and produced relatively small ice blocks. ***(No impact on the Harðaskriða area due to the formation of a proglacial trench diverting flow in a westward direction).***
1948	No	Recession	A jökulhlaup with a duration of 17 days, a volume of 2.2 km^3 and a peak discharge of 5,000 m^3s^{-1}. ***(No impact on the Harðaskriða area due to the formation of a proglacial trench diverting flow in a westward direction).***
1954	No	Recession	A jökulhlaup with a duration of 14 days, a volume of 3.2 km^3 and a peak discharge of 10,000 m^3s^{-1}. Jökulhlaup flowed in the Skeiðará and Sandgígjukvísl with peak discharges of 6,000 m^3s^{-1} 4,000 m^3s^{-1} respectively. ***(No impact on the Harðaskriða area due to the formation of a proglacial trench diverting flow in a westward direction).***

Table 1 Chronology of glacier margin fluctuations and jökulhlaups (1598-1954) from the drainage of Grímsvötn subglacial lake draining from Skeiðarárjökull. Information in this table is sourced from Thórarinsson (1974), Björnsson (1997), Glacier risks database (2005) and Ives (2007).

Photo Year	Ave Z dif (m)	RMS (m)	SD (m)	95% confidence (2xSD) (m)
1965	0.0773	3.4536	3.6062	7.2124
1968	1.8190	2.5760	1.8769	3.7538
1997*	1.5005~~.1436~~	2.727~~4884~~	2.3369~~6015~~	4.6738~~5.2030~~
2003*	-0.9224	2.7059	2.6221	5.2442
2007	0.1575	1.6187	1.6442	3.2884

Table 2 Average height difference between DEM and control (check) points surveyed at the field site with error estimates given as root mean square (RMS) errors. Random errors are reported at the 95th percentile limit (all units are in metres). Note '*' designates 1997 and 2003 Loftmyndir DEMs compared with field data.

818

819 **Figures**

820

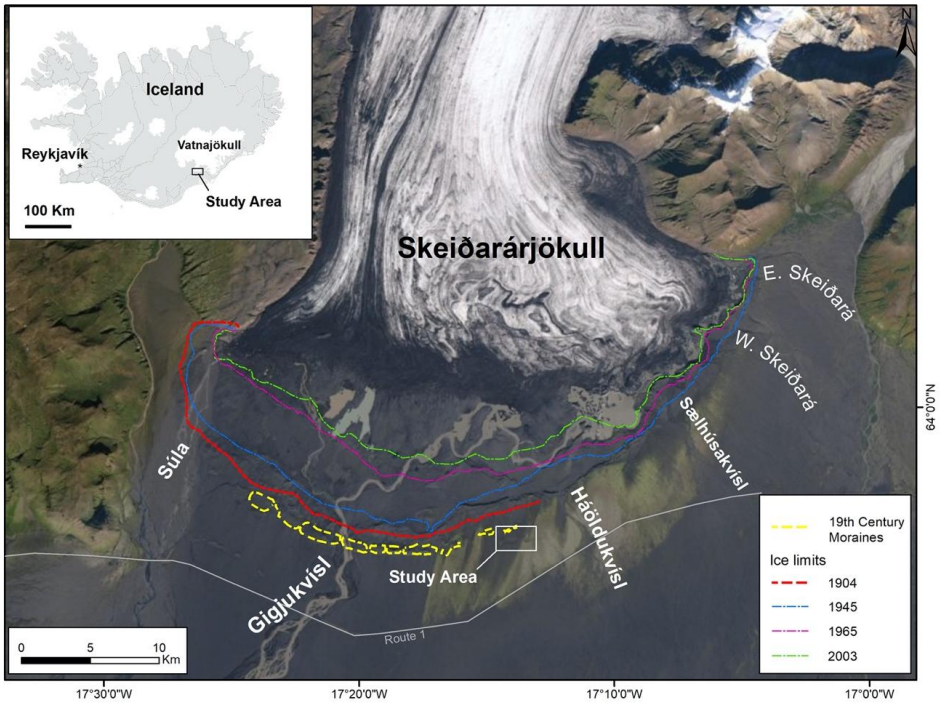

821

822 **Figure 1.** Skeiðarárjökull in Iceland (top inset) and its margin showing the three major lobes, the retreat of
823 the margin since 1945, the location of the 19th century moraines and the major proglacial river channels
824 (Imagery: 2010 Google Earth; Iceland Inset - Justus Lyons).

825

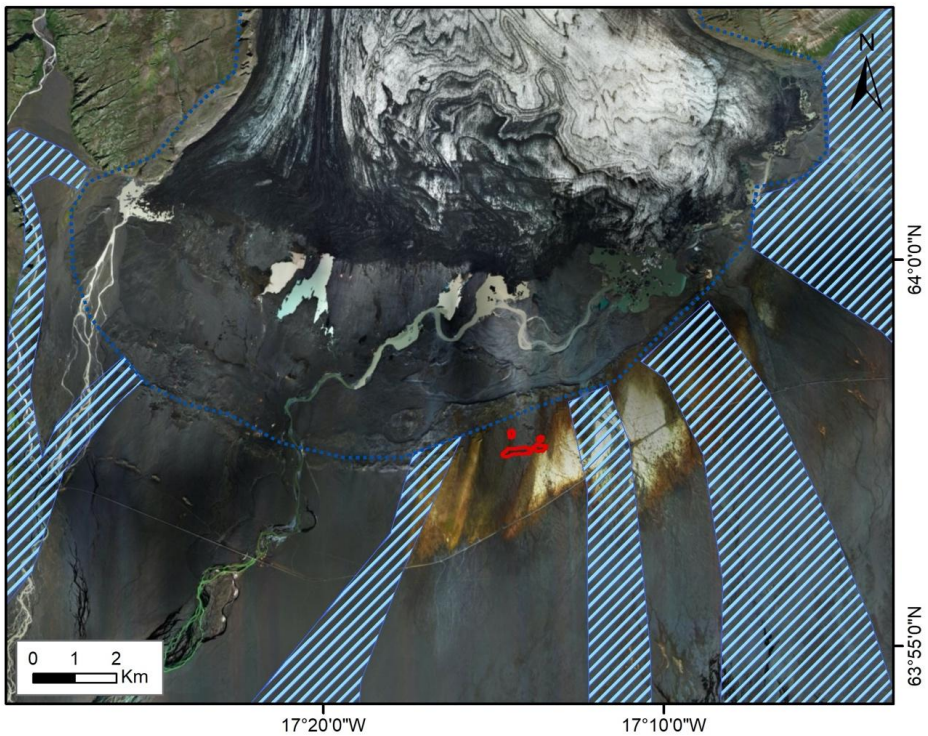

Figure 2. Approximate extent of 1934 ice margin (dashed blue line) and location of jökulhlaup routing (blue hashed polygons) on top of 2016~~03~~ ~~(~~Digital Globe photomosaic~~, (1997 photomosaic underlain to fill gaps).~~ Red polygons delineate location of depressions (Thórarinsson, 1974).

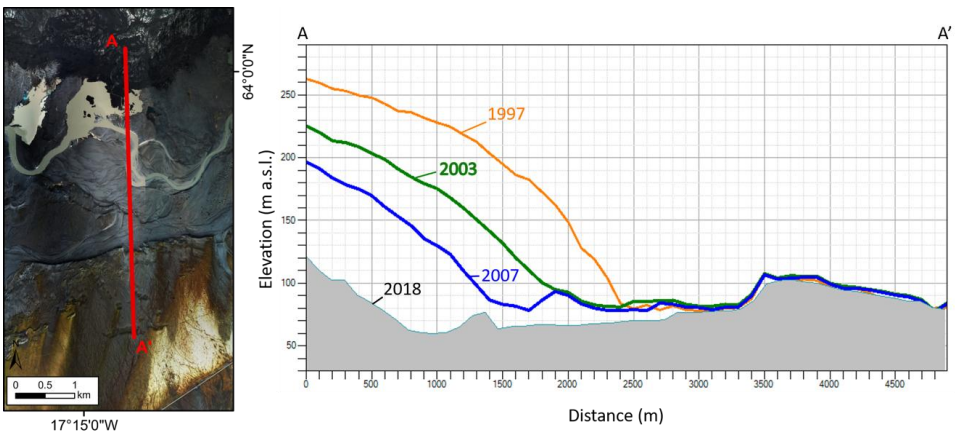

Figure 3. Proximal to distal ~~Long~~ profiles of the glacier and the sandur, demonstrating the retreat of the margin and the base level lowering of drainage within the proglacial depression, and assumed lowering of groundwater table. The 1997, 2003, 2007 profiles are derived DEMs from imagery acquired by Landmælingar Íslands, Loftmyndir ehf. and NERC ARSF, respectively. The 2018 profile is derived from ArcticDEM.

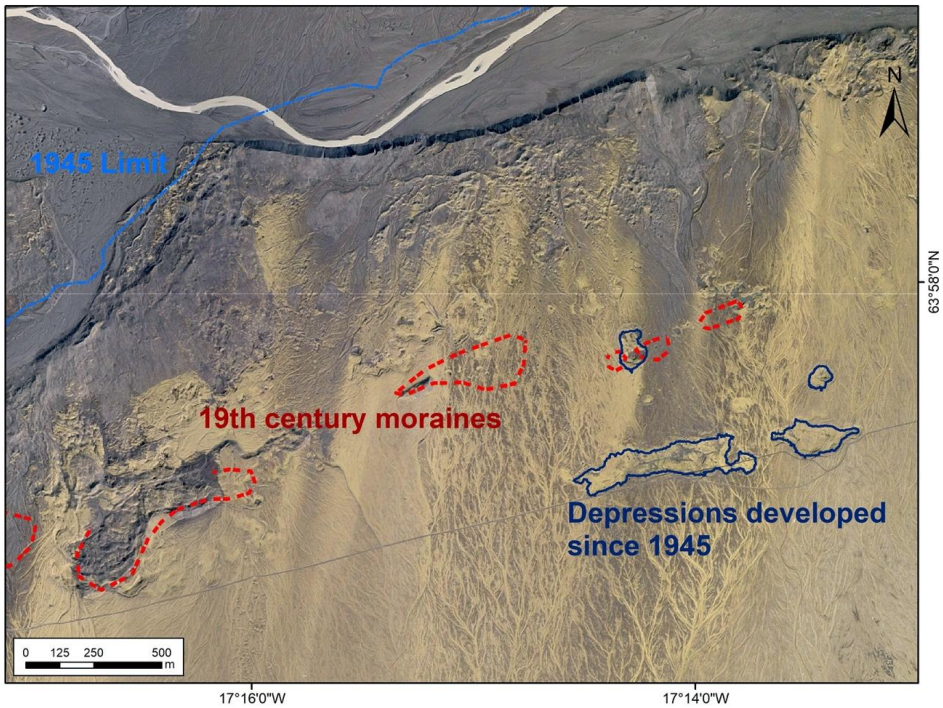

Figure 4. Approximate locations of 19th century moraines estimated from georeferenced 1904 topographic map (red line) on 2003 imagery~~and position of 19th century moraines~~. Blue indicates depressions that have developed since 1945.

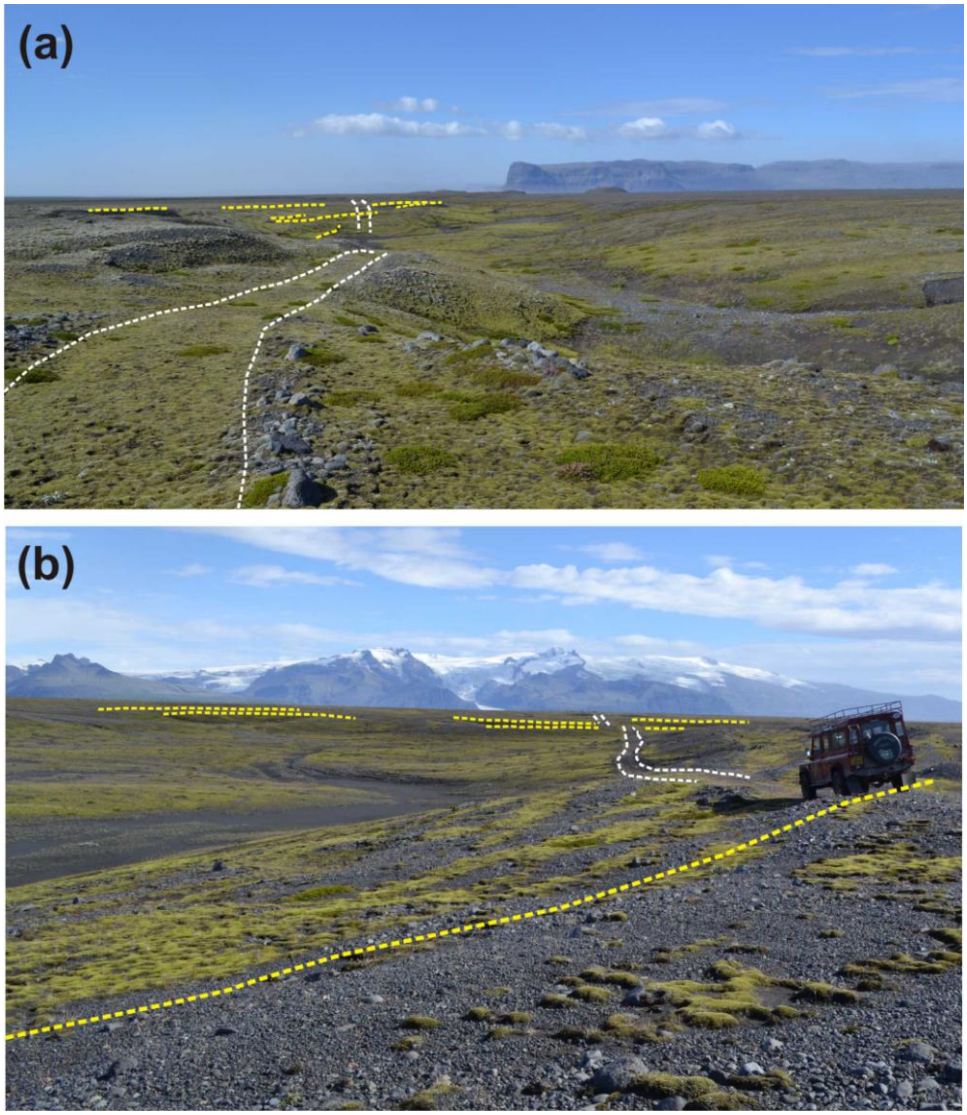

Figure 5. (a) Top. A view towards the west of depression 4 (for location see figs 2 & 4). The upper surfaces of well-defined normally faulted blocks are indicated by the yellow dashed lines. The path of the old gravel road is indicated by the white dashed lines indicating substantial deformation and subsidence. (b) View towards the east of depression 4 showing concentric rings associated with individual fault blocks indicated by yellow lines. The path of the old gravel road is indicated by the white dashed lines indicating substantial deformation and subsidence.

Comment [AR2]: Figure caption has been revised to reflect changes to this figure.

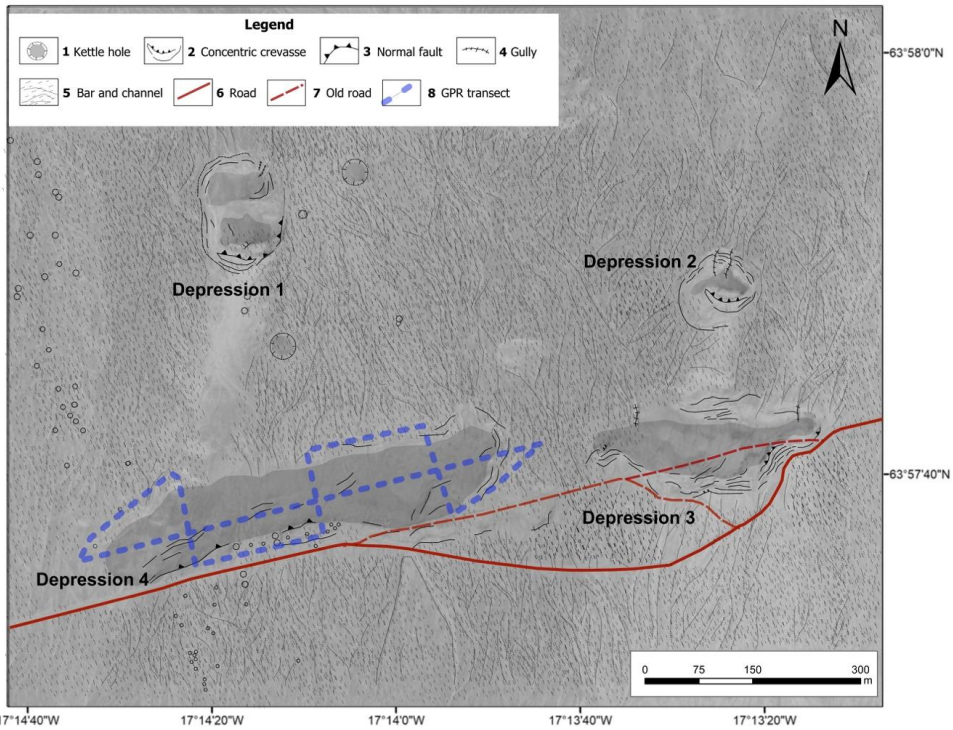

Figure 6. Geomorphological map of depressions and GPR transects (dashed blue lines). Red broken line represents the original course of a gravel road that has been re-routed to the south due to on-going subsidence of depression.

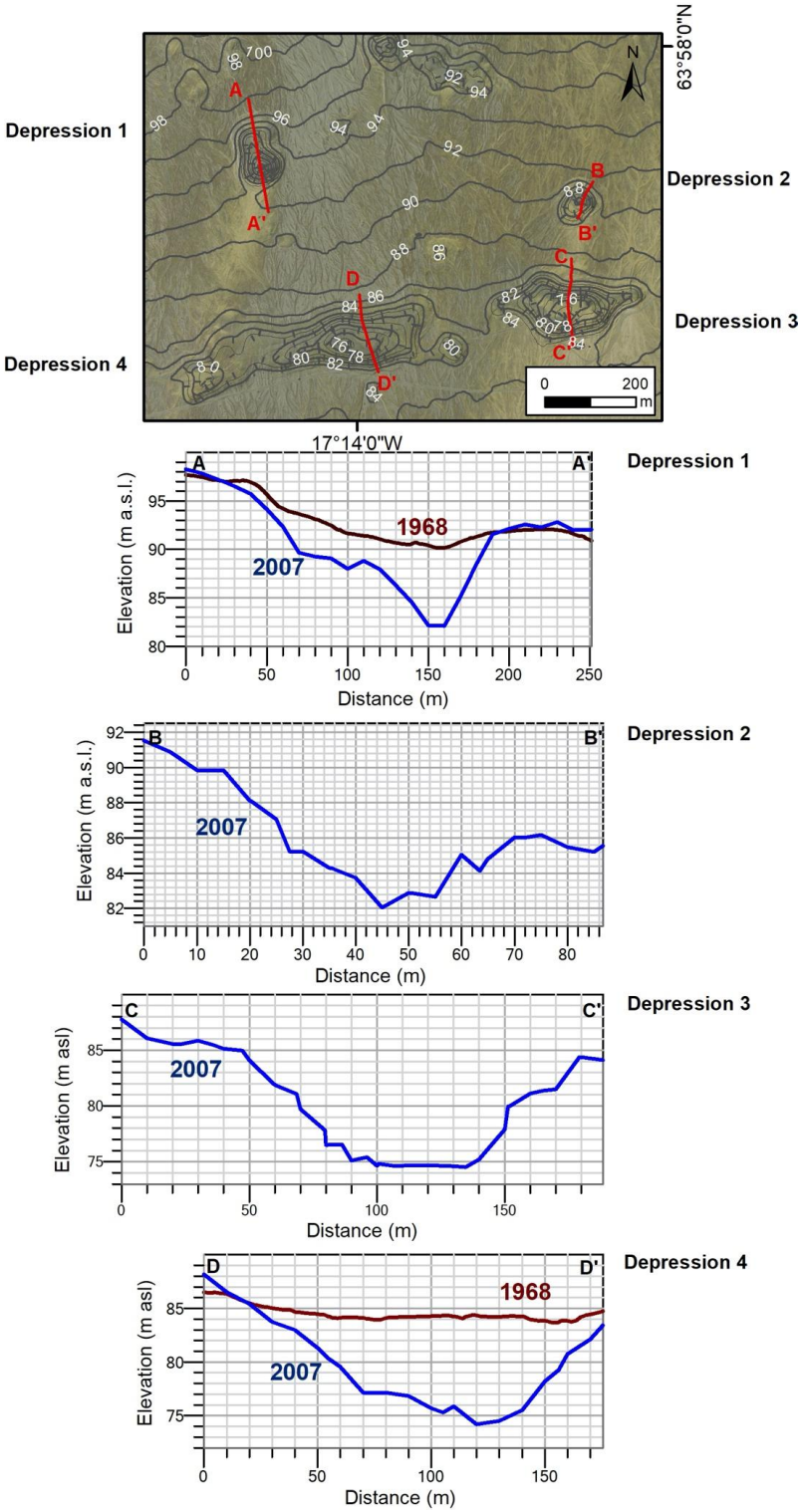

Figure 7. Profiles of depressions 1 –4 in 2007 (dGPS survey transects) are shown in blue; the 1968 surfaces, when available, are~~is~~ shown in red.

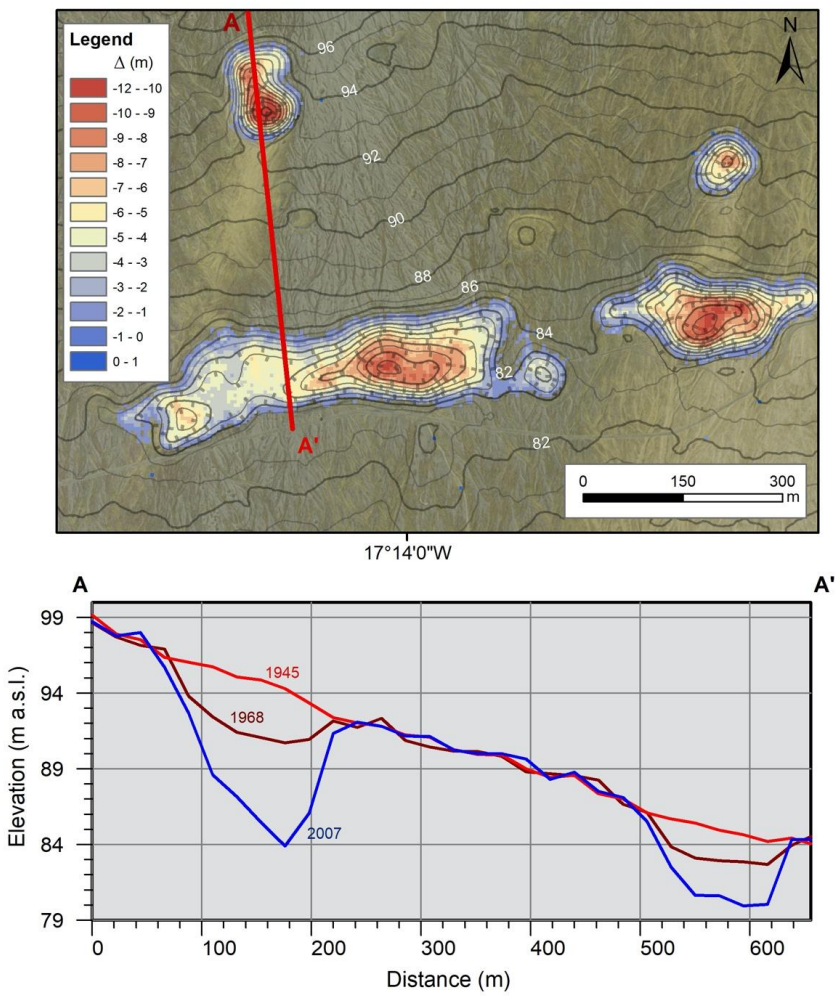

Figure 8. Total elevation loss (m) between 1945 – 2007 and estimated volume loss estimated by using an artificial 1945 surface (top); profiles of depressions between 1945 (red), 1968 (brown) and 2007 (blue) (bottom).

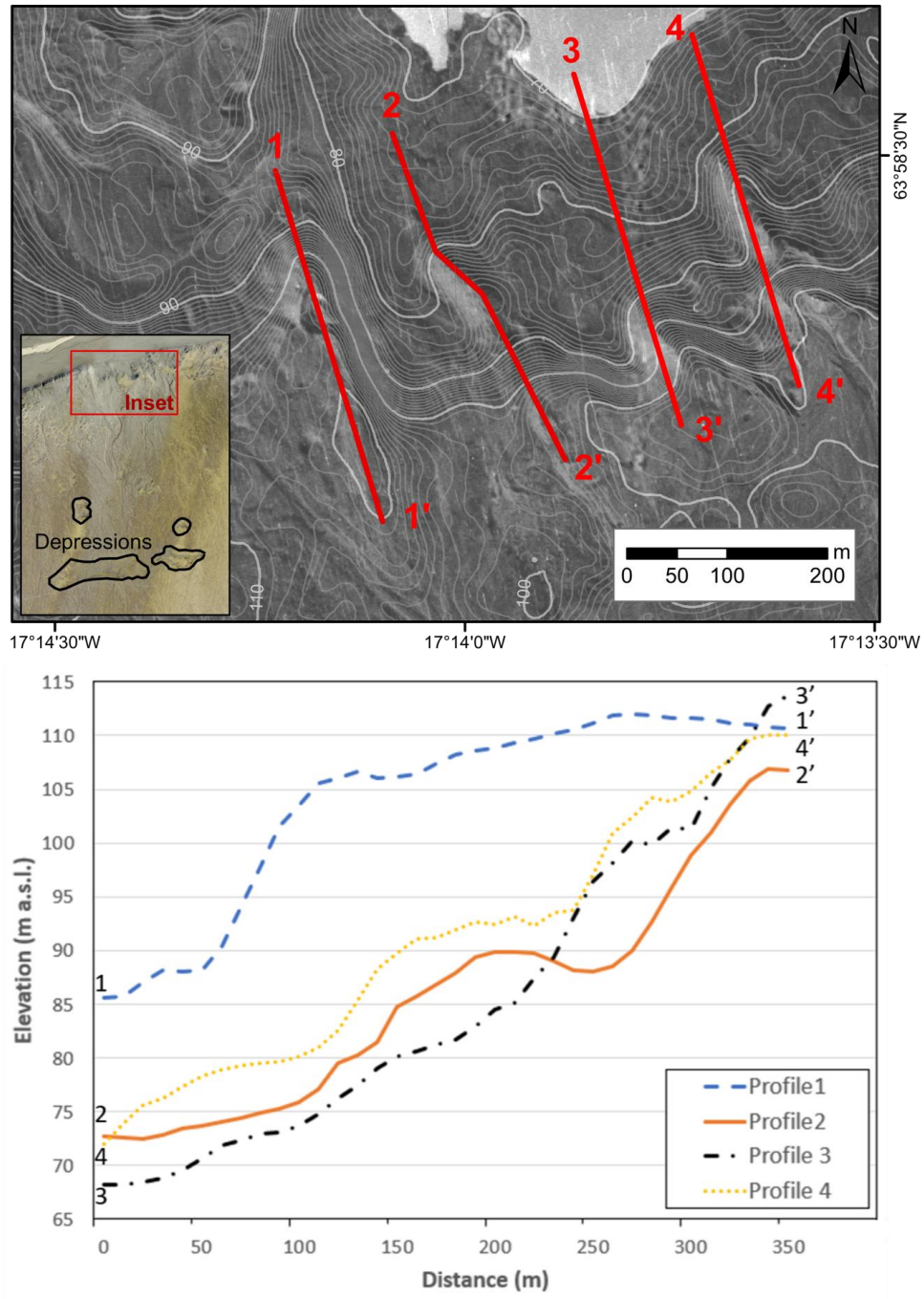

Figure 9. (a) The location 1965 drumlinised ridges exposed by the retreat of the glacier margin since 1945. (b) Elevation profile of the proglacial depression (profile 1) and drumlinised ridges (profiles 2-4).

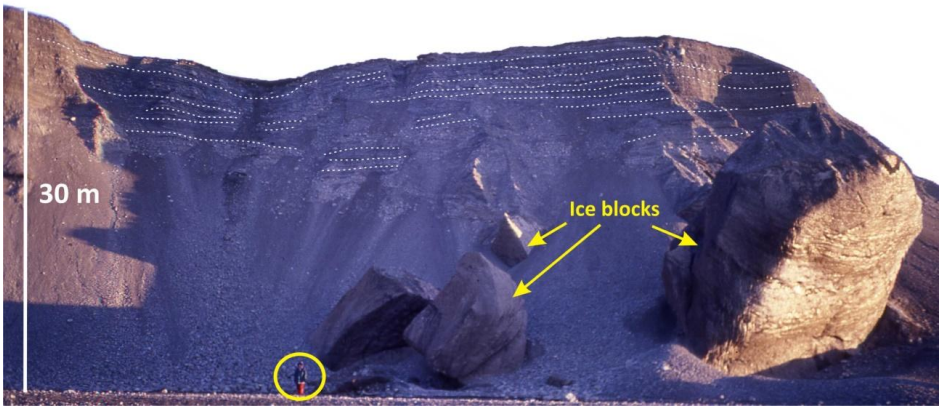

Figure 10. Photograph taken in May 1997 showing the presence of large isolated blocks of glacier ice within jökulhlaup deposits.

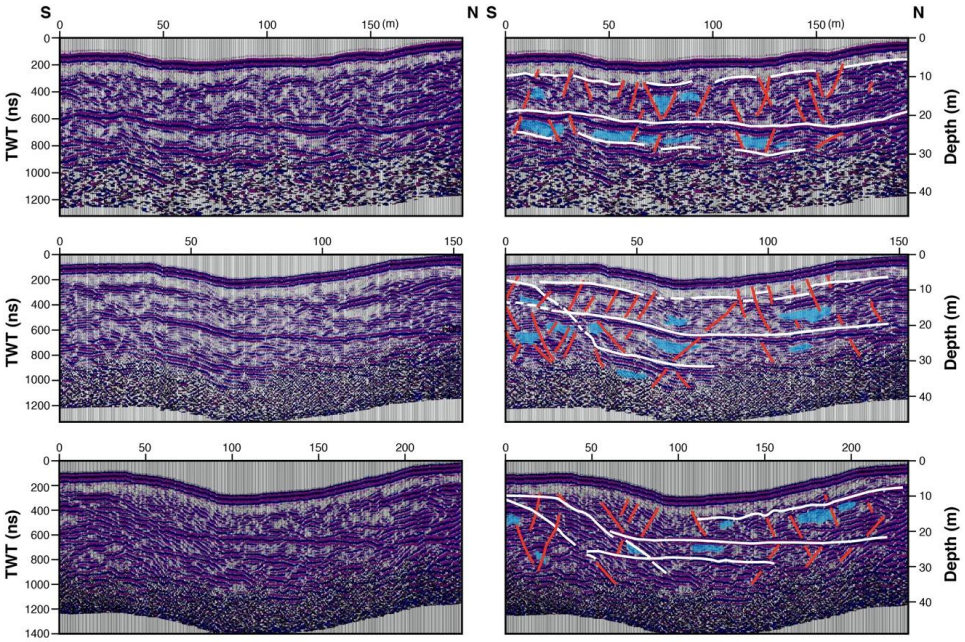

Figure 11. N-S cross-sectional radargrams through Depression 4. From top to bottom: west line, central line and east line (see Fig. 6). Main reflectors are shown in white, structural features in red, and buried ice remnants in blue. For further explanations, see main text.

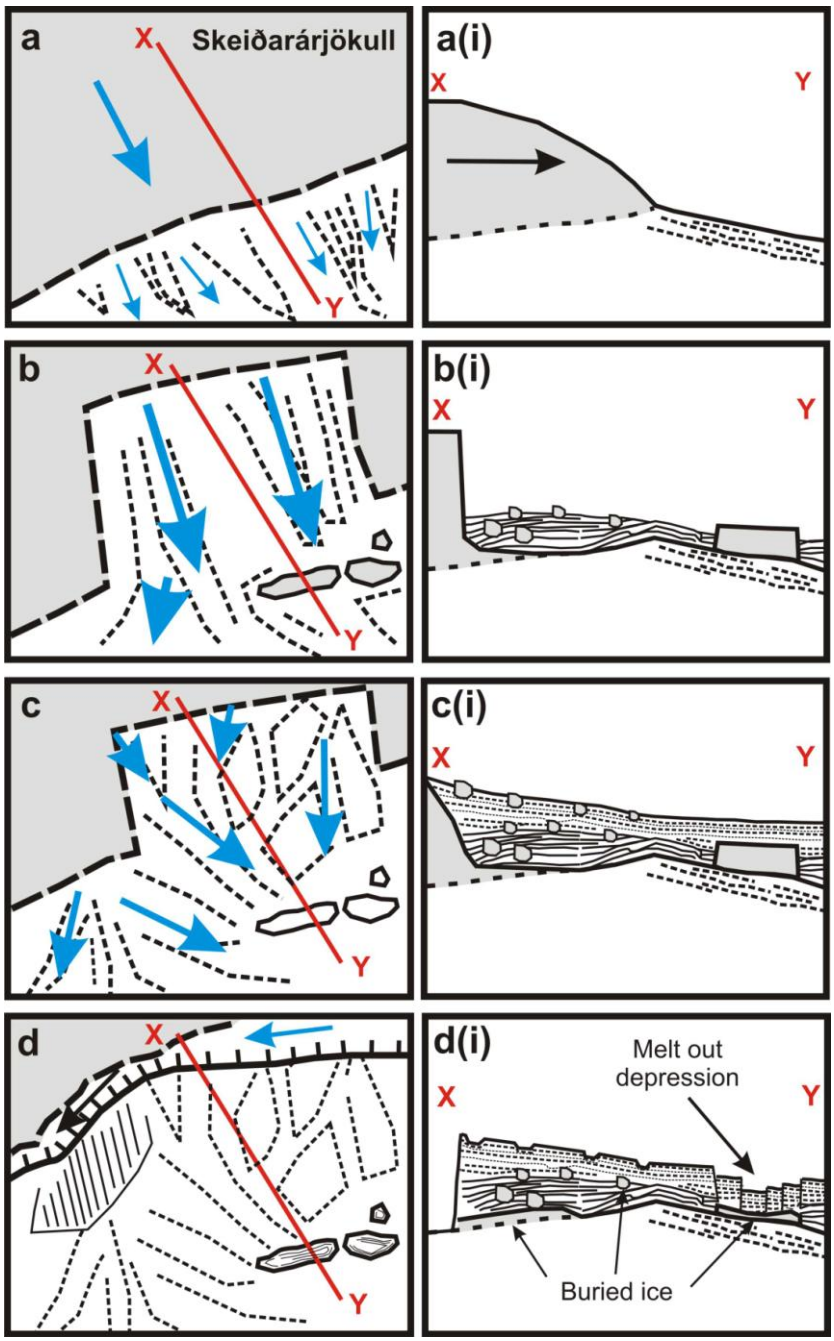

Figure 12. Model showing the proposed sequence of events responsible for the formation of the Harðaskriða melt out depressions on Skeiðarársandur. (a & ai) Initial glacier position before the 1903 jökulhlaup. (b) Erosion of ice-walled re-entrant into the snout of Skeiðarárjökull during 1903 jökulhlaup and transport of large ice blocks onto sandur. (bi) Partial burial of large 1903 jökulhlaup-transported ice blocks. (c & ci) Burial of 1903 jökulhlaup emplaced ice blocks by 1913 and 1922 jökulhlaup deposits. (d) Glacier margin position in 1945 allows meltwater to drain in a westerly direction along the ice margin abandoning the sandur surface. (di) Abandoned sandur surface showing the presence of isolated buried ice blocks (see Fig. 10) and the development of the large melt out depression.

Controls on jökulhlaup-transported buried ice melt-out at Skeiðarársandur, Iceland: implications for the evolution of ice-marginal environments

David J. Blauvelt[1], Andrew J. Russell[1*], Andrew R.G. Large[2], Fiona S. Tweed[3], John F. Hiemstra[4], Bernd Kulessa[4,5], David J.A. Evans[6] and Richard I. Waller[7]

[1] 116 East Glebe Rd, Alexandria VA, 22305, USA
[2] Newcastle University, School of Geography Politics and Sociology, NE1 7RU, UK
[3]Geography, Staffordshire University, College Road, Stoke-on-Trent, ST4 2DE, UK
[4]College of Science, Swansea University, Singleton Park, SA2 8PP, Wales, UK
[5]School of Technology, Environments and Design, University of Tasmania, Hobart, Tasmania 7001, Australia
[6]Department of Geography, Durham University, Lower Mountjoy, South Road, Durham, DH1 3LE, UK
[7]School of Geography, Geology and the Environment, Keele University, Staffordshire, ST5 5BG, UK

[*]*Corresponding Author*: andy.russell@ncl.ac.uk

Abstract

High-magnitude jökulhlaups, glacier margin position and ice-thickness have been identified as key controls on sandur evolution. Existing models however have focused primarily on observations made during short windows of time and often do not account for the subsequent modification of proglacial landsystems by repeated jökulhlaups or post-depositional modification due to melt out over decadal time-scales. Digital Elevation Models (DEMs) were used to reconstruct the development of large depressions on Skeiðarársandur, an outwash plain in southeast Iceland. These depressions measure up to 1 km in width and up to 13 m in depth and are associated with ice bodies up to 1 km in length and up to 150 m in height emplaced during a high-magnitude jökulhlaup in 1903 and subsequently buried by jökulhlaups in 1913 and 1922. The continued melting of the Harðaskriða ice bodies over a century following their emplacement, together with subsequent repeated burial, by high-magnitude jökulhlaups demonstrates that jökulhlaups may continue to serve as important controls on sandur evolution on a decadal to centennial timescale (10^1 – 10^2 years). The Harðaskriða depressions developed only following the retreat of the glacier margin after 1945, which highlights the controls of margin position on the evolution of the sandur. Margin position and thickness of the glacier profile was seen to affect not only the distribution and thickness of sediment emplaced during jökulhaups but also the rate and pattern of melt in the decades following the decoupling of the margin from the sandur. The jökulhlaup landsystem model signatures identified at this site may provide a useful analogue for interpreting landforms and strata emplaced by glacier margin fluctuations, jökulhlaups and melt out generated by retreating continental Pleistocene ice sheets.

1. Introduction

Glaciers are frequently used as indicators of climate change as they respond dynamically to changes in the climate driven components of their mass balance. Knowledge of the former extent of glaciers can be used to reconstruct palaeo-climate and to define the former position of contemporary glaciers. Distinctive assemblages of landforms and deposits at modern glacier-margins have stimulated the development of models which can be used to reconstruct ice-marginal processes. Models such as the ice-marginal landsystem (e.g. Krüger, 1994; Evans and Twigg, 2002; Evans et al., 2019) were developed from the detailed investigation of contemporary glacier margins and have been used to reconstruct palaeo-glacier margins in the Quaternary record (e.g. Evans et al., 1999). By definition, many studies of contemporary ice-marginal processes provide only a snapshot of the geomorphological and sedimentological evolution of an ice-marginal zone, as they do not take account of post-depositional landscape modification processes and are not always able to constrain the influences of previous landsystems on landscape evolution. Palimpsest landscapes comprising a number of superimposed landsystems allow landform overprinting and the potential for landsystem legacy to persist for periods of 10^1-10^2 yr^{-1} modifying subsequent landsystems (Kleman, 1992; Kleman and Stroeven, 1997; Schomacker and Kjær, 2007; Korsgaard et al., 2015).

Ice-marginal and proglacial geomorphology can be modified by a number of post-depositional processes such as aeolian deflation and deposition, fluvial erosion and deposition, periglacial and paraglacial slope processes (e.g. Ballantyne, 2002; Mountney and Russell, 2006, 2009). Melt-out of buried glacier ice has been well-documented from modern ice-margins (Price, 1969; Schomacker and Kjær, 2007; Tonkin et al., 2016) as well as being interpreted from the Quaternary record (Eyles et al., 1999; Fard, 2003). Buried ice melt-out has been invoked to account for a number of distinctive landforms such as ‘kame and kettle’ topography and ‘hummocky moraine’, both of which result from topographic inversion as buried ice melts, causing slow collapse of overlying sediment (e.g. Everest and Bradwell, 2003; Lukas et al. 2005; Bennett and Glasser, 2009).

Despite widespread acknowledgement of the importance of buried ice within former glacier margins, relatively little attention has been paid to the process of ice emplacement and how this may determine buried ice distribution and melt-out styles. Studies of buried ice melt out also tend to have focussed on the immediate ice proximal areas of proglacial outwash plains. Similarly, there are scant data on the rates of ice melting beneath thick debris mantles; exceptions include McKenzie (1969) and Schomacker (2008). Buried ice is known to have survived for decades to centuries (e.g. French and Harry, 1990; Evans and England, 1992; Everest and Bradwell, 2003; Schomacker, 2008) however there have been few detailed studies of melt-out rates over these timescales.

Processes occurring in the ice-marginal zones of glaciers and ice sheets are complex. Subaerial processes re-work glacially-deposited debris and the melt-out of buried ice leads to collapse structures and topographic inversion (Price, 1969; Bennett and Glasser, 2009). Even a thin (> 0.01 m) layer of debris covering glacier ice can provide sufficient insulation to retard ablation (e.g. Lister, 1953; Østrem, 1959; Nakawo and Young, 1981, 1982; Nicholson and Benn, 2006) and ablation can be very slow under thick debris mantles. Very slow melt rates can therefore permit the survival of buried glacier ice for long periods of time. The sustained collapse of overlying sediment due to buried ice melt-out is a significant post-depositional modification process in deglaciated landscapes with ice-cored topography (Ballantyne, 2002). The correlation between climatic parameters and melt rates of buried ice bodies is weak however, suggesting that both burial processes and topography play a key role in the rates of ice melting (Nicholson and Benn, 2006; Schomacker, 2008).

Glacier ice can also be buried '*in situ*' by supraglacial sediment deposition on top of an active or stagnant glacier margin (e.g. Russell and Knudsen, 2002; Schomacker and Kjær, 2007; Schomacker et al., 2006). During jökulhlaups, ice blocks become detached by englacial hydrofracturing, meltwater conduit collapse and ice cliff collapse (Roberts et al. 2000; Roberts, 2005). Ice-blocks up to 10^2 m in diameter are known to have been washed from glacier margins by jökulhlaups on to outwash plains (sandar) and subsequently either partially or completely buried by sandur aggradation (Tómasson, 1996; Russell and Knudsen, 1999; Roberts et al., 2000; Fay 2001, 2002a,b; Roberts, 2005;

Russell et al., 2006). Melt out of ice blocks transported by the 2010 Eyjafjallajökull eruption generated jökulhlaups is thought to have played a major role in post depositional landscape evolution (Harrison et al., 2019).

During the November 1996 jökulhlaup, ~8.3 x 10^6 m^3 of ice was removed from Skeiðarárjökull (Fay, 2002; Russell et al., 2001a, 2005). Sections of the snout of Skeiðarárjökull were fractured *in situ* into blocks up to 200 m x 400 m in size (Roberts et al., 2000). Ice blocks as large as 45 m in diameter were transported from the glacier margin (Fay, 2002; Russell et al., 2005). Some of these ice blocks were deposited as a linear jökulhlaup flow-parallel cluster, resulting in a single coalesced kettle hole approximately 130 m wide and 40 m long (Fay, 2002a; Russell and Knudsen, 1999, 2002). The largest accumulation of ice blocks was over 1 km in length with a width of up to 300 m (Fay, 2002a; Russell and Knudsen, 2002). Ice blocks transported and buried by such single high-magnitude jökulhlaups are known to persist for 10^1-10^2 yr^{-1} (e.g. Fay, 2002; Everest and Bradwell, 2003; Russell et al., 2005).

The aims of this paper are to: (1) determine the origin of a series of actively developing depressions within the proglacial area of Skeiðarársandur, southeast Iceland; (2) evaluate the mode and significance of buried ice emplacement and subsequent melt for depression development; and (3) explain their significance for sandur evolution. To fulfil these aims we quantify the decadal evolution of the depressions and characterise their sub-surface sedimentary architecture and relate to the wider record of jökulhlaups on Skeiðarársandur.

2. Study area

Harðaskriða is located 3.6 km from the current margin of Skeiðarárjökull within the central zone of Skeiðarársandur, a 1300 km^2 outwash plain fed by Skeiðarárjökull in southeast Iceland (Fig. 1). Skeiðarárjökull is a temperate, surge-type, outlet glacier of Vatnajökull ice cap with a 23 km wide piedmont snout (Björnsson, 1998). Skeiðarársandur has a strong maritime climate, where the maximum depth of winter freezing is only of the order of centimetres (Douglas and Harrison, 1996; Thórhallsdóttir, 1996) making the presence of permafrost impossible. Skeiðarárjökull and Skeiðarársandur have been subject to repeated high-magnitude jökulhlaups generated

both by subglacial volcanic eruptions and the drainage of subglacial and ice-marginal lakes (Thórarinsson et al., 1974; Björnsson, 1992; 1997). The Harðaskriða area of Skeiðarársandur last experienced meltwater flow during the 1922 jökulhlaup, after which glacier margin recession created incised proglacial channels at the Háöldukvísl and Gígjukvísl; subsequently a proglacial trench developed, allowing all subsequent meltwater to be routed westward (Galon, 1973) (Figs 2, 3 and 4; Table 1). The Harðaskriða area is now part of an elevated sandur surface which was unaffected by the large November 1996 jökulhlaup (Snorrason et al., 2002). The Harðaskriða area was however inundated by eleven large jökulhlaups between 1861 and 1938 when Skeiðarárjökull was at its Little Ice Age maximum extent (Thórarinsson, 1974; Björnsson, 1997; Glaciorisk, 2005) (Table 1). These high frequency high-magnitude jökulhlaups resulted in significant aggradation on the eastern and central proximal areas of Skeiðarársandur with accumulated elevations of up to ~125 m above sea level (a.s.l.) compared with elevations of below 90 m a.s.l. for equivalent-aged sandur surfaces to the west (Blauvelt, 2013). Historic accounts indicate a number of large jökulhlaups associated with glacier margin disruption and ice block release in the Harðaskriða area between 1861 and 1938 (Thórarinsson, 1974; Glaciorisk, 2005) (Fig. 2; Table 1). The 1897 and 1903 jökulhlaups can also be specifically linked to the Harðaskriða area (Thórarinsson, 1974). A 1 km long, 150 m high piece of the glacier margin was washed out on to the sandur during the 1903 jökulhlaup possibly associated with detachment along a large, ice flow transverse, hydrofracture generating a large 'embayment' (Roberts et al., 2000, Roberts, 2005).

The Harðaskriða comprises outwash surfaces characterised by a well-developed channel and bar pattern supporting numerous ice block obstacle marks up to 10 m in diameter (Fig. 4). These outwash surfaces are however disrupted by four large depressions the largest of which has maximum dimensions of 604 x 108 m and a depth of ~13 m (Figs 5, 6 and 7). Although there are historic accounts of high magnitude jökulhlaup processes and immediate impacts at Harðaskriða there has been no detailed examination of the development of the resulting landforms and deposits.

3. Methods

3.1. Topographic survey and DEM generation

DEMs for 1968 and 2007 were produced using stereophotogrammetry on digital aerial imagery. Vertical aerial photographs collected for DEM creation were obtained from the National Land Survey of Iceland, Landmælingar Íslands. Images were scanned by Landmælingar Íslands with an Eversmart Jazz+ Scitex scanner, at a resolution of 2000 dpi and delivered as tagged image format (tif) files. Camera calibration documentation and flight lines drawn on 1:100,000 topographic maps were provided for all photographs taken after 1954. Photographs from 1945, taken by the U.S. Air Force, were purchased from Landmælingar Íslands, who provided known flight elevations and camera focal lengths. Colour digital images acquired in 2007 by NERC ARSF (IPY07/13) were also used in this study. Digital elevation models (20 m resolution) and photo mosaics were purchased from Loftmyndir HF for 1997 and 2003 datasets.

A differential GPS (dGPS) survey was conducted in 2007 between the glacier margin and Iceland's ring road (Fig. 1). Transects of four of the Harðaskriða depressions were surveyed (Fig. 7). Additionally, large-scale, persistent features across Skeiðarársandur including kettle holes, boulders and ridges that were visible on all historical aerial photographs were utilised for ground control points (GCPs). Survey points were collected using a Thales ProMark III unit, corrected to Icelandic Roads Authority survey sites.

BAE's *SocetSet* 5.5 (*Ngate*) software was used to generate the DEMs. Triangulation (interior and exterior orientation) was accomplished for all photosets. Once an internal coordinate system was established within the photographs, the control points measured in the field could be used to relate the image to the ground (absolute orientation). The ISN93 coordinates of the GCPs were used to identify points on the images. Once the x, y and z values of GCPs were identified on both (or more) images, SocetSet then performed point measurement automatically, using digital image matching (Baily et al., 2003).

Systematic errors and random errors were evaluated by comparing apparent elevation differences between the DEMs and ground control points measured with the dGPS. The location of the check points and ground control points are summarised in Table 2. Systematic errors are given as root-mean-square error (RMS) measures and the 95th percentile limit is given for random errors a technique commonly used in DEM

quality analysis (Schiefer and Gilbert, 2007). All units are in metres above sea level (m a.s.l.). Following manual clean up ('post pushing') of the study area, all check points fell under 1 m. Due to the comparatively small scale and dynamic terrain of the study area, no additional registration was applied.

Elevation differences were used to provide an approximate estimate of the volumetric loss for four of the major Harðaskriða depressions (Fig. 8) and the elevation loss of the adjoining glacier (Fig. 3). Whilst the poor quality of the 1945 images precluded the production of a 1945 DEM surface to quantify subsidence over the last sixty-two years, an attempt was made to provide as close an approximation as possible. Comparing surfaces constructed from two subsequent time periods (before and after) is often utilised as a cost-effective method to quickly quantify large-scale volumetric changes due to melt out, subsidence, flooding, human interference or other causes (Schiefer and Gilbert, 2007). By removing elevation points that lay within the depressions on the 2007 imagery and generating a triangular irregular network, or TIN, across the missing data points, a 1945 DEM surface could be simulated.

Although the 2018 ArcticDEM was used to provide a general comparison of glacier recession and proglacial fluvial system incision (Porter et al., 2018) (Fig. 3), offsets between the 2018 ArcticDEM and photogrammetrically-derived DEMs, as well as the difficulty in removing bias in this type of terrain, precluded its use for quantification of rates of lowering of the Harðaskriða depressions.

3.2. Ground Penetrating Radar survey

Ground-Penetrating Radar (GPR) profiles were collected from depression 4 (Figs. 5 and 6) using the MALÅ ProEx system with a 13 m long (distance Tx – Rx = 6 m), low-frequency (30 MHz) Rough Terrain Antenna (RTA). GPR-lines (all corrected for topography), both outside and across the depression, were collected in 2013 (i.e. 6 years after the GPS surveys). The objectives were to gain insight in the subsurface sediment architecture, deformation or collapse structures, and to investigate the possibility of the presence of remnants of buried ice.

234 The basic principles of GPR surveying are that electromagnetic waves travel at
235 different velocities dependent on the electrical and magnetic properties of the earth
236 materials, and that incident waves are refracted or reflected on interfaces between
237 materials with contrasting dielectric permittivities. The nature of the signal that is
238 returned to the surface (i.e. its intensity, polarity and propagation velocity) can then be
239 analysed using processing software (ReflexW; cf. Sandmeier, 2012) which allows the
240 reconstruction and modelling of the architecture of the subsurface.
241
242 Figure 6 shows the survey plan with a single E-W profile capturing the length of the
243 depression, and three shorter N-S profiles across the depression. Data were collected as
244 a continuous array with additional transects surveyed to connect the long and cross
245 profiles (the radar profiles outside the depression were used for reference only).
246 Assuming an average propagation velocity of c. 0.07 m ns^{-1} (cf. Cassidy et al., 2003),
247 depth penetration in the sandur sediments was c. 30 m. This is a value typical for
248 velocities in wet, sandy to gravelly materials and may be an underestimation in case of
249 significant quantities of buried ice present in the subsurface.
250
251 **4. Results**

252 *4.1. Morphology of Harðaskriða depressions*
253 All depression measurements are based on their 2007 dimensions. Depression 1 is
254 approximately oval in shape and ranges in width from 164 m (north-south) to 108 m
255 (east-west) (Figs. 7 and 8). The northern and southern rims are characterised by
256 outwardly dipping arcuate and concentric normal faults. Along the southern rim, normal
257 faulting has resulted in the rotation of two large blocks (up to 60 m in length and 15 m
258 wide). The base of this depression is characterised by sagging, uneven terrain, and is
259 divided into two portions of unequal depth. The northernmost part of the depression
260 measured 10 ± 1.64 m in depth, while the southern part of the depression measured 12
261 ± 1.64 m in depth. Recent satellite imagery (DigitalGlobe, 2016) indicates further
262 depression widening attributed to continued melt-out.
263
264 Depression 2 is approximately circular in shape and ranges in width from 89 m (north-
265 south) to 104 m (east-west) and 13 ± 1.64 m deep (Fig. 7). The northern portion contains

concentric normal faults and two extensional faults that trend north-south (40 m and 50 m in length). Along the southernmost rim of this depression, normal faulting has resulted in the rotation of two blocks, the largest 60 m long and 13 m wide.

Depression 3 possesses an irregular, elongate morphology that trends east-west. The depression ranges in width from 342 m (east-west) and 116 m (north-south) and is 12 ±1.64 m deep (Fig. 7). The margin, while not circular in shape, contains numerous normal faults and recesses that surround the depression. The southern margin is marked by several rotated blocks and steep walls. The margin appears to slump in rotational blocks towards the centre, resulting in 'steps' that dip outwards from the depression. A dirt road observed on the 1945 aerial photographs remains visible on the 2007 aerial photographs. Its original surface, although now undulating, remains discernible as it traverses depression 3, suggesting that subsidence has been gradual in nature.

Depression 4, the widest of the depressions, is similar in shape to depression 3, possessing an irregular shape and trending east-west (Fig. 7). The depression ranges in width from 604 m (east-west) to 148 m (north-south). Similar to the other depressions, the walls are steepest along the southern margin, and the margin is characterised by horst and graben blocks and concentric extensional fractures (Figs 5a, b and 6). Numerous recesses have developed along the northern, eastern and western margin and possess a relatively gentle, stepped slope, compared to those along the steeper southern margin.

Directly 800 m north of these depressions and visible on the 1965 photographs are three drumlinised, elongate ridges that lead to the elevated sandur (Fig. 9a). These ridges trend north-south and, from east to west, are 176 m, 79 m and 151 m in length and 30, 37, and 34 ±1.64 m in height respectively. Elevation profiles were extracted of the area immediately adjacent to these ridges (Profile 1) and the prominent ridges (Profiles 2-4) that rose towards the elevated sandur surface (Fig. 9b). While varying in height, the ridges all span an average of 33 m from the base of the depression to the sandur. Later photo series (1965 - 1997) indicate that these ridges were largely removed by the fluvial erosion of shifting proglacial drainage channels and by the November 1996 jökulhlaup. The sedimentary section revealed by erosion during the November 1996 jökulhlaup shows a number of large ice blocks up to 30 m in diameter

299 contained within stratified coarse grained jökulhlaup deposits (Fig. 10). Vertical lowering
300 of 12 ± 1.64 m over the 62 years since 1947 was calculated from the height difference
301 between the 1945 and 2007 sandur surfaces, representing an average rate of 19.4 ± 2.6
302 cm of lowering per year (Figs 7 and 8).
303
304
305 *4.2. Sub-surface structure of Harðaskriða depressions*
306 Using a relatively low radar frequency, and assuming that the subsurface sediment
307 mostly comprises sand and small to medium gravel (with no outsized boulders to cause
308 'disruptive' hyperbolae) it may be expected that the signal-to-noise ratio is adequate for
309 resolving metre-scale sandur sedimentology down to a depth of c. 30 m.
310
311 There are two main sub horizontal reflectors in the GPR cross-profiles: one at an
312 estimated depth of 6 m and one at c. 20 m below the surface (white solid lines in Fig.
313 11). A third discontinuous reflector is visible just above the noise which starts at 30 m.
314 As it is right at the detection limit, interpreting this reflector will not be attempted
315 below. The 6 m reflector tends to mirror the surface topography and the 20 m reflector
316 is generally less undulating and continuous across the depression. All three profiles also
317 show shorter sub horizontal reflectors that are thought to represent prominent bedding
318 surfaces. Northward dipping reflectors, a single one in the central cross-profile and two
319 parallel features in the east cross-profile (white dashed lines in Fig. 11), appear to
320 extend down from the 6 m reflector, cross and deflect the 20 m reflector and then
321 connect in a stepped fashion with the reflector at 30 m depth.
322
323 In all three cross-profiles, high-angle linear or curvilinear structures (indicated in red in
324 Fig. 11) intersect, or terminate onto the aforementioned reflectors. They are interpreted
325 as joints or normal faults. Particularly near the margins of the depression, they can be
326 seen to disrupt or offset reflectors. Most structures are outward dipping, but there are
327 also less common, apparently younger, inward-dipping faults. All such fractures seem to
328 have developed to accommodate the flexure in the depression and are attributed to
329 progressive subsidence due to gradual melt-out of buried ice. At the surface around the
330 periphery of the depression, the structures present as stepped ring-structures (Figs 5a, b
331 and 6), which are very similar to the 'concentric' ring-fractures described for collapsing

calderas and other ice-melt phenomena by Branney (1995) and Branney and Gilbert (1995).

Whilst confident about the interpretation of the joint and fault structures, the characterisation of the subsurface materials from the radargrams is more challenging, particularly without the possibility of direct ground truthing. There are good exposures near the Gígjukvísl, 5 km kilometres to the west (see Russell et al., 2001), but they are developed into proglacial surfaces which lack the 'pitted' surfaces diagnostic of jökulhlaup deposits. Fortuitously, the 1996 jökulhlaup cut a 30 m high section into sandur sediments 1.3 km north of the Harðaskriða depressions (Fig. 10) so there is at least some information available on textural heterogeneity of the sandur sediments and the distribution and dimensions of buried ice.

Apart from the aforementioned reflectors, the most conspicuous zones in the GPR profiles are those that seem to be devoid of energy returns. Such zones (indicated in blue in Fig. 11), can be observed mostly away from the centre of the depression and below the 6 m reflector, but there are also a few at greater depths. Assuming that these features are not processing artefacts, they must represent homogeneous materials with a low relative dielectric permittivity ε_r. Where a reflector - mostly that at 6 m depth, forms the upper surface of such zones - the polarity is opposite to that of the air wave (phase change of 180°) which would suggest that the overlying sediment has a relatively high ε_r. Since ice has an ε_r of 3-4 (Brandt et al., 2007) and overlying materials, which can logically assumed to be relatively (wet) jökulhlaup sediments may be expected to have an ε_r in the order of 10-30 - and drawing analogies with nearby exposures - the zones are tentatively interpreted as remnants of buried ice.

The observation that the interpreted blocks of buried ice are ubiquitous at the north and south sides of the cross-profiles, but less common in the central parts is compatible with the idea that subsidence has been greatest in the centre of the depression. The inward dipping reflector on the south side in the central and east cross-profiles (Fig. 11, middle and lower panels) may delineate the upper surface of relatively intact buried ice. The deeper parts of this surface may have served as a slip-plane extending into one of the deeper identified normal faults.

Although its strength is variable, it is clear that the reflector at 20 m is more continuous than the 6 m reflector. Interestingly, its polarity is the same as the air wave which suggests that it represents a contact between a lower permittivity (above) to a higher permittivity material below. The fact that it does not show significant offsets where intersected by high angle faults is taken as evidence that the reflector is not a sedimentary surface. Instead it is proposed that it represents the local groundwater table (wet/saturated sand: ε_r = 10-30; Brandt et al., 2007), although it is noted that other studies on the sandur (cf. Cassidy et al., 2003; Burke et al., 2010) have found the groundwater table to be significantly shallower.

5. Discussion

The average rate of 19.4 ± 2.6 cm of lowering per year between 1945 and 2007 determined from this study is an order of magnitude lower than the 1.88 ma^{-1} reported for immediate post jökulhlaup ice-melt out within the Gígjökull basin between 2010 and 2016 (Harrison et al., 2019). Higher buried ice melt rate at Gígjökull can be attributed to the simultaneous deposition of smaller ice fragments with jökulhlaup deposits rather than the melt of large isolated blocks.

Combined DEMs, dGPS measurements and GPR surveys reveal that the Harðaskriða depressions experienced the greatest vertical loss within their centres, due to slump in rotational blocks towards the centres, characteristic of 'horst and graben' structures. This process has resulted in 'steps' that have developed along the side of each of the features into the centre. The concentric rings of normal faulting, horst and graben and normal and extensional faults described at the Harðaskriða depressions 1 - 4 are consistent with observations made at other field sites involving the melt-out of smaller bodies of ice that have been transported by lahars and jökulhlaups (Maizels, 1992; Branney, 1995; Branney and Gilbert, 1995; Olszewski and Weckwerth, 1998). Such features have also been used as indirect evidence of buried bodies of ice at other locations (e.g. Boulton, 1972; Hambrey, 1984; Krüger and Kjær, 2000; Kjær and Krüger, 2001; Dickson and Head, 2006).

As the ice bodies buried at Harðaskriða began to melt, the loss of volume and drainage of subsurface water may have resulted in the subsidence of the overlying sediment (McDonald and Shilts, 1975, Maizels, 1992). This sort of subsidence can produce outwardly-dipping arcuate hairline fractures that can elongate into a ring, causing the subsidence of a coherent block of sediment as seen in depressions 1 and 2 (Branney, 1995; Branney and Gilbert, 1995). These overhanging scarps become unstable and collapse along new arcuate faults, resulting in the development of extensional crevasses that may continue to expand along small vertical and normal faults causing some walls to collapse, resulting in keystone graben (Sanford, 1959; McDonald and Shilts, 1975). Continued collapse leads to intersection of arcuate fractures resulting in blocks that tilt and subside into the pit, while mass movements and slumping may accelerate the melting rate of a buried ice body (Johnson, 1992).

At larger collapse pits, such as depressions 3 and 4, irregular topographic margins with embayments also developed (Branney, 1995; Branney and Gilbert, 1995). These features, combined with the steep walls of the depressions and undisturbed nature of the surrounding outwash plain are consistent with bodies of ice that have been surrounded by sediment (Maizels, 1991). The gentle slopes of the northern walls and the steeper slopes of the southern walls are consistent with the development of a 'normal' kettle hole (Maizels, 1992; Olszewski and Weckwerth, 1998), as proglacial outwash would have resulted in the development of gravitational flow on the northern side, while block displacement and subsidence developed on the southern side following melt out.

The existence of large bodies of buried ice greater than 30 m in thickness on Skeiðarársandur have been identified and documented using resistivity studies (Everest and Bradwell, 2003) and confirmed at exposures (Klimek, 1972; Bogacki, 1973; Churski, 1973; Jewtuchowicz, 1973; Russell and Knudsen, 1999; Molewski, 2000). Ridges and detached slabs of dead ice in the eastern and western parts of Skeiðarársandur have also been identified and described and are attributed to deposition by the retreating ice margin (Galon, 1973; Jewtuchowicz, 1973; Wojcik, 1973). Unlike ice-cored ridges, plains or moraines elsewhere on the sandur, the geometry, orientation and size of the bodies of ice that resulted in the Harðaskriða depressions are consistent with other descriptions

of isolated blocks of ice emplaced during high-magnitude jökulhlaups (Maizels, 1992; Maizels and Russell, 1992; Branney, 1995; Branney and Gilbert, 1995; Harrison et al., 2019).

A topographic map published in 1904 (Danish Staff Map) depicts several elongated, east-west trending ridges extending across central Skeiðarársandur that appear to be continuations of the 19th century moraines that persist today in the western region of the sandur (Fig. 2). By 1945, aerial photographs reveal that these moraines are no longer visible on the central sandur, and reportedly buried or removed by jökulhlaups (Galon, 1973; Jewtuchowicz, 1973; Wojcik, 1973; Wisniewski, 1997; Knudsen et al., 2001). While some of the depressions and landforms correspond to the approximate positions of the 19th century moraines, largest Harðaskriða depressions are developed approximately 400 m south of this limit, suggesting that they are not related to buried ice bodies contained within the pre-existing 19th century moraines (Fig. 4).

According to Thórarinsson (1974), a large piece of the glacier margin detached during the 1903 jökulhlaup approximately 1 km in length and up to 150 m in height; it was also documented that a fracture of similar size and length developed up glacier located where the floodwaters burst from the glacier margin. During this same flood, house-size ice blocks were emplaced on the sandur and the flood waters *"dug into the sand a deep, 'many persons high', steep-sided channel"* (Thórarinsson, 1974). Ice blocks, regardless of their original shapes, result in circular depressions, such as Depression 2, however dumbbell-shaped pits may form where circular collapse pits from two closely adjacent buried blocks of ice overlap, such as Depression 1 (Branney and Gilbert, 1995). The geometry and orientation of the largest elongated depressions (Depressions 3 and 4) may therefore correspond to the 1 km wide portion of the margin that was detached during the 1903 jökulhlaup described by Thórarinsson (1974). In the absence of evidence of a disrupted glacier snout or ice blocks on the topographic map published in 1904, it is presumed that the field survey that formed the basis for this map pre-dated the 1903 jökulhlaup.

Thórarinsson (1974) stated that jökulhlaups in 1913 and 1922 inundated the central sandur with floodwaters and sediment. During later periods of glacier stillstand,

meltwater runoff was concentrated in the central part of the sandur, resulting in the formation of wide outwash channels (Galon, 1973). In common with glacier termini elsewhere in Iceland, the margin of Skeiðarárjökull experienced climate-forced recession from their Little Ice Age maximum extents (Thórarinsson, 1943; Sigurðsson, 2005). Recession of Skeiðarárjökull resulted in meltwater drainage from the glacier margin at progressively lower elevations leading to sandur incision (Galon, 1973). As such, subsequent jökulhlaups in 1934 and 1938 did not affect Harðaskriða, as the floodwaters were routed through other channels such as the Háöldukvísl, 1.5 km to the east (Fig. 1). Aerial photographs taken in 1945 show the formation of a proglacial trench and meltwater flow in a westerly direction towards the Gígjukvísl (Figs 1 and 3).

While the jökulhlaup-transported ice bodies may have been emplaced as early as 1897 and as late as 1922, any melting that occurred during that time is not captured due to a lack of available imagery. The rate of melt of a buried ice body may be affected by a variety of factors, including the amount of sediment within the ice, depth of burial and geothermal heat flux (Nakawo and Young, 1981; Nicholson and Benn, 2006), making it difficult to estimate the initial size of the buried ice body. Ice blocks emplaced and completely buried by the 1903 jökulhlaup would have been further insulated by additional sediment aggradation during the 1913 and 1922 jökulhlaups (Thórarinsson, 1974). That glacier ice buried by November 1996 jökulhlaup deposits has survived for 23 years illustrates the feasibility of buried ice preservation between the 1903 and 1913 jökulhlaups.

It is noticeable that the Harðaskriða depressions are not visible on the 1945 photographs, suggesting that the buried ice has not exhibited high melting rates. It is not until the 1965 photographs, following the retreat of the central lobe of the glacier margin and the subsequent formation of the proglacial trench post-1945, that subsidence is visible. This observation and the sequence of events presented in this study suggests that the melt rate of the buried ice bodies may have been accelerated as a result of the retreat and decoupling of the glacier margin and the associated rise in ambient temperatures and lowering of local groundwater table. This demonstrates the control that glacier margin stability has on post-depositional modification processes, as buried ice bodies may be capable of persisting for much longer periods at a stable or

advancing margin, characterised by proglacial aggradation, rather than at a retreating or stagnating margin characterised by proglacial incision.

According to Björnsson et al. (1999) profiles of the surface of Skeiðarárjökull in 1904 were ~100 m higher than in 1945, which would have resulted in a steeper ice surface gradient and therefore increased hydraulic gradient during high-magnitude jökulhlaups (Roberts et al., 2000, 2001; Roberts, 2005). This would have increased the capacity of jökulhlaups to excavate and transport sediment. The elongate, drumlinised ridges observed on the 1965 images on the down-glacier side of the proglacial trench generated by the retreat of the glacier margin are interpreted as conduit-fill eskers created by sediment deposition as meltwater ascended by at least 30 m over a distance of ~200 m from the proglacial depression to innundate Harðaskriða (Fig. 9).

The landform and sediment assemblage at Harðaskriða reflect the role of multiple jökulhlaups just after the Little Ice Age maximum extent of Skeiðarárjökull. Initial glacier position before the 1903 jökulhlaup is associated with unconfined proglacial drainage (Russell and Knudsen, 1999, 2002; Russell et al., 2005, 2006) (Figures 11a and 11a(i)). Erosion of a 1 km wide ice-walled re-entrant into the snout of Skeiðarárjökull by the 1903 jökulhlaup liberated large ice blocks which were transported by the jökulhlaup onto the sandur for distances of up to 0.5 – 0.8 km (Fig. 11b). The largest 1903 jökulhlaup-transported ice blocks were probably partially buried as was the case with the largest ice blocks during the 1996 jökulhlaup (Russell and Knudsen, 1999; Fay, 2001, 2002a) (Fig. 11b(i)). Sediment aggradation during the 1913 and 1922 jökulhlaups buried the ice blocks emplaced in 1903 (Fig. 11c(i)). It is likely that the ice blocks had reduced in size by ablation between 1903 and 1913. Continued glacier recession resulted in the abandonment of the Harðaskriða sandur surface between 1933 and 1945 (Fig. 11d). Melt of buried ice results in depressions which have deepened and expanded in surface area between 1968 and 2007 (Fig. 11d(i)). The GPR survey undertaken in 2013 of the largest depression indicates the presence of buried glacier ice which together with the recent satellite observations of depression widening, suggests that the melt out processes are ongoing.

6. Conclusions

Continued melting of the Harðaskriða ice bodies nearly a century following their emplacement and burial demonstrates that jökulhlaups may continue to be an important control on sandur evolution over decadal to centennial timescales (10^1 – 10^2 years). Buried ice meltout associated with the development of the Harðaskriða depressions was enhanced by the lowering of the groundwater table following abandonment of the sandur brought about by glacier margin recession during the second half of the twentieth century. The occurrence of three high magnitude jökulhlaups within an 18-year period following the Little Ice Age glacier maximum extent resulted in significant sandur aggradation and ice block burial, assisting the long term preservation of ice. By contrast, a similar succession of jökulhlaups during a period of glacier margin recession will reduce the potential for jökulhlaup-transported ice blocks to be buried as repeated 'decoupling' of the glacier margin from the its sandur reduces the potential for stacking of jökulhlaup deposits.

Our model of the jökulhlaup landsystem at Harðaskriða and the ability to identify them at other warm-based sediment-rich glaciers that may be subject to some or all the large-scale processes including margin fluctuations, jökulhlaup dynamics and secondary modification may provide a useful analogue for interpreting landforms and strata emplaced by margin fluctuations, jökulhlaups and melt out generated by the retreating continental Pleistocene ice sheets.

Acknowledgements

AJR, DJB, ARGL and FST acknowledge the Earthwatch Institute for fieldwork funding. AJR and ARGL thank the NERC ARSF (IPY07/13) for acquisition of 2007 aerial photography and AJR's fieldwork in 1996-97 was funded by (GR3/10960). We thank Ragnar Frank Kristjánsson and Regína Hreinsdóttir for valuable support for jökulhlaup-related research within Skaftafell/Vatnajökull National Park. We thank Marek Ewertowski for acquiring the 2013 GPS data and Chris Williams for conducting the topographic corrections of the GPR data. We thank Anders Schomacker and an anonymous reviewer for their constructive comments on this paper. Achim Belich is thanked for editorial oversight. Thanks to Salvatore G. Candela for assistance with digital elevation models.

560 **References**

561

562 Ballantyne, C.K., 2002. Paraglacial Geomorphology. Quaternary Science Reviews 21, 18-
563 19, 1935-2017.
564 Baily, B., Collier, P., Farres, P., Inkpen, R. and Pearson, A. 2003. Comparative assessment
565 of analytical and digital photogrammetric methods in the construction of DEMS
566 and geomorphological forms, Earth Surface Processes and Landforms 28, 307-
567 320.
568 Bennett, M.R., Glasser, N.F. 2009. Glacial geology: ice sheets and landforms. Second
569 edition. Oxford, Wiley-Blackwell. 385pp.
570 Brandt, O., Langley, K., Kohler, J., Hamran, S.E., 2007. Detection of buried ice and
571 sediment layers in permafrost using multi-frequency Ground Penetrating Radar:
572 a case examination on Svalbard. Remote Sensing in the Environment 111, 212-
573 227.
574 Björnsson, H., 1974 Explanation of jökulhlaups from Grímsvötn, Vatnajökull, Iceland,
575 Jökull 24, 1-26.
576 Björnsson, H., 1992 Jökulhlaups in Iceland: prediction, characteristics and simulation.
577 Annals of Glaciology 16, 95-106.
578 Björnsson, H., 1997. Grímsvatnahlaup Fyrr og Nu. In Haraldsson, H. (ed.) Vatnajökull:
579 Gos og hlaup 1996. Reykjavík: Vegagerðin, 61-77.
580 Björnsson, H., 1998. Hydrological characteristics of the drainage system beneath a
581 surging glacier. Nature 395, 771-774.
582 Björnsson, H., Pálsson, F., Magnússon, E., 1999. Skeiðarárjökull: Landslag og
583 rennslisleiður vatns undir sporði. Raunvísindastofnun Háslólans. RH-11-1999.
584 Blauvelt, D., 2013. Evolution of a Sandur: sixty years of change, Skeiðarársandur, Iceland.
585 PhD Thesis, Newcastle University, 301pp.
586 Bogacki, M., 1973 Geomorphological and geological analysis of the proglacial area of
587 Skeiðarárjökull. Central, western and eastern sections, Geographia Polonica 26,
588 57-88.
589 Boulton, G.S., 1972. Modern Arctic glaciers as depositional models for former ice sheets.
590 Journal of the Geological Society of London 128, 361-393.

591 Branney, M.J., 1995. Downsag and extension at calderas: new perspectives on collapse
592 geometries from ice-melt, mining and volcanic subsidence. Bulletin of
593 Volcanology 57, 303-318.
594 Branney, M.J., Gilbert, J.S. 1995. Ice-melt collapse pits and associated features in the
595 1991 lahar deposits of Volcan Hudson, Chile: criteria to distinguish eruption-
596 induced glacier melt. Bulletin of Volcanology 57, 293-302.
597 Burke, M.J., Woodward, J., Russell, A.J., Fleisher, P.J., Bailey, P.K. 2010. The sedimentary
598 architecture of outburst flood eskers: a comparison of ground-penetrating radar
599 from Bering Glacier, Alaska and Skeiðarárjökull, Iceland. GSA Bulletin 122, 9-10,
600 1637-1645.
601 Cassidy, N.J., Russell, A.J., Marren, P.M., Fay, H., Rushmer, E.L., Van Dijk, T.A.G.P.,
602 Knudsen Ó., 2003. GPR-derived architecture of November 1996 jökulhlaup
603 deposits, Skeiðarársandur, Iceland. in: Bristow, C.S., Jol, H.M., (Eds.) Ground
604 Penetrating Radar in Sedimentation, Spec. Publ. Geol. Soc. 211, pp. 153-166.
605 Churski, Z., 1973. Hydrographic features of the proglacial area of Skeiðarárjökull.
606 Geographia Polonica 26, 209-254.
607 Dickson, J., Head, J.W., 2006. Evidence for an Hesperian-aged South circum-Polar lake
608 margin environment on Mars. Planetary and Space Science 54, 251-272.
609 Douglas, T.D., Harrison, S. 1996. Turf-banked terraces in Öræfi, southeast Iceland:
610 morphology, rates of movement, and environmental controls. Arctic and Alpine
611 Research 28, 228-236.
612 Evans, D.J.A., England, J., 1992. Geomorphological evidence of Holocene climate change
613 from northwest Ellesmere Island, Canadian High Arctic. Holocene 2, 148-158.
614 Evans, D.J.A., Twigg, D.R., 2002. The active temperate glacial landsystem: A model based
615 on Breiðamerkurjökull and Fjallsjökull, Iceland. Quaternary Science Reviews 21,
616 20-22, 2143-2177.
617 Evans, D.J.A., Lemmen, D.S., Rea, B.R., 1999. Glacial landsystems of the southwest
618 Laurentide Ice Sheet: modern Icelandic analogues. Geomorphology 14, 673-691.
619 Evans D.J.A., Ewertowski, M.W. & Orton, C. 2019. The glacial landsystem of
620 Hoffellsjökull, SE Iceland: contrasting geomorphological signatures of active
621 temperate glacier recession driven by ice lobe and bed morphology. Geografiska
622 Annaler 101A, 249–276.

623 Everest, J., Bradwell, T., 2003. Buried glacier ice in southern Iceland and its wider
624 significance, Geomorphology 52, 347-358.
625 Eyles. N., Boyce, J.I., Barendregt, R.W. 1999. Hummocky moraine: sedimentary record of
626 stagnant Laurentide Ice Sheet lobes resting on soft beds. Sedimentary Geology
627 123, 3–4, 163-174.
628 Fay, H., 2001. The role of ice blocks in the creation of distinctive proglacial landscapes
629 during and following glacier outburst floods (jökulhlaups). PhD thesis, Keele
630 University.
631 Fay, H., 2002a. Formation of ice-block obstacle marks during the November 1996 glacier-
632 outburst flood (jökulhlaup), Skeiðarársandur, southern Iceland. in Martini, I.P.,
633 Baker, V.R. and Garzon, G. (eds) Flood and Megaflood Processes and Deposits:
634 Recent and Ancient Examples. International Association of Sedimentologists
635 Special Publication *32,* pp. 85-97.
636 Fay, H., 2002b. Formation of kettle holes following a glacial outburst flood (jökulhlaup),
637 Skeiðarársandur, southern Iceland. in: Snorasson, A., Finnsdóttir, H.P., Moss, M.,
638 (Eds.) The Extremes of the Extremes: Extraordinary Floods. Proceedings of a
639 symposium held at Reykjavik, Iceland, July 2000. IAHS Publication Number 271,
640 pp. 205-210.
641 Fard, A.M., 2003. Large dead-ice depressions in flat-topped eskers: evidence of a
642 Preboreal jökulhlaup in the Stockholm area, Sweden. Global and Planetary
643 Change 35, 3–4, 273-295.
644 French, H.M., Harry, D.G. 1990. Observations on buried ice and massive segregated ice,
645 western arctic coast, Canada. Permafrost and Periglacial Processes 1, 31-43.
646 Galon, R., 1973. Geomorphological and geological analysis of the proglacial area of
647 Skeiðarárjökull: central section. Geographica Polonica 26, 15-57.
648 Glacier risks database 2005. http://www.nimbus.it/glaciorisk/gridabasemainmenu.asp
649 Accessed 25/04/2019.
650 Hambrey, M.J., 1984. Sedimentary processes and buried ice phenomena in the
651 proglacial areas of Spitsbergen glaciers. Journal of Glaciology 30, 104,116-119.
652 Harrison, D., Ross, N., Russell, A.J., Dunning, S.A. 2019. Post-jökulhlaup geomorphic
653 evolution of the Gígjökull Basin, Iceland. Annals of Glaciology 60(80), 1-11.
654 Hjulström, F., 1952. The geomorphology of the alluvial outwash plains (sandurs) of
655 Iceland and the mechanics of braided rivers. Proceedings of the XVIIth

International Congress of the International Geographical Union, Washington, pp. 337-342.

Hooke, R.L., Jennings, C.E., 2006. On the formation of tunnel valleys of the southern Laurentide ice sheet. Quaternary Science Reviews 25, 1364-1372.

Ives, J.D., 2007. Skaftafell in Iceland: a thousand years of change. Ormstunga: Reykjavik, 256pp.

Jewtuchowicz, S., 1973. The present-day marginal zone of Skeiðarárjökull. Geographia Polonica 26, 115-138.

Johnson, P.G., 1992. Stagnant glacier ice, St. Elias Mountains, Yukon. Geografiska Annaler 74A, 1, 13-19.

Kleman, J., 1992. The palimpsest glacial landscape in northwestern Sweden. Late Weichselian deglaciation landforms and traces of older west-centered ice sheets. Geografiska Annaler 74A, 4, 305-325.

Kleman, J., Stroeven, A.P., 1997. Preglacial surface remnants and Quaternary glacial regimes in northwestern Sweden. Geomorphology 19, 1–2, 35–54.

Klimek, K., 1972. Present-day fluvial processes and relief of Skeiðarársandur plain (Iceland). Polska Academia Nauk Institut Geografi 94, 129-139.

Knudsen, Ó., Jóhannesson, H., Russell, A.J., Haraldsson, H., 2001. Changes in the Gígjukvísl river channel during the November 1996 jökulhlaup, Skeiðarársandur, Iceland, Jökull 50, 19-32.

Korsgaard, N.J., Schomacker, A., Benediktsson, Í.Ö., Larsen,N.K., Ingólfsson,Ó., Kjær, K.H. 2015. Spatial distribution of erosion and deposition during a glacier surge: Brúarjökull, Iceland. Geomorphology 250, 258-270

Krüger, J. 1994. Glacial processes, sediments, landforms and stratigraphy in the terminus region of Mýrdalsjökull, Iceland. Folia Geographica Danica 21, 1–233.

Krüger, J. and Kjær, K.H. 2000. De-icing progression of ice-cored moraine in a humid, subpolar climate, Kötlujökull, Iceland. Holocene 10, 721-731.

Kjær, K.H. and Krüger, J. 2001. The final phase of dead-ice moraine development: processes and sediment architecture, Kötlujökull, Iceland. Sedimentology 48, 935-952.

Levy, A., Robinson, Z. Krause, S., Waller, R., Weatherill, J. 2015. Long-term variability of proglacial groundwater-fed hydrological systems in an area of glacier retreat, Skeiðarársandur, Iceland. Earth Surface Processes and Landforms 40, 981–994.

689 Lister, H., 1953. Report on glaciology at Breiðamerkurjökull, 1951. Jökull 1, 23-31.
690 Lukas, S., Nicholson, L.I., Ross, F.H., Humlum, O., 2005. Formation, meltout processes
691 and landscape alteration of High-Arctic ice-cored moraines-examples from
692 Nordenskiold Land, Central Spitsbergen. Polar Geography 29, 157-187.
693 Maizels, J.K., 1977. Experiments on the origin of kettle-holes. Journal of Glaciology 18,
694 291-303.
695 Maizels, J.K., 1991. Origin and evolution of Holocene sandurs in areas of jökulhlaup
696 drainage, South Iceland. in: Maizels, J.K. and Caseldine, C. (eds) Environmental
697 change in Iceland: past and present. Dordrecht: Kluwer, pp. 267-300.
698 Maizels, J.K., 1992. Boulder ring structures produced during jökulhlaup flows-origin and
699 hydraulic significance. Geografiska Annaler 74A, 21-33.
700 Maizels, J.K., 1997. Jökulhlaup deposits in proglacial areas. Quaternary Science Reviews
701 16, 7, 93-819.
702 Maizels, J.K., Russell, A.J., 1992. Quaternary perspectives on jökulhlaup prediction. In
703 Gray, J.M. (ed.) Applications of Quaternary Research. Quaternary Proceedings 2,
704 133-153.
705 McDonald, B.C., Shilts, W.W., 1975. Interpretation of faults in glaciofluvial sediments. in
706 Jopling, A. V. and McDonald, B. C. (eds), Glaciofluvial and glaciolacustrine
707 sedimentation. SEPM Special Publication 23, pp. 123-131.
708 McKenzie, G.D., 1969. Observations on a collapsing kame terrace in Glacier Bay National
709 Monument, southeast Alaska. Journal of Glaciology 8, 413-414.
710 Nakawo, M., Young, G.J., 1981. Field experiments to determine the effect of a debris
711 layer on ablation of glacier ice. Annals of Glaciology 2, 85-91.
712 Nakawo, M., Young, G.J., 1982. Estimate of glacier ablation under debris layer from
713 surface temperature and meteorological variables. Journal of Glaciology 28, 29-
714 34.
715 Nicholson, L., Benn, D.I., 2006. Calculating ice melt beneath a debris layer using
716 meteorological data. Journal of Glaciology 52, 178, 463-470.
717 Nye, J.F., 1976. Water flow in glaciers: jökulhlaups, tunnels and veins. Journal of
718 Glaciology 17, 181-207.
719 Olszewski, A., Weckwerth, P., 1999. The morphogenesis of kettles in the
720 Höfðabrekkujökull forefield, Mýrdalssandur, Iceland. Jökull 47, 71-88.

Østrem, G., 1959. Ice melting under a thin layer of moraine and the existence of ice cores in moraine ridges. Geografiska Annaler 41A, 228-230.

Porter C and 28 others. 2018. ArcticDEM. doi: 10.7910/DVN/OHHUKH.

Price, R.J., 1969. Moraines, sandar, kames and eskers near Breiðamerkurjökull, Iceland. Transactions of the Institute of British Geographers 46, 17-43.

Price, R.J., Howarth, P.J., 1970. The evolution of the drainage system (1904 - 1965) in front of Breiðamerkurjökull, Iceland. Jökull 20, 27-37.

Roberts, M.J., 2005. Jökulhlaups: a reassessment of floodwater flow through glaciers. Reviews of Geophysics 43, RG1002, doi:10.1029/2003RG000147.

Roberts, M.J., Russell, A.J., Tweed, F.S., Knudsen, Ó. 2000. Ice fracturing during jökulhlaups; implications for englacial floodwater routing and outlet development. Earth Surface Processes and Landforms 25, 1429-1446.

Roberts, M.J., Russell, A.J., Tweed, F.S., Knudsen, Ó., 2001. Controls on englacial sediment deposition during the November 1996 jökulhlaup, Skeiðarárjökull, Iceland. Earth Surface Processes and Landforms 26, 935-952.

Roberts, M.J., Tweed, F.S., Russell, A.J., Knudsen, Ó., Lawson, D.E., Larson, G.J., Evenson, E.B., Björnsson, H., 2002. Glaciohydraulic supercooling in Iceland. Geology 30, 439-442.

Robinson, Z.P., Fairchild, I.J., Russell, A.J., 2008. Hydrogeological implications of glacial landscape evolution at Skeiðarársandur, SE Iceland. Geomorphology 97, 218-236.

Russell, A.J., Knudsen, Ó., 1999. Controls on the sedimentology of November 1996 jökulhlaup deposits, Skeiðarársandur, Iceland. in: Fluvial Sedimentology VI (ed. by N. D. Smith, & J. Rogers), I.A.S. Spec., Publ. 28, pp. 315-329.

Russell, A.J., Knudsen, Ó., 2002. The effects of glacier-outburst flood flow dynamics on ice-contact deposits: November 1996 jökulhlaup, Skeiðarársandur, Iceland. in: Martini, I.P., Baker, V.R., Garzon, G. (eds) Flood and megaflood deposits: recent and ancient examples. Oxford: Blackwell Science, pp. 67-83.

Russell, A.J., Knudsen, Ó., Fay, H., Marren, P.M., Heinz, J., Tronicke, J., 2001a. Morphology and sedimentology of a giant supraglacial, ice-walled, jökulhlaup channel, Skeiðarársandur, Iceland. Global Planetary Change 28, 203-226.

Russell, A.J., Knight, P.G., van Dijk, T.A.G.P., 2001b. Glacier surging as a control on the development of proglacial, fluvial landforms and deposits, Skeiðarársandur, Iceland. Global and Planetary Change 28, 163-174.

754 Russell, A.J. Fay, H., Marren, P.M., Tweed, F.S., Knudsen Ó., 2005. Icelandic jökulhlaup
755 impacts. in: Caseldine, C.J., Russell, A.J., Knudsen, Ó., & Harðardóttir, (eds.)
756 Iceland: Modern Processes and Past Environments. Elsevier Book. pp. 153-204.
757 Russell, A.J., Roberts, M.J., Fay, H., Marren, P.M., Cassidy, N.J., Tweed, F.S. and Harris, T.
758 2006. Icelandic jökulhlaup impacts: implications for ice-sheet hydrology,
759 sediment transfer and geomorphology. Geomorphology 75, 33-64.
760 Sanford, A.R., 1959. Analytical and experimental study of simple geologic structures.
761 Geological Society of America Bulletin 70, 19-52.
762 Schiefer, R., Gilbert, R., 2007. Reconstructing morphometric change in a proglacial
763 landscape using historical aerial photography and automated DEM generation.
764 Geomorphology 88, 167-178.
765 Sandmeier, K.J., 2012. ReflexW 8.1, Program for the Processing of Seismic, Acoustic or
766 Electromagnetic Reflection, Refraction and Transmission Data; Software Manual:
767 Karlsruhe, Germany.
768 Schomacker, A., 2008. What controls dead-ice melting under different climate
769 conditions? A discussion. Earth Science Reviews 90, 3–4, 103-113.
770 Schomacker, A., Kjær, K.H., 2007. Origin and de-icing of multiple generations of
771 ice-cored moraines at Brúarjökull, Iceland. Boreas 36, 4, 411-425.
772 Sigurðsson, O., 2005. Variations of termini of glaciers in Iceland in recent centuries and
773 their connection with climate. Developments in Quaternary Sciences 5, 241-255.
774 Smith, L.C., Sheng, Y., Magilligan, F.J., Smith, N.D., Gomez, B., Mertes, L.A.K., Krabill,
775 W.B., Garvin, J.B., 2006. Geomorphic impact and rapid subsequent recovery from
776 the 1996 Skeiðarársandur jökulhlaup, Iceland, measured with multi-year airborne
777 lidar. Geomorphology 75, 65-75.
778 Snorrason, Á., Jónsson, P., Pálsson, S., Árnason, S., Víkingsson, S., Kaldal, I., 2002.
779 November 1996 jökulhlaup on Skeiðarársandur outwash plain, Iceland. in:
780 Martini, I.P., Baker, V.R., Garzón, G., (Eds.), Flood and megaflood processes and
781 deposits: recent and ancient examples. Special Publication of the International
782 Association of Sedimentologists 32, pp. 55-65.
783 Thórarinsson, S., 1943. Oscillations of the Iceland Glaciers in the last 250 years.
784 Geografiska Annaler 25A, 1-54.
785 Thórarinsson, S. 1974. Vötnin Strið: Saga Skeiðarárhlaupa og Grimsvatnagosa.
786 Bókaútgáfa Menningarsjods, Reykjavik, 254p.

787 Thórarinsson, S., Sæmundsson, K., Williams, S.W.J., 1951. ERTS-1 image of Vatnajökull:
788 analysis of glaciological, structural and volcanic features. Jökull 23, 7-17.
789 Thórhallsdóttir, T.E. 1996. Seasonal and annual dynamics of frozen ground in the central
790 highland of Iceland. Arctic and Alpine Research 28, 237-243.
791 Tonkin, N., Midgley, N.G., Cook, S.J., Graham, D.J. 2016. Ice-cored moraine degradation
792 mapped and quantified using an unmanned aerial vehicle: A case study from a
793 polythermal glacier in Svalbard. Geomorphology 258, 1-10.
794 Wisniewski, E., Andrzejewski, L., Molewski, P., 1997. Fluctuations of the snout of
795 Skeiðarárjökull in Iceland in the last 100 years and some of their consequences in
796 the central part of its forefield. Landform Analysis 1, 73-78.
797 Wojcik, G., 1973. Glaciological studies on the Skeiðarárjökull. Geographia Polonica 26,
798 185-208.

799 # Tables

800

Year	Eruption	Glacier margin advance/recession	Jökulhlaup impacts *(Impacts on the Harðaskriða area)*
1598	Yes	Advance	No detailed information available.
1629	Yes	Advance	Huge jökulhlaup with at least five enormous flood paths across Skeiðarársandur. Fertile land flooded, one family died and at least one man isolated 5 days on a high hill in the flood area.
1816	?	Little Ice Age Maximum	No detailed information available.
1838	?	Little Ice Age Maximum	No detailed information available.
1851	Yes	Little Ice Age Maximum	No detailed information available.
1861	Yes?	Little Ice Age Maximum	Large jökulhlaup (Stórahlaup) which destroyed much land close to the farms Svínafell, Hof and Hofsnes. Icebergs and large quicksand areas (kettle holes) formed in the flood path.
1867	Yes	Little Ice Age Maximum	Large jökulhlaup, 13 days duration, waning on the 4th day. Icebergs washed out onto Skeiðarársandur, which was completely covered by water.
1873	Yes	Little Ice Age Maximum	Fairly small jökulhlaup The discharge in the river Súla increased right after the beginning of the jökulhlaup in river Skeiðará.
1883	yes	Little Ice Age Maximum	No detailed information available.
1892	Yes?	Little Ice Age Maximum	One of the largest jökulhlaups in river Skeiðará with a duration of four days. Peak discharge reached after two days accompanied by tremendous noise. The next day ice blocks were covering the sandur all the way to the ocean. Ice blocks were up to 20 m in diameter and very tightly packed. South of the main flood outlet, icebergs, up to 20 m high, covered a 7 km wide region. Mud was spread over the flooded area and was unusually thick. Melting icebergs and quicksand made it difficult to cross the Skeiðarársandur for several months after the flood.
1897	Yes	Little Ice Age Maximum	This jökulhlaup was smaller than the one in 1892 and had a duration of 10 days with a 6 day rising stage. It burst from Skeiðarárjökull near Harðaskriða, a steep moraine south of central Skeiðarárjökull. Ice blocks up to 20m in diameter were spread over a 6 km wide area between Harðaskriða and the Skeiðará. ***(Potential source of jökulhlaup transported ice blocks to the Harðaskriða area).***
1903	Yes		Large jökulhlaup with a duration of 4 days reaching discharge peak very quickly and covering more of the western outwash plain than usual. Ice blocks were carried all the way to the ocean. A large piece of the glacier margin detached during the 1903 jökulhlaup approximately 1 km in length and up to 150 m in height; it was also documented that a fracture of similar size and length developed up glacier located where the floodwaters burst from the glacier margin. ***(Potential source of jökulhlaup transported ice blocks to the Harðaskriða area).***
1913	No	Recession	Large jökulhlaup of 12 days duration. The flood was focussed on the eastern part of Skeiðarársandur. Large amounts of ice detached from snout of Skeiðarárjökull with ice blocks described as being the size of houses.
1922	Yes	Recession	This large jökulhlaup had a duration of 14 days and had its main outlet on the eastern side of Skeiðarársandur. Rising stage

			discharge increased slowly for 6 days before any ice blocks were observed being transported downstream. Followed by 8 days of recession. The jökulhlaup waned within one day. ***(Potential for aggradation in the Harðaskriða area).***
1934	Yes	Recession	A large jökulhlaup with a volume of 4.5 km^3 with a 16 day duration and a peak discharge of 25,000 to 30,000 m^3s^{-1}. The eastern most outlet was 2.5 km wide and ice blocks carried to ocean. ***(Potential for aggradation in the Harðaskriða area).***
1938	Yes	Recession	A large jökulhlaup with a volume of 4.7 km^3, a peak discharge of 25,000 to 30,000 m^3s^{-1} and a 16 day duration. Almost all Skeiðarársandur was flooded with ice blocks covering the sandur, although they were smaller than those generated by the 1934 jökulhlaup. ***(Potential for aggradation in the Harðaskriða area).***
1941	No	Recession	A small jökulhlaup with a duration of 17 days and a volume of 1.4 km^3. Relatively small ice blocks released from the glacier snout. ***(No impact on the Harðaskriða area due to the formation of a proglacial trench diverting flow in a westward direction).***
1945	No	Recession	A jökulhlaup with a duration of 12 days, a volume of 2.6 km^3 and a peak discharge of 10,000 m^3s^{-1}. Jökulhlaup flowed in the Skeiðará, Sandgígjukvísl and Núpsá river and produced relatively small ice blocks. ***(No impact on the Harðaskriða area due to the formation of a proglacial trench diverting flow in a westward direction).***
1948	No	Recession	A jökulhlaup with a duration of 17 days, a volume of 2.2 km^3 and a peak discharge of 5,000 m^3s^{-1}. ***(No impact on the Harðaskriða area due to the formation of a proglacial trench diverting flow in a westward direction).***
1954	No	Recession	A jökulhlaup with a duration of 14 days, a volume of 3.2 km^3 and a peak discharge of 10,000 m^3s^{-1}. Jökulhlaup flowed in the Skeiðará and Sandgígjukvísl with peak discharges of 6,000 m^3s^{-1} 4,000 m^3s^{-1} respectively. ***(No impact on the Harðaskriða area due to the formation of a proglacial trench diverting flow in a westward direction).***

Table 1 Chronology of glacier margin fluctuations and jökulhlaups (1598-1954) from the drainage of Grímsvötn subglacial lake draining from Skeiðarárjökull. Information in this table is sourced from Thórarinsson (1974), Björnsson (1997), Glacier risks database (2005) and Ives (2007).

Photo Year	Ave Z dif (m)	RMS (m)	SD (m)	95% confidence (2xSD) (m)
1965	0.0773	3.4536	3.6062	7.2124
1968	1.8190	2.5760	1.8769	3.7538
1997*	1.5005	2.7248	2.3369	4.6738
2003*	-0.9224	2.7059	2.6221	5.2442
2007	0.1575	1.6187	1.6442	3.2884

820

821 **Table 2** Average height difference between DEM and control (check) points surveyed at the field site with
822 error estimates given as root mean square (RMS) errors. Random errors are reported at the 95th
823 percentile limit (all units are in metres). Note '*' designates 1997 and 2003 Loftmyndir DEMs compared
824 with field data.

825

826

Figures

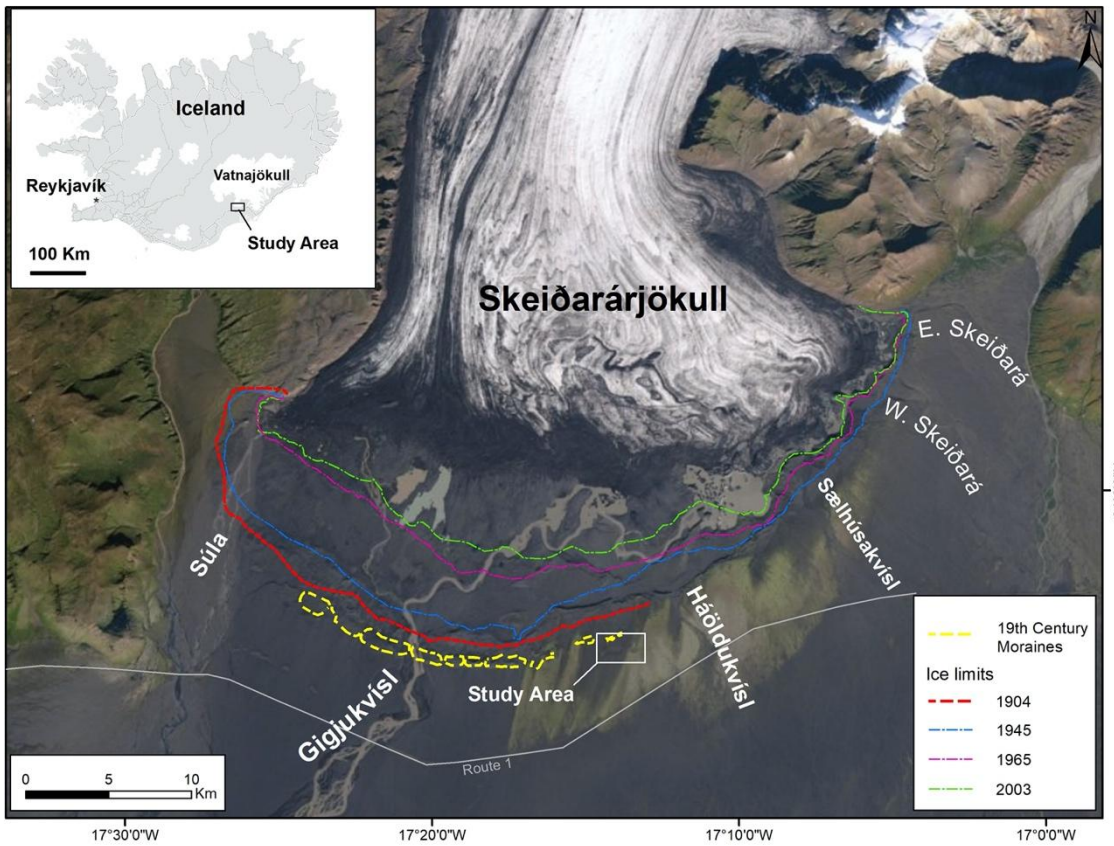

Figure 1. Skeiðarárjökull in Iceland (top inset) and its margin showing the three major lobes, the retreat of the margin since 1945, the location of the 19th century moraines and the major proglacial river channels (Imagery: 2010 Google Earth; Iceland Inset - Justus Lyons).

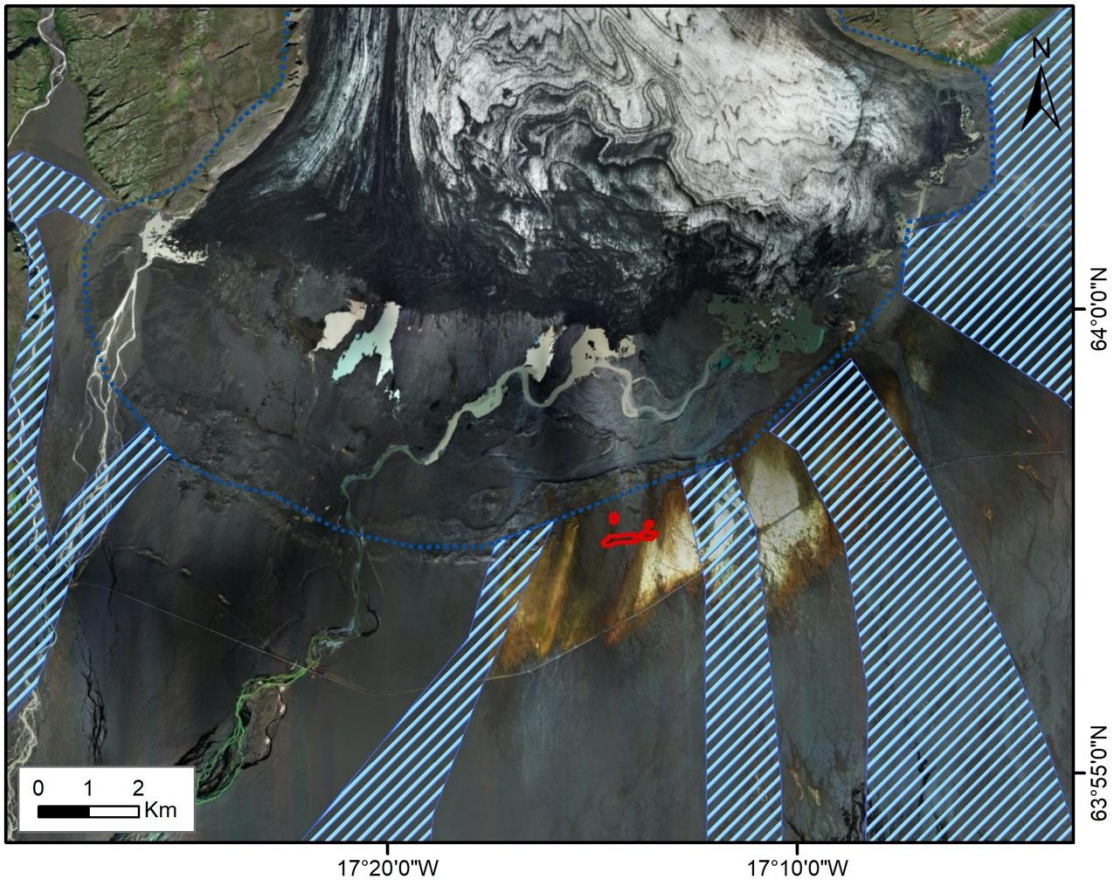

Figure 2. Approximate extent of 1934 ice margin (dashed blue line) and location of jökulhlaup routing (blue hashed polygons) on top of 2016 (Digital Globe photomosaic. Red polygons delineate location of depressions (Thórarinsson, 1974).

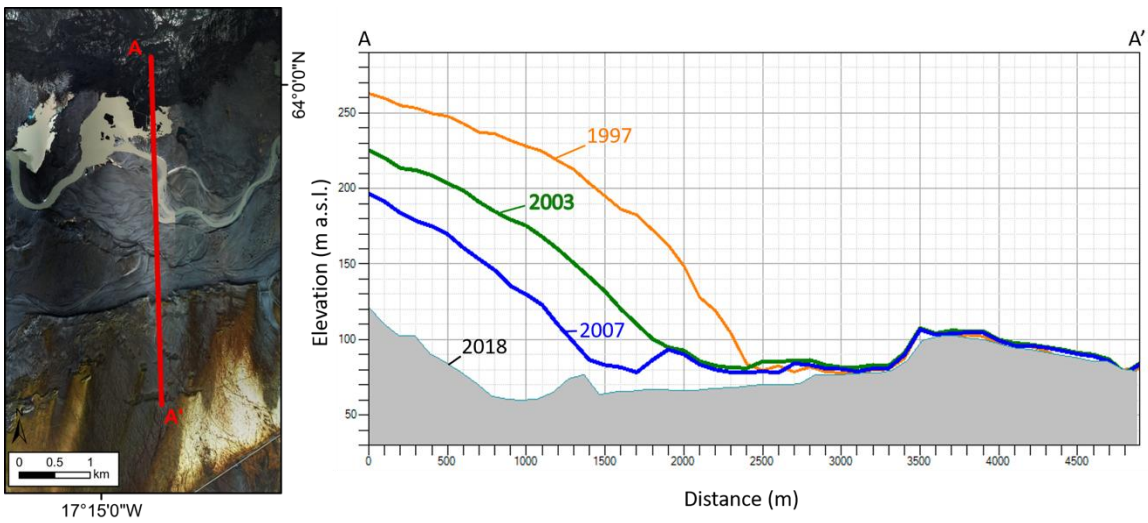

Figure 3. Proximal to distal profiles of the glacier and the sandur, demonstrating the retreat of the margin and the base level lowering of drainage within the proglacial depression, and assumed lowering of groundwater table. The 1997, 2003, 2007 profiles are derived DEMs from imagery acquired by Landmælingar Íslands, Loftmyndir ehf. and NERC ARSF, respectively. The 2018 profile is derived from ArcticDEM.

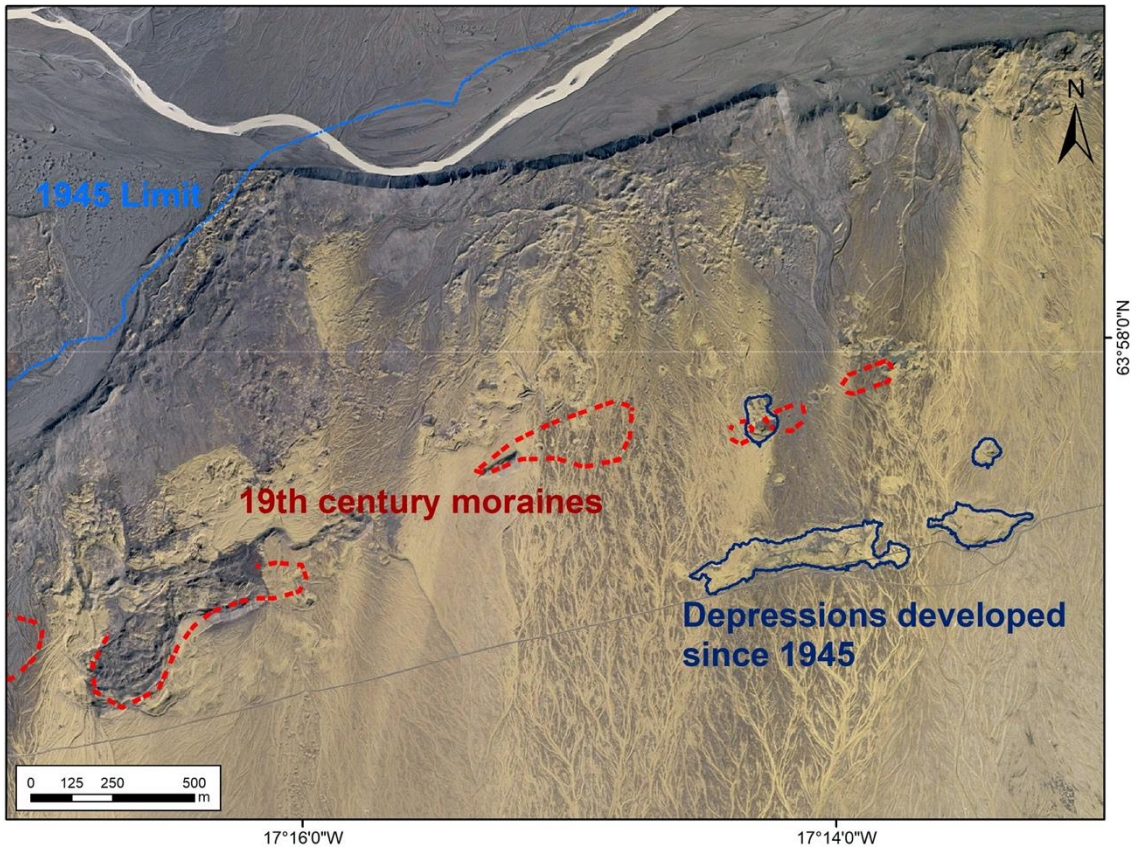

Figure 4. Approximate locations of 19th century moraines estimated from georeferenced 1904 topographic map (red line) on 2003 imagery. Blue indicates depressions that have developed since 1945.

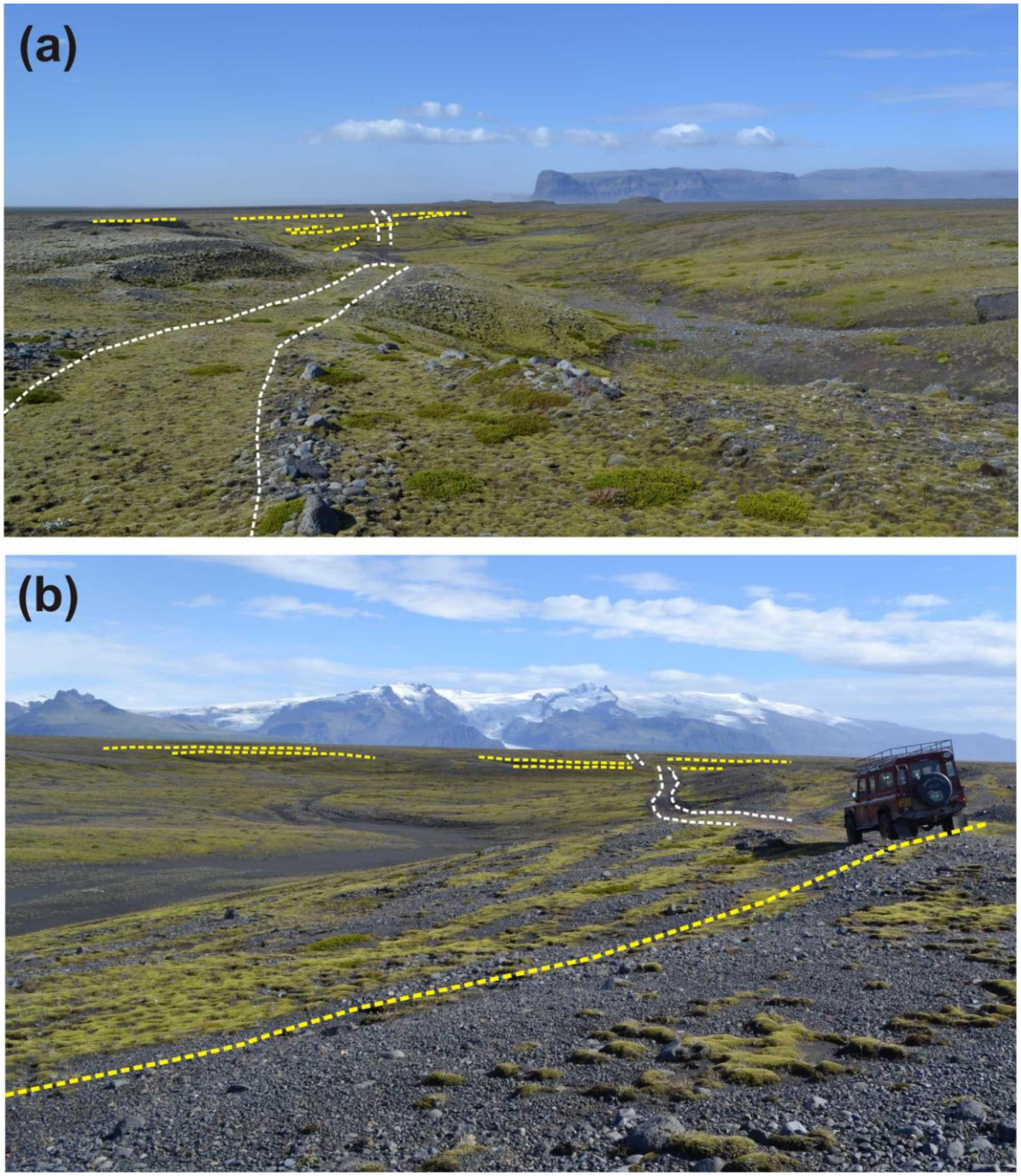

Figure 5. (a) Top. A view towards the west of depression 4 (for location see figs 2 & 4). The upper surfaces of well-defined normally faulted blocks are indicated by the yellow dashed lines. The path of the old gravel road is indicated by the white dashed lines indicating substantial deformation and subsidence. (b) View towards the east of depression 4 showing concentric rings associated with individual fault blocks indicated by yellow lines. The path of the old gravel road is indicated by the white dashed lines indicating substantial deformation and subsidence.

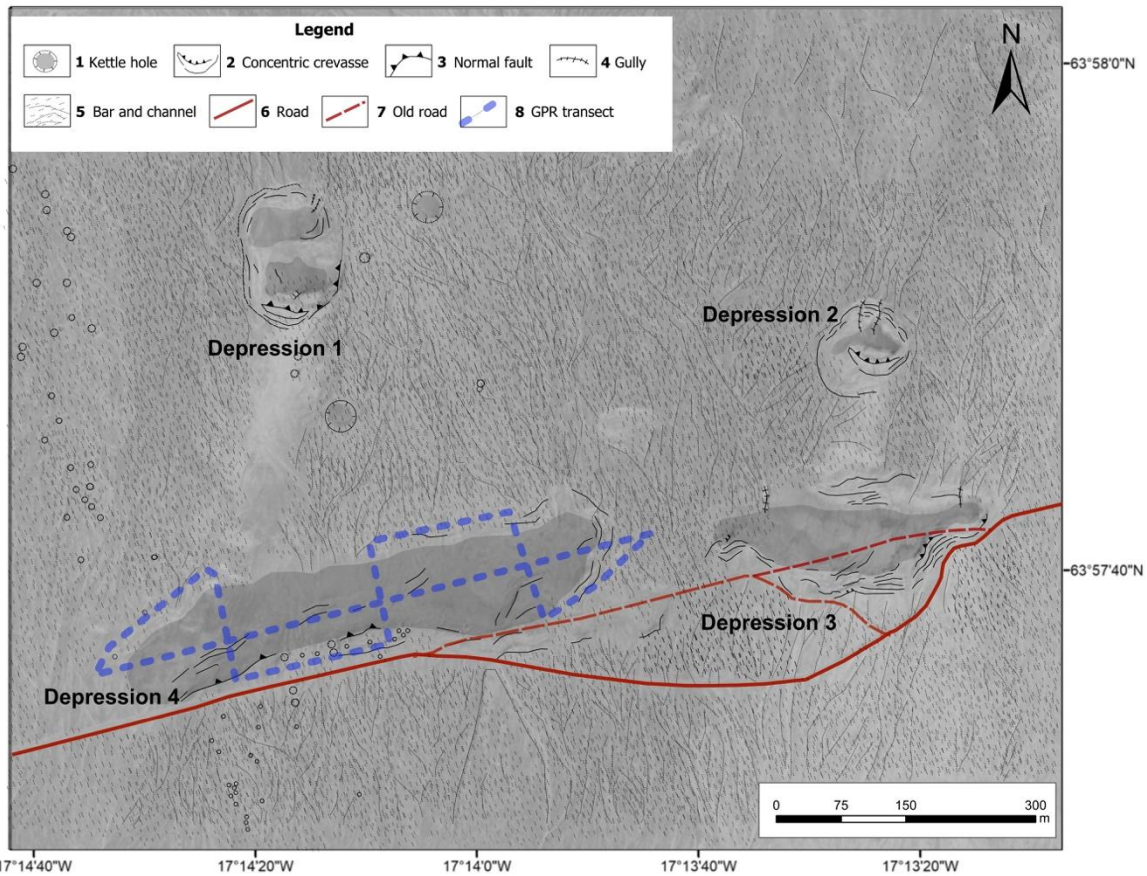

Figure 6. Geomorphological map of depressions and GPR transects (dashed blue lines). Red broken line represents the original course of a gravel road that has been re-routed to the south due to on-going subsidence of depression.

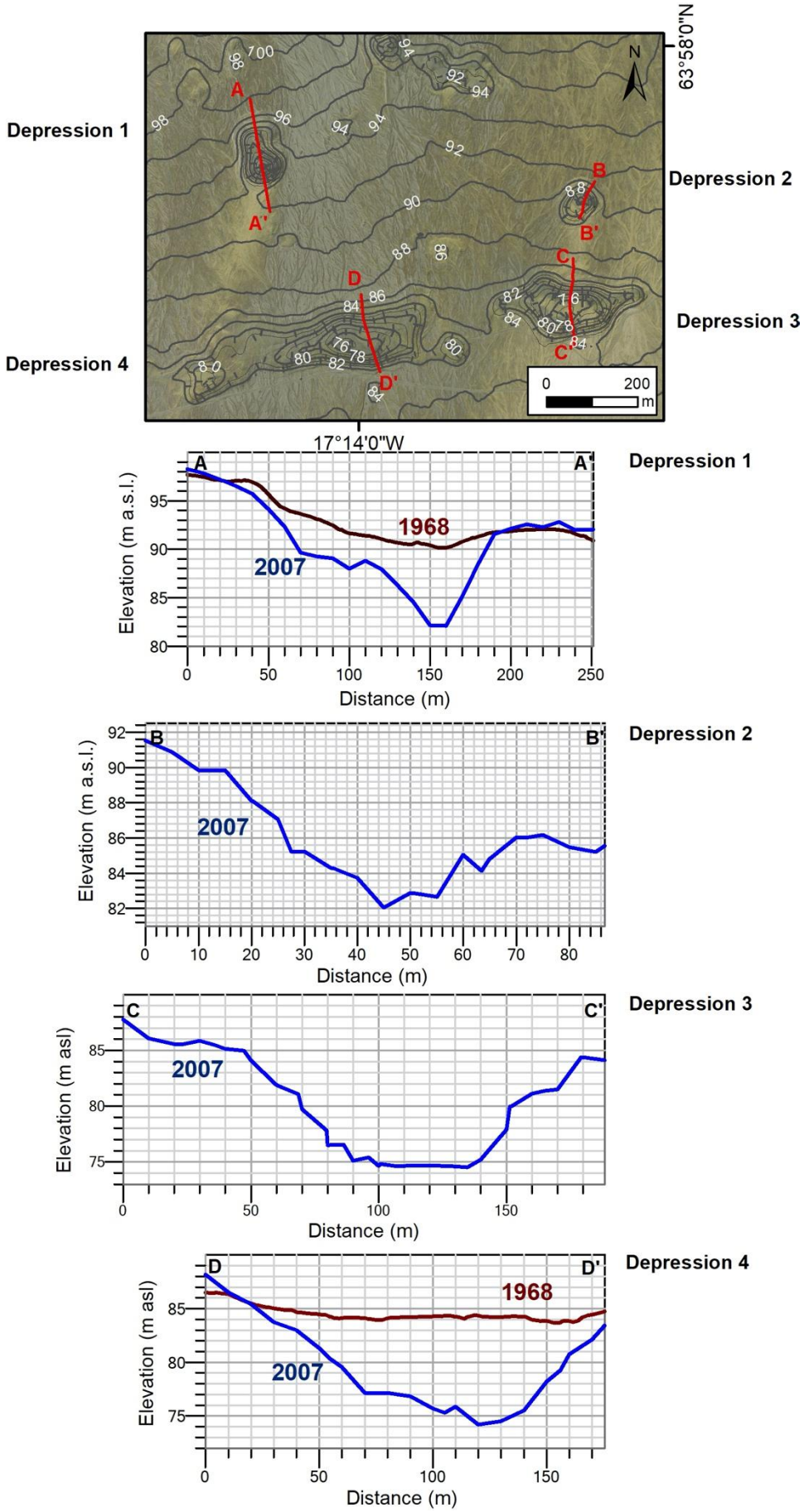

865

866 **Figure 7.** Profiles of depressions 1 –4 in 2007 (dGPS survey transects) are shown in blue; the 1968
867 surfaces, when available, are shown in red.

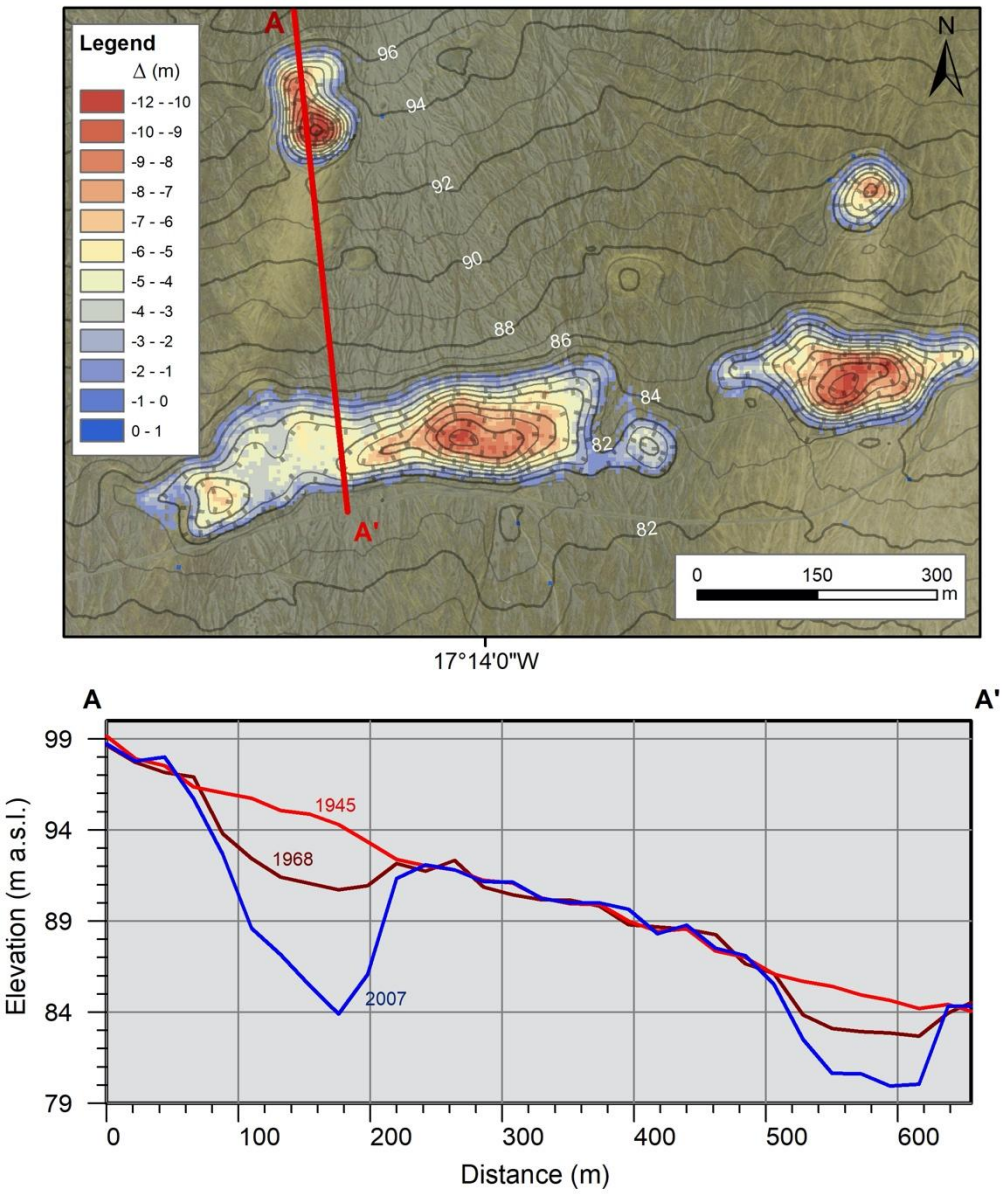

Figure 8. Total elevation loss (m) between 1945 – 2007 and estimated volume loss estimated by using an artificial 1945 surface (top); profiles of depressions between 1945 (red), 1968 (brown) and 2007 (blue) (bottom).

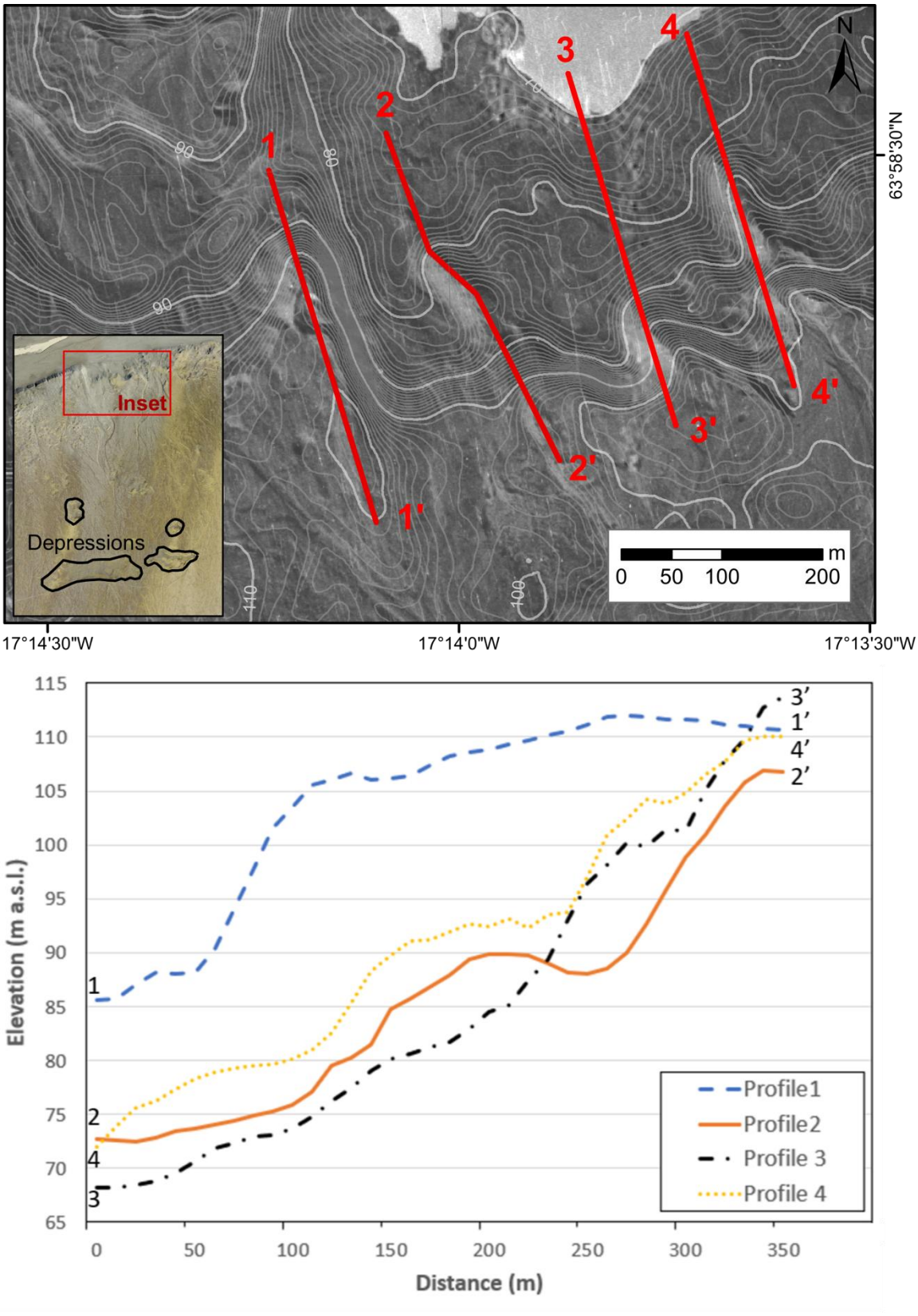

Figure 9. (a) The location 1965 drumlinised ridges exposed by the retreat of the glacier margin since 1945. (b) Elevation profile of the proglacial depression (profile 1) and drumlinised ridges (profiles 2-4).

878

879

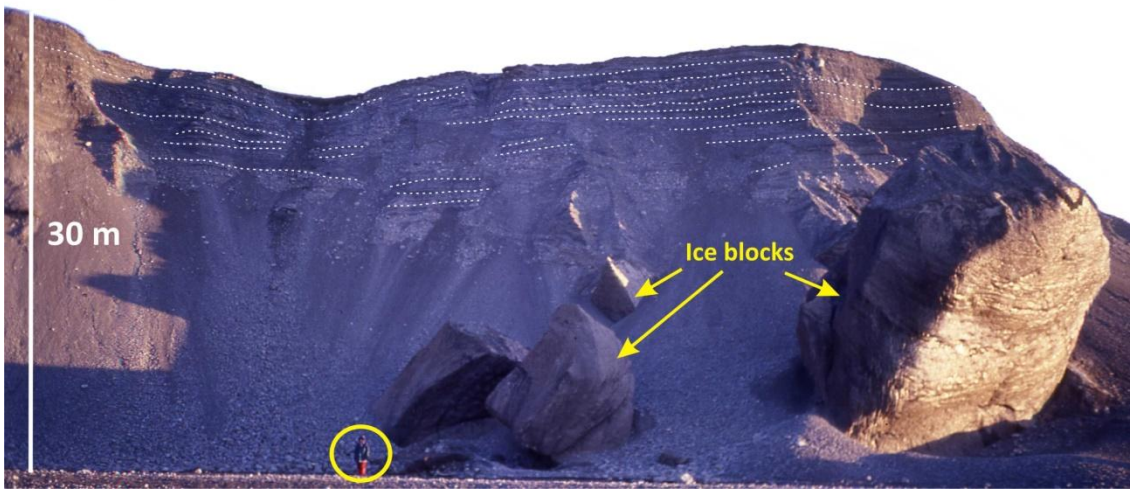

880
881 **Figure 10.** Photograph taken in May 1997 showing the presence of large isolated blocks of glacier ice
882 within jökulhlaup deposits.
883
884

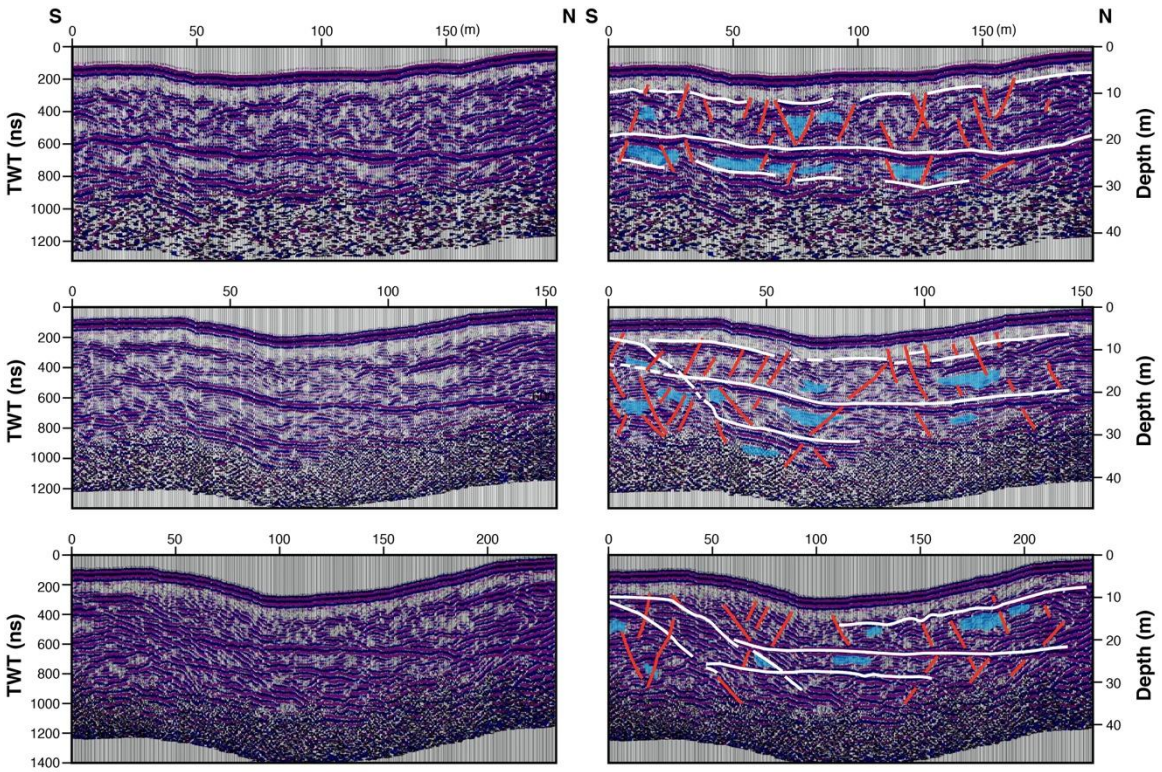

Figure 11. N-S cross-sectional radargrams through Depression 4. From top to bottom: west line, central line and east line (see Fig. 6). Main reflectors are shown in white, structural features in red, and buried ice remnants in blue. For further explanations, see main text.

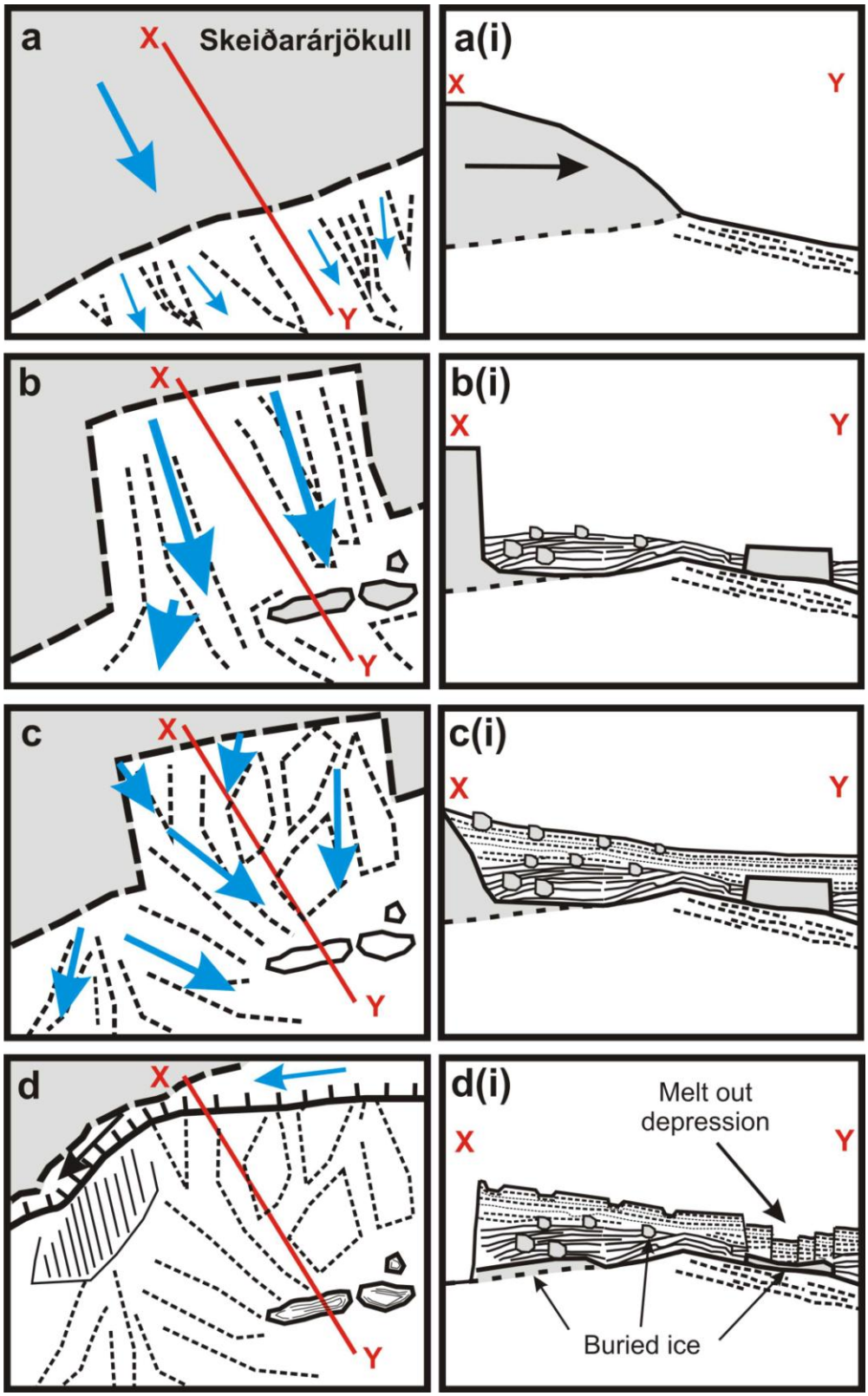

Figure 12. Model showing the proposed sequence of events responsible for the formation of the Harðaskriða melt out depressions on Skeiðarársandur. (a & ai) Initial glacier position before the 1903 jökulhlaup. (b) Erosion of ice-walled re-entrant into the snout of Skeiðarárjökull during 1903 jökulhlaup and transport of large ice blocks onto sandur. (bi) Partial burial of large 1903 jökulhlaup-transported ice blocks. (c & ci) Burial of 1903 jökulhlaup emplaced ice blocks by 1913 and 1922 jökulhlaup deposits. (d) Glacier margin position in 1945 allows meltwater to drain in a westerly direction along the ice margin abandoning the sandur surface. (di) Abandoned sandur surface showing the presence of isolated buried ice blocks (see Fig. 10) and the development of the large melt out depression.

Figure (Color)

Click here to download high resolution image

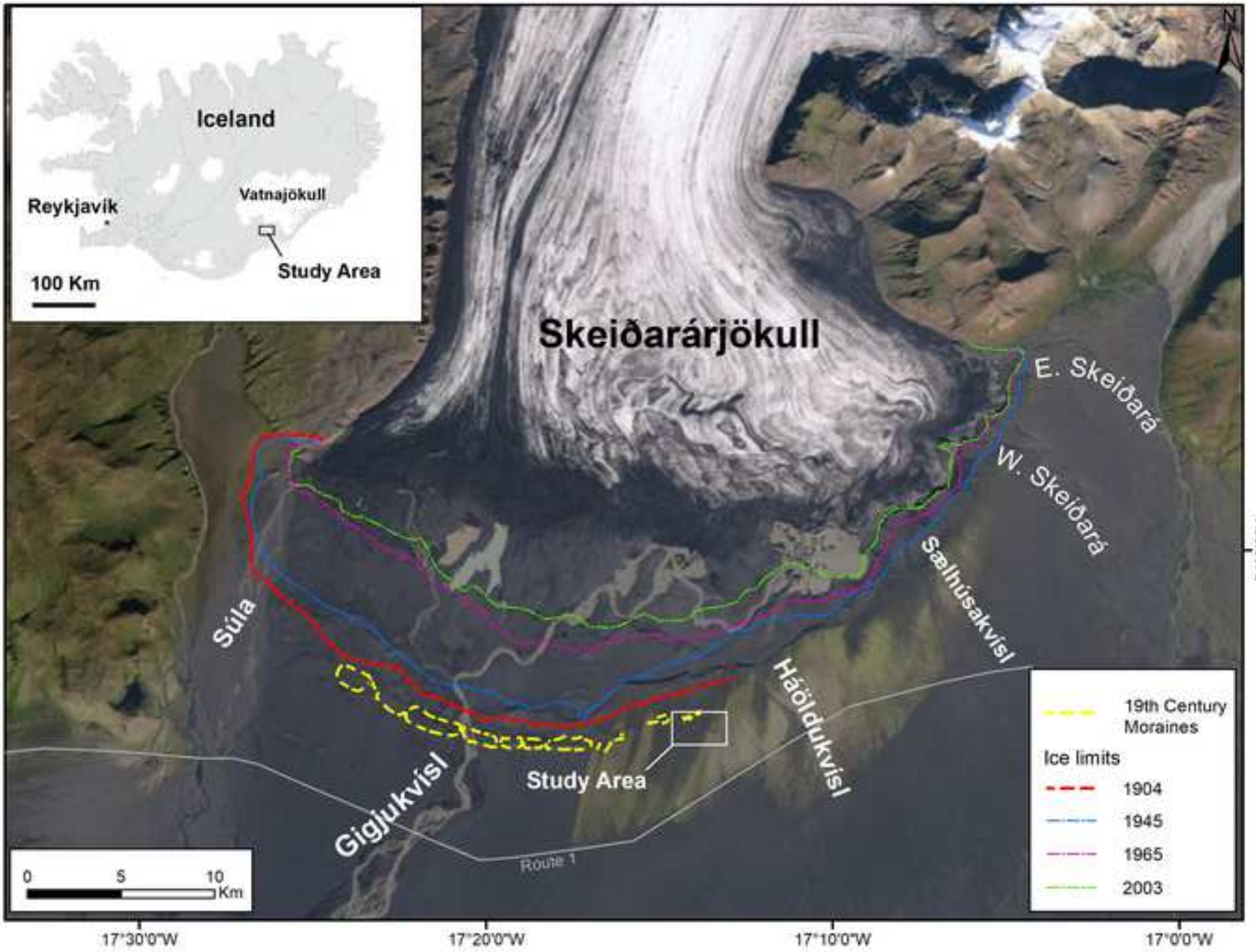

Figure (Color)

Click here to download high resolution image

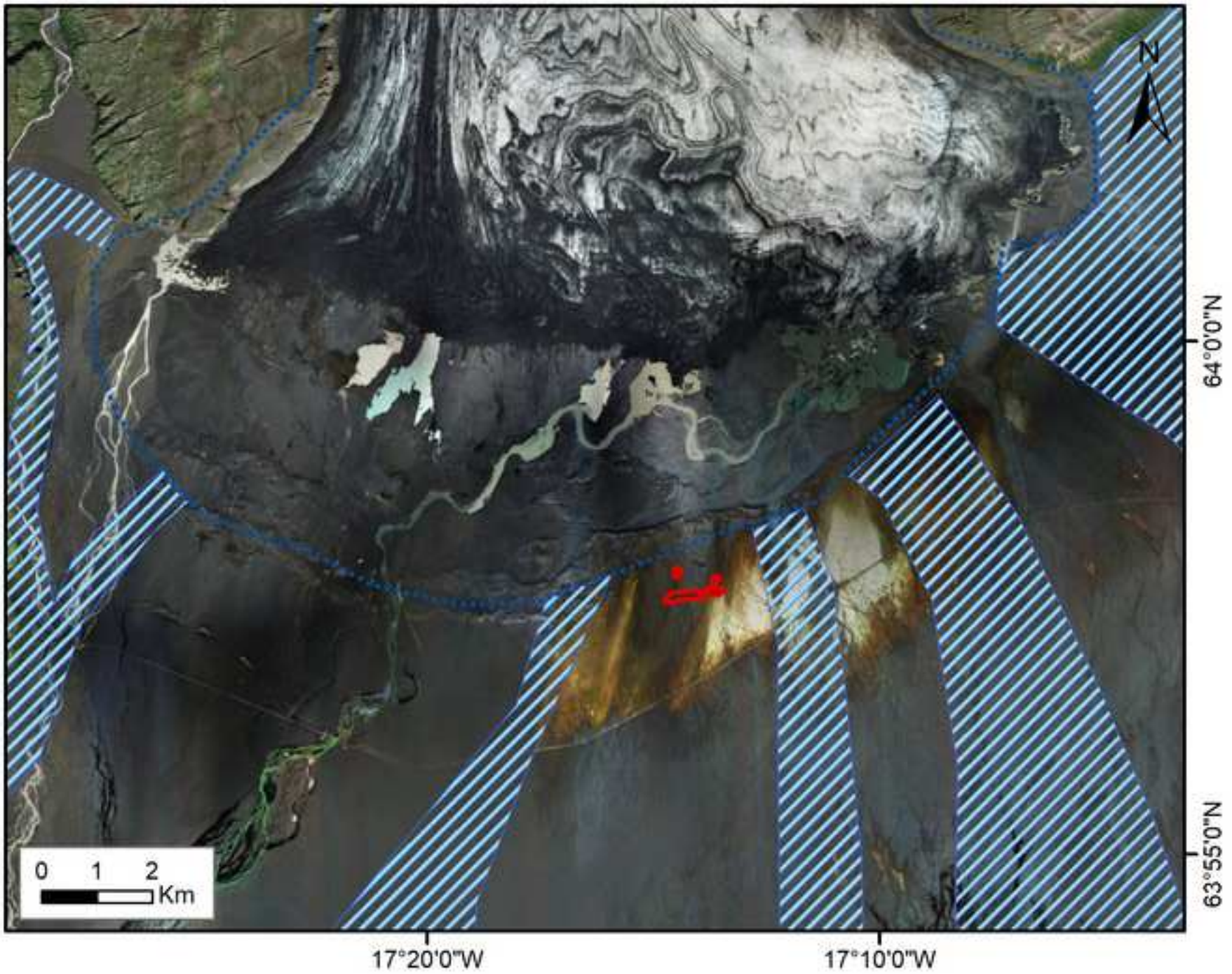

Figure (Color)

Click here to download high resolution image

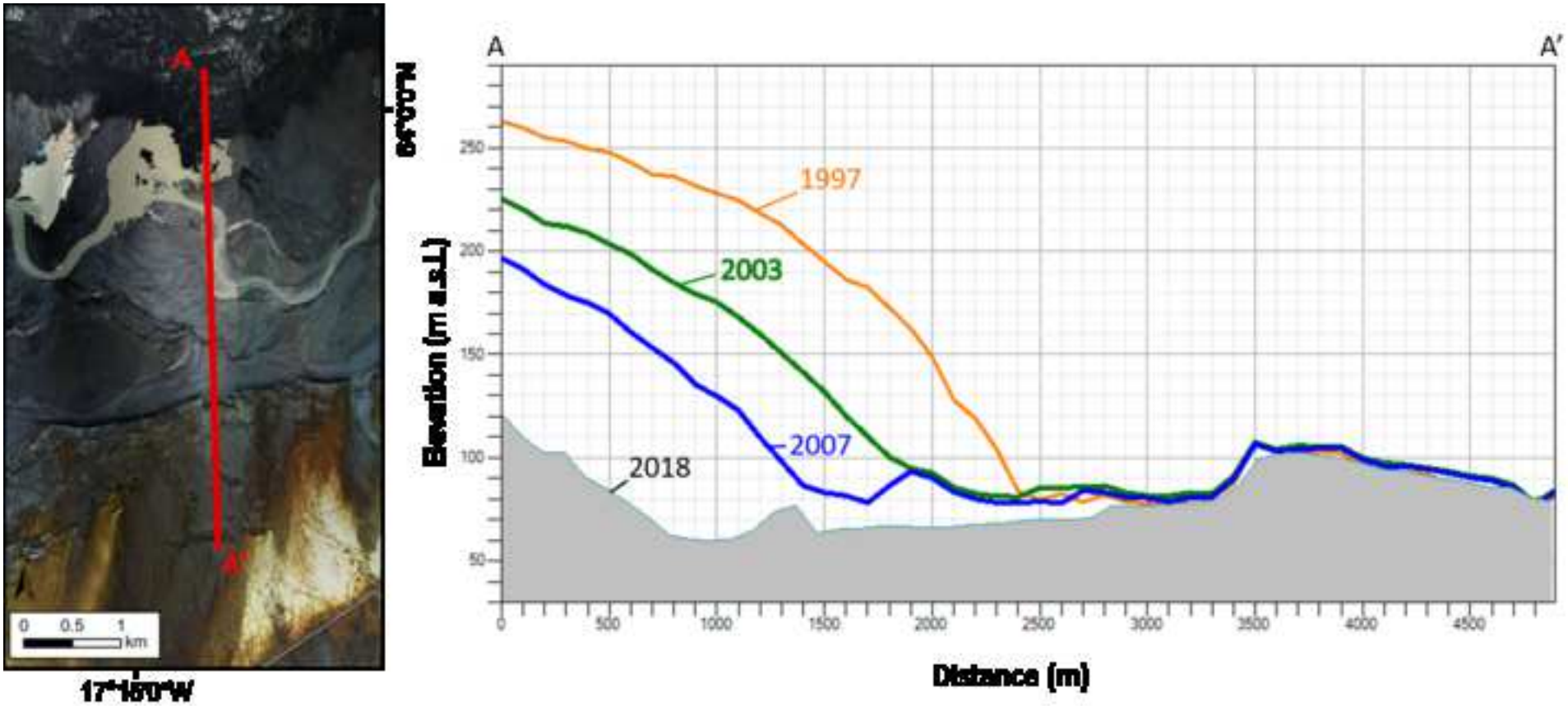

Figure (Color)
Click here to download high resolution image

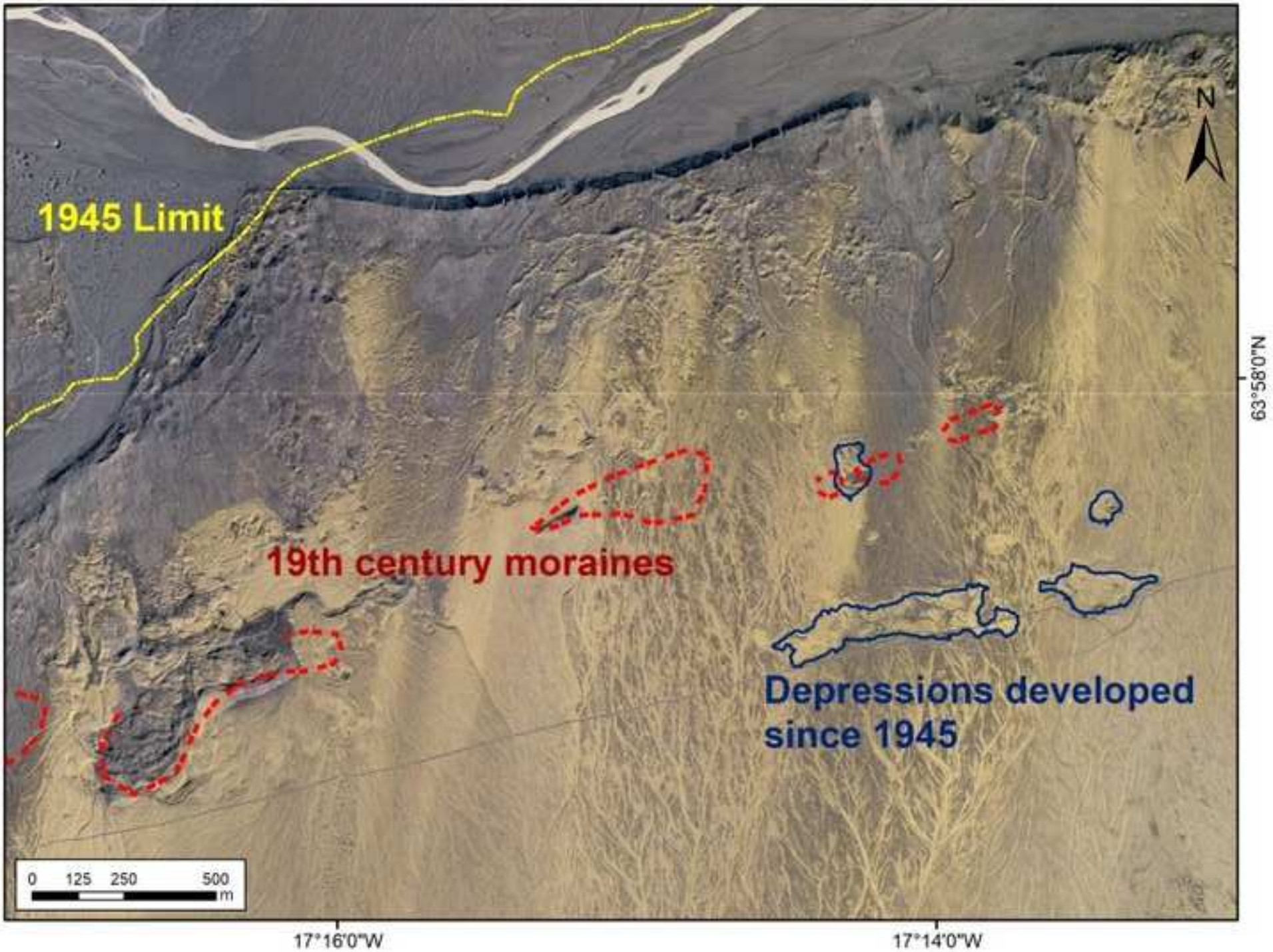

Figure (Color)
Click here to download high resolution image

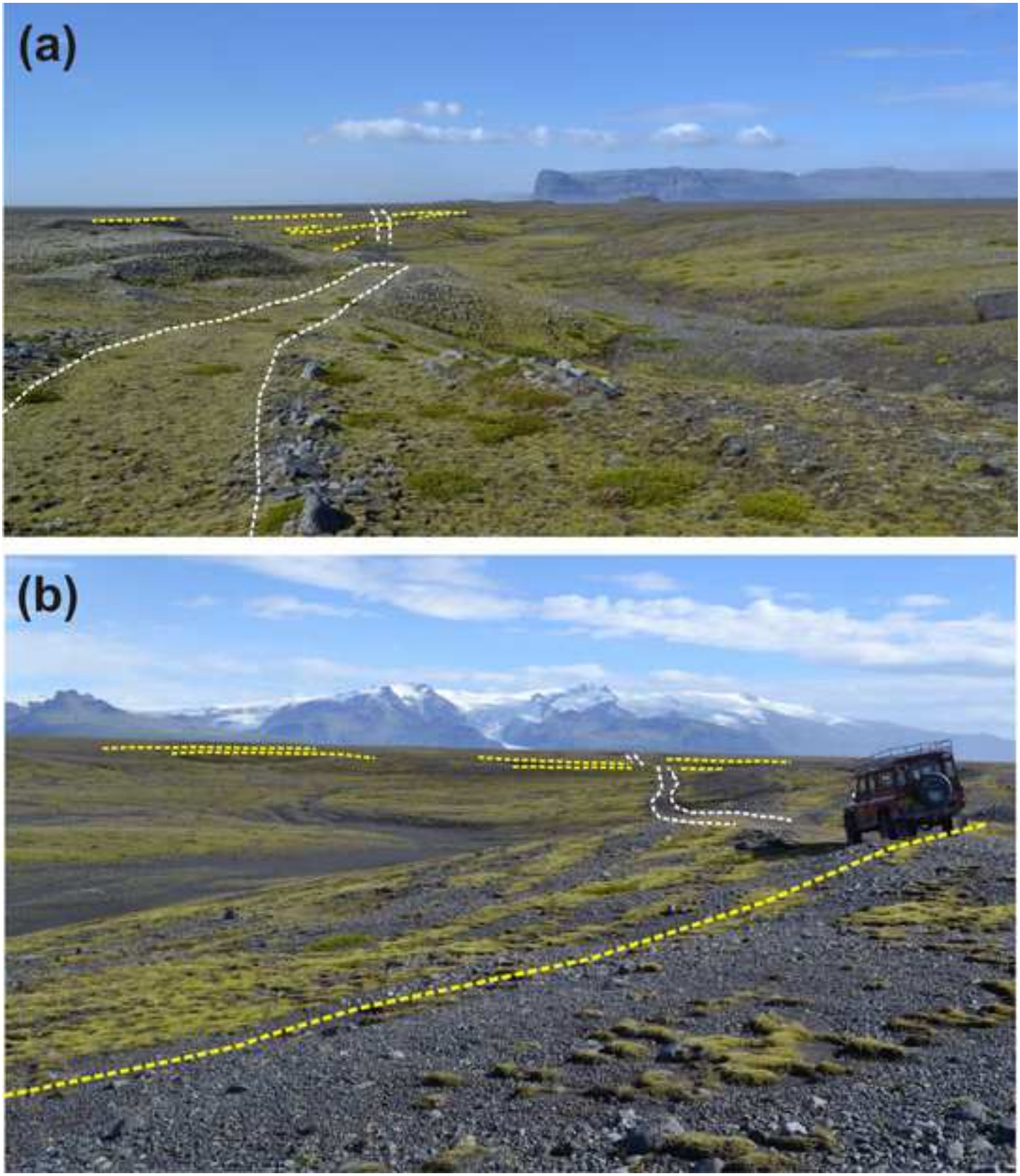

Figure (Color)

Click here to download high resolution image

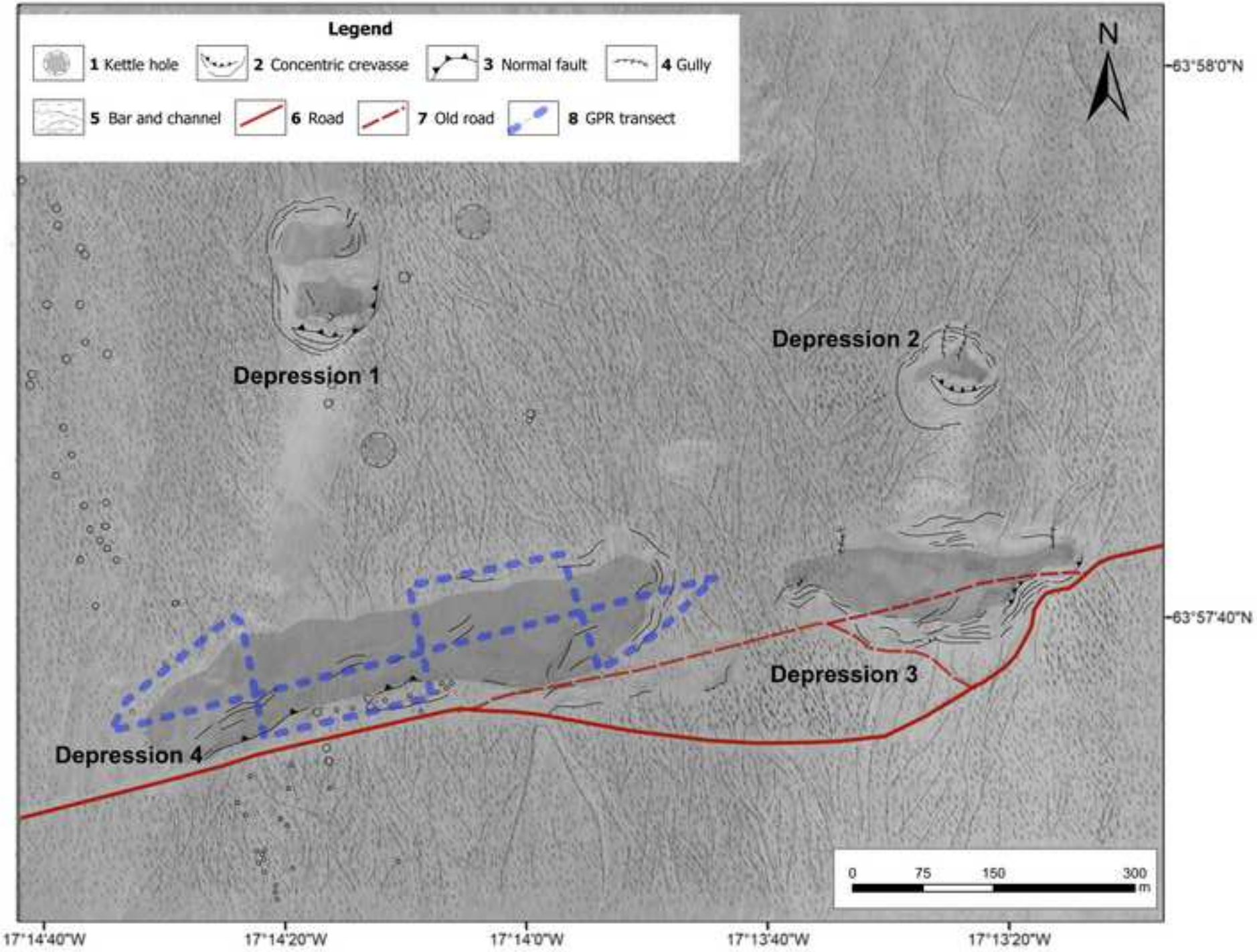

Figure (Color)

Click here to download high resolution image

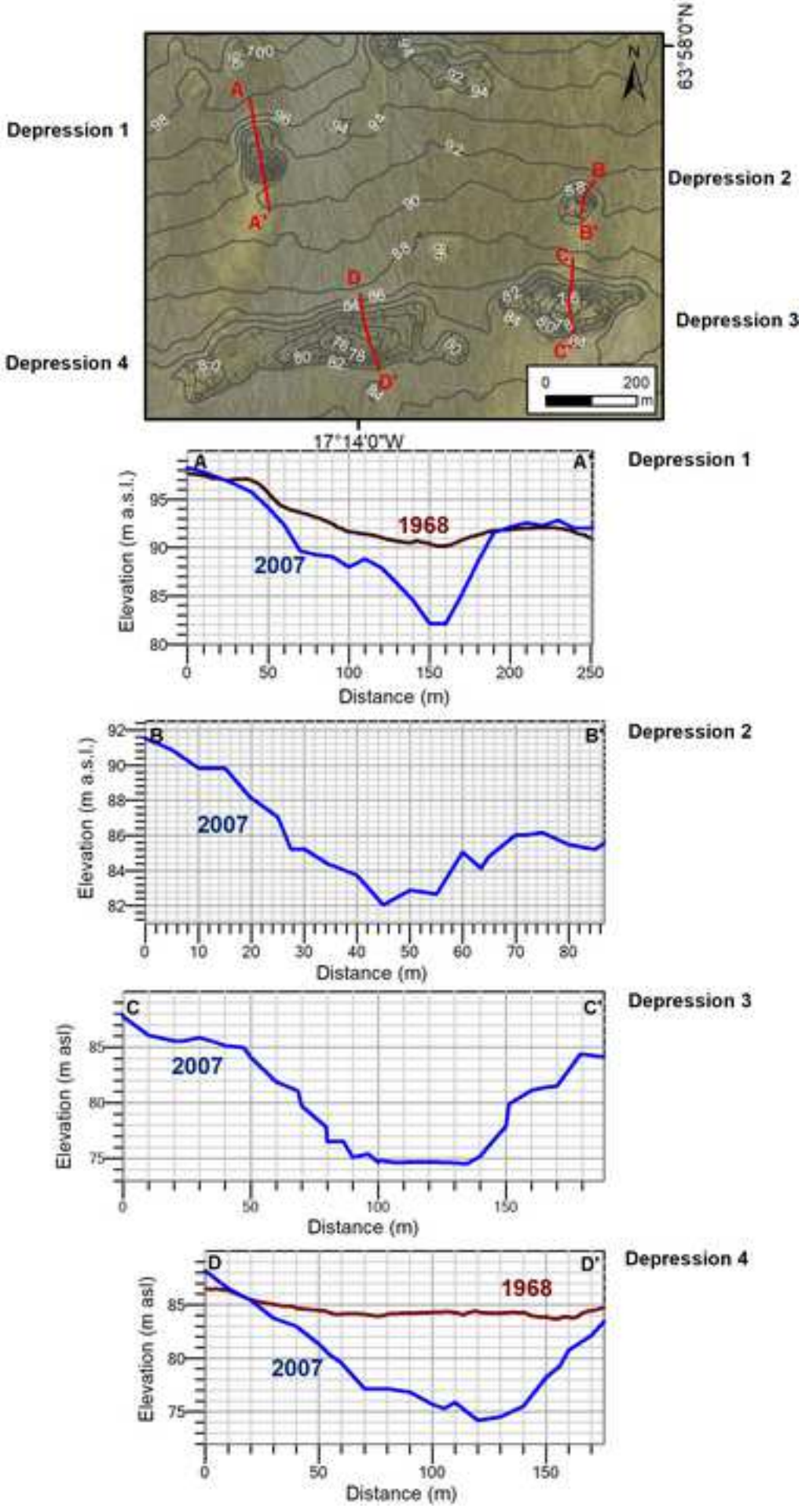

Figure (Color)
Click here to download high resolution image

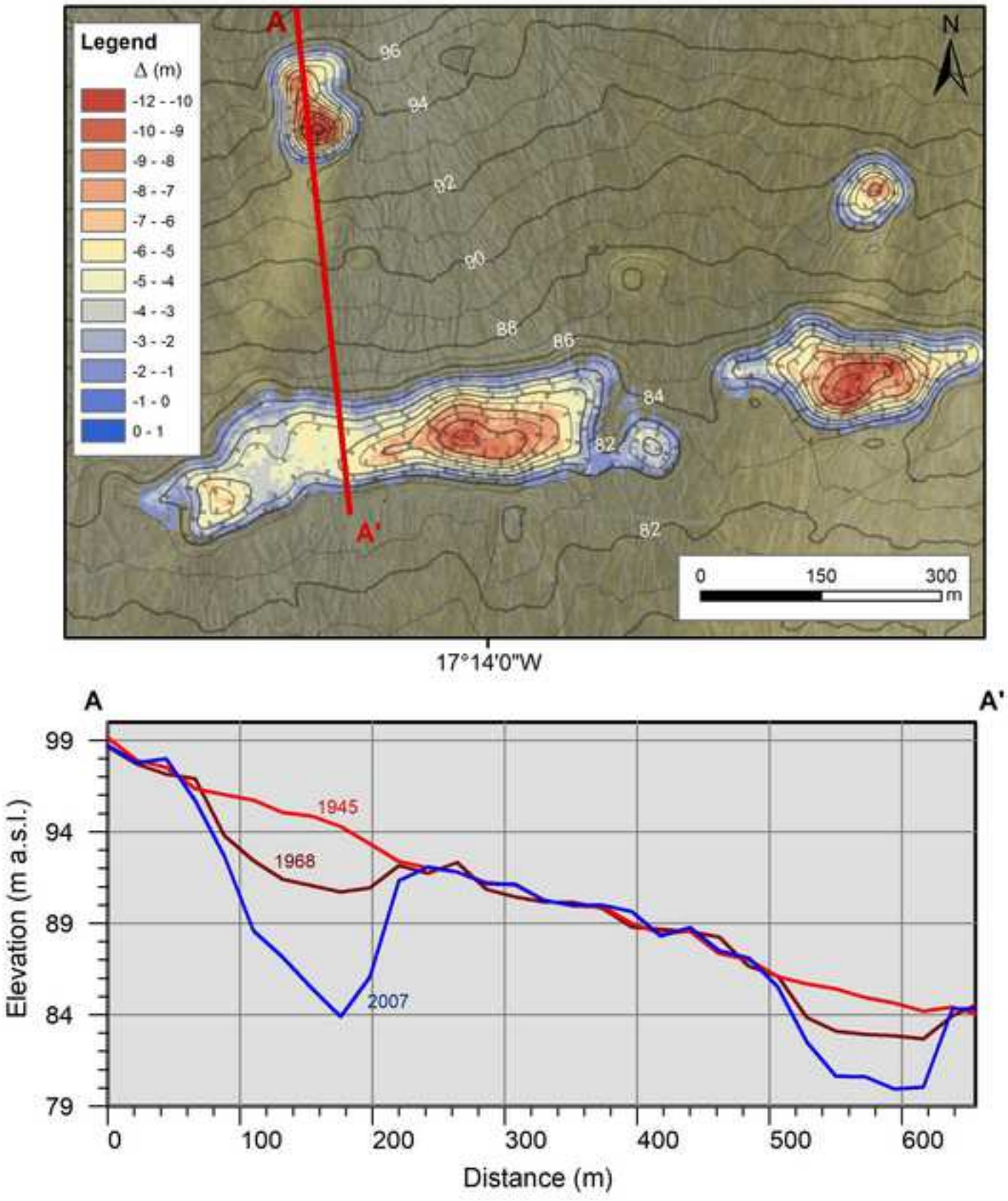

Figure (Color)

Click here to download high resolution image

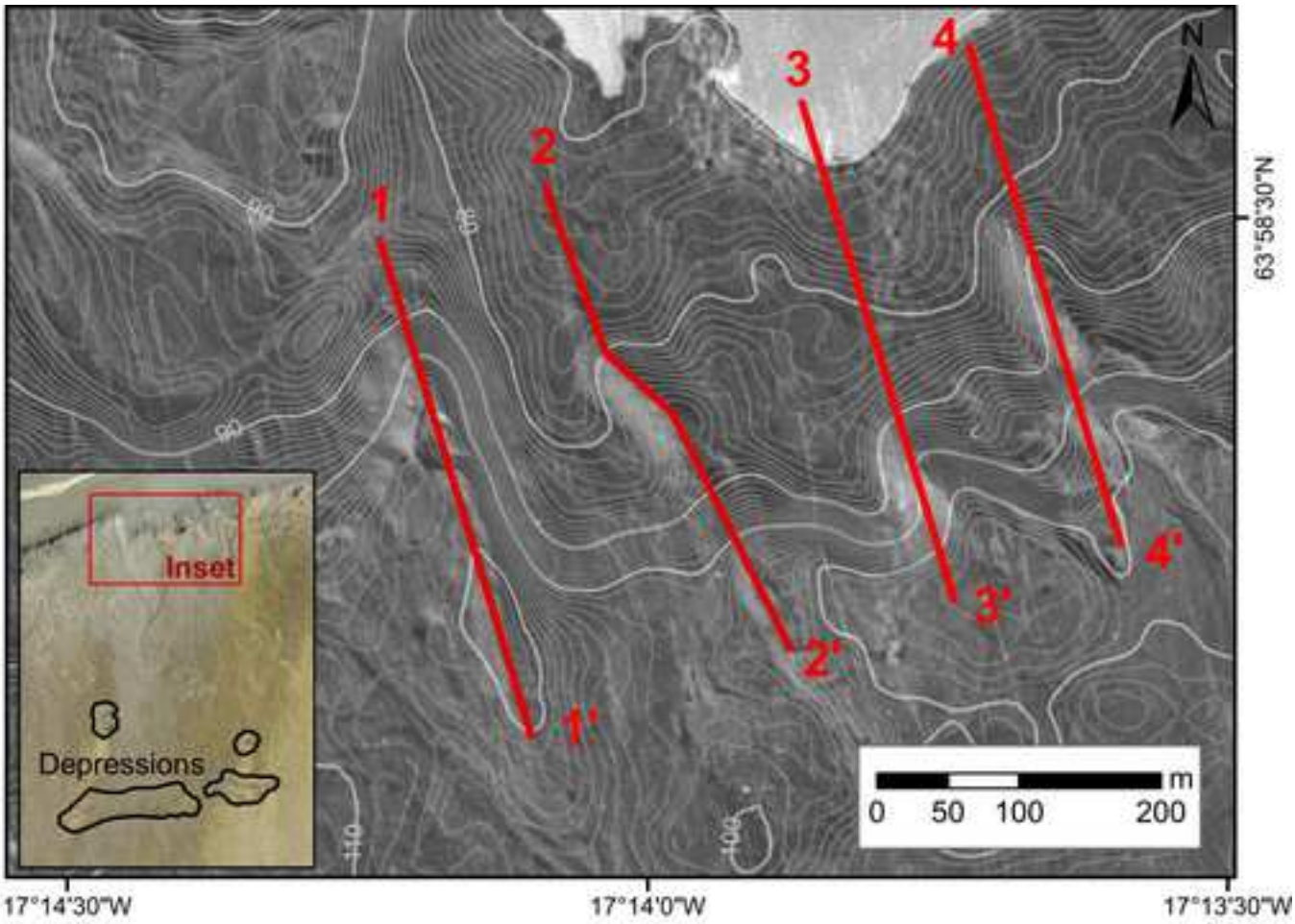

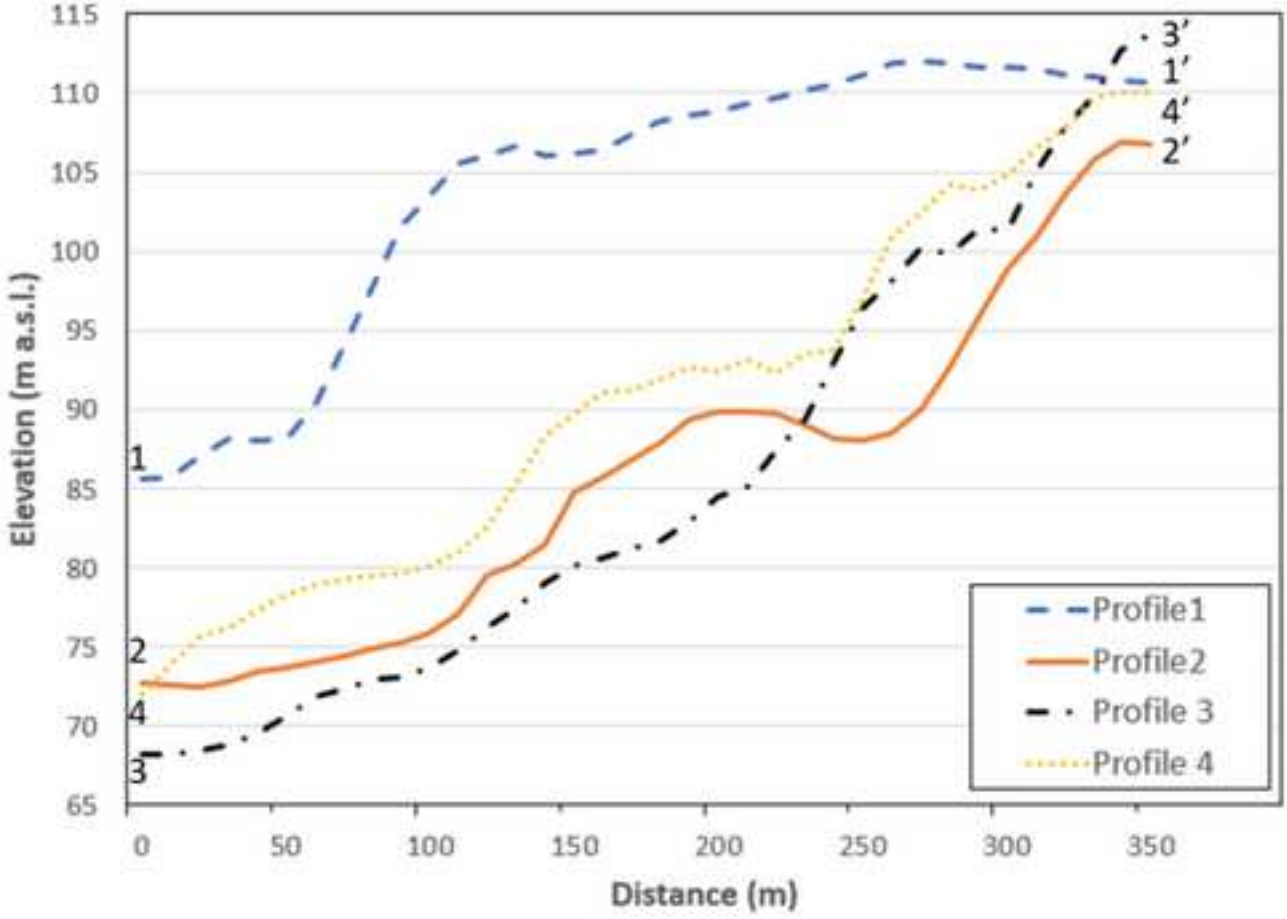

Figure (Color)

Click here to download high resolution image

Figure (Color)

Click here to download high resolution image

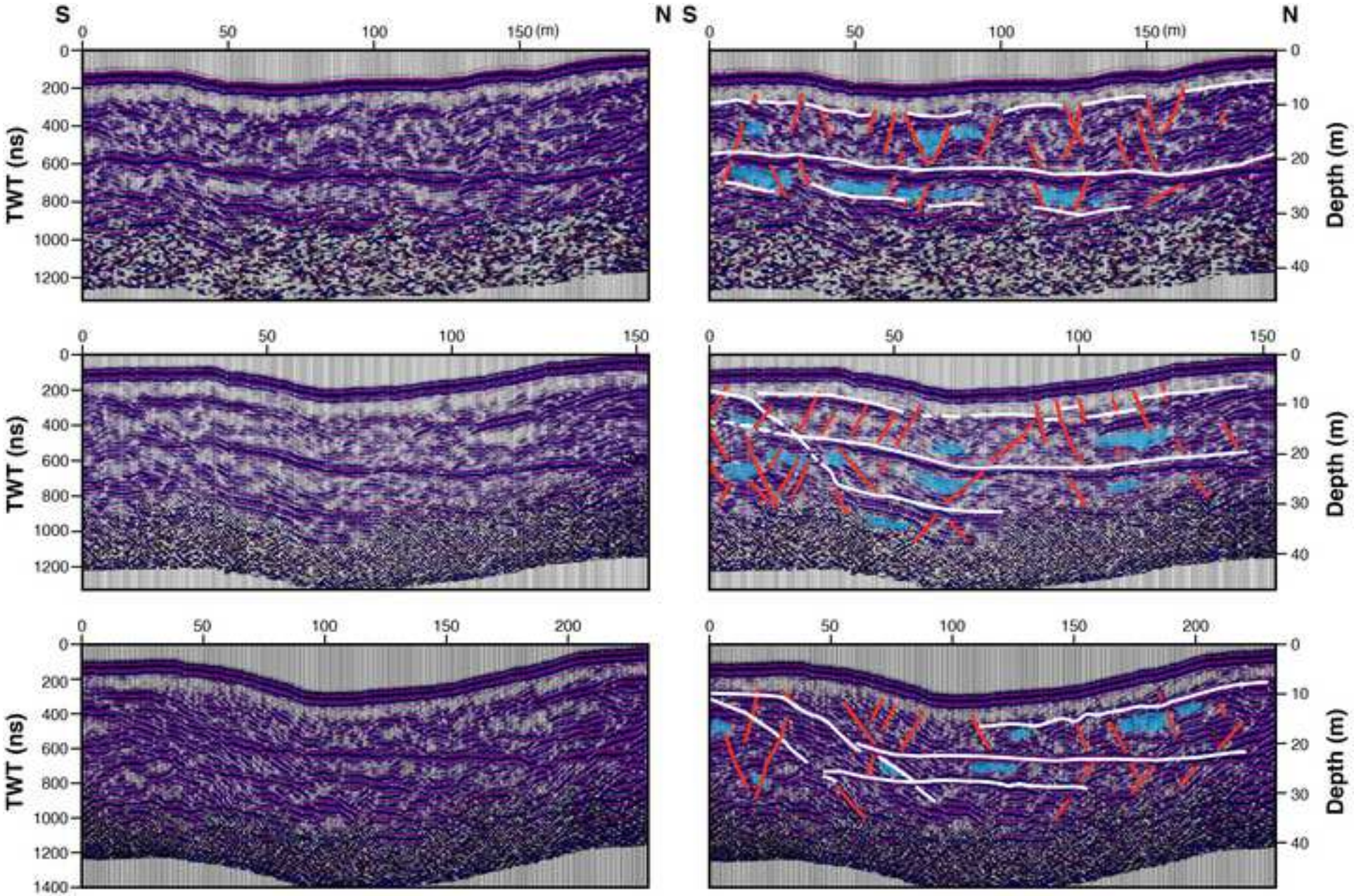

Figure (Color)
Click here to download high resolution image

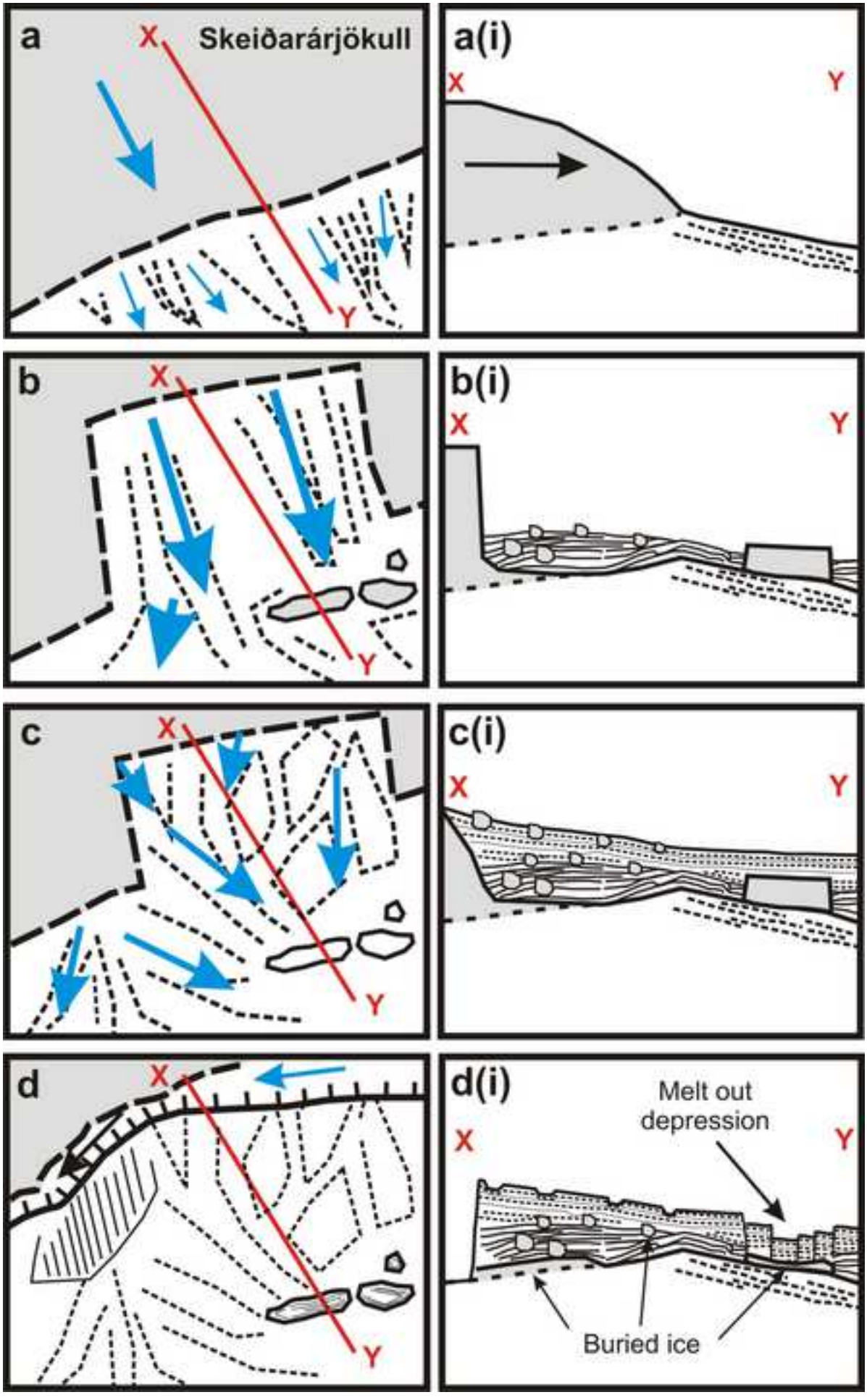

Figure (Greyscale)
Click here to download high resolution image

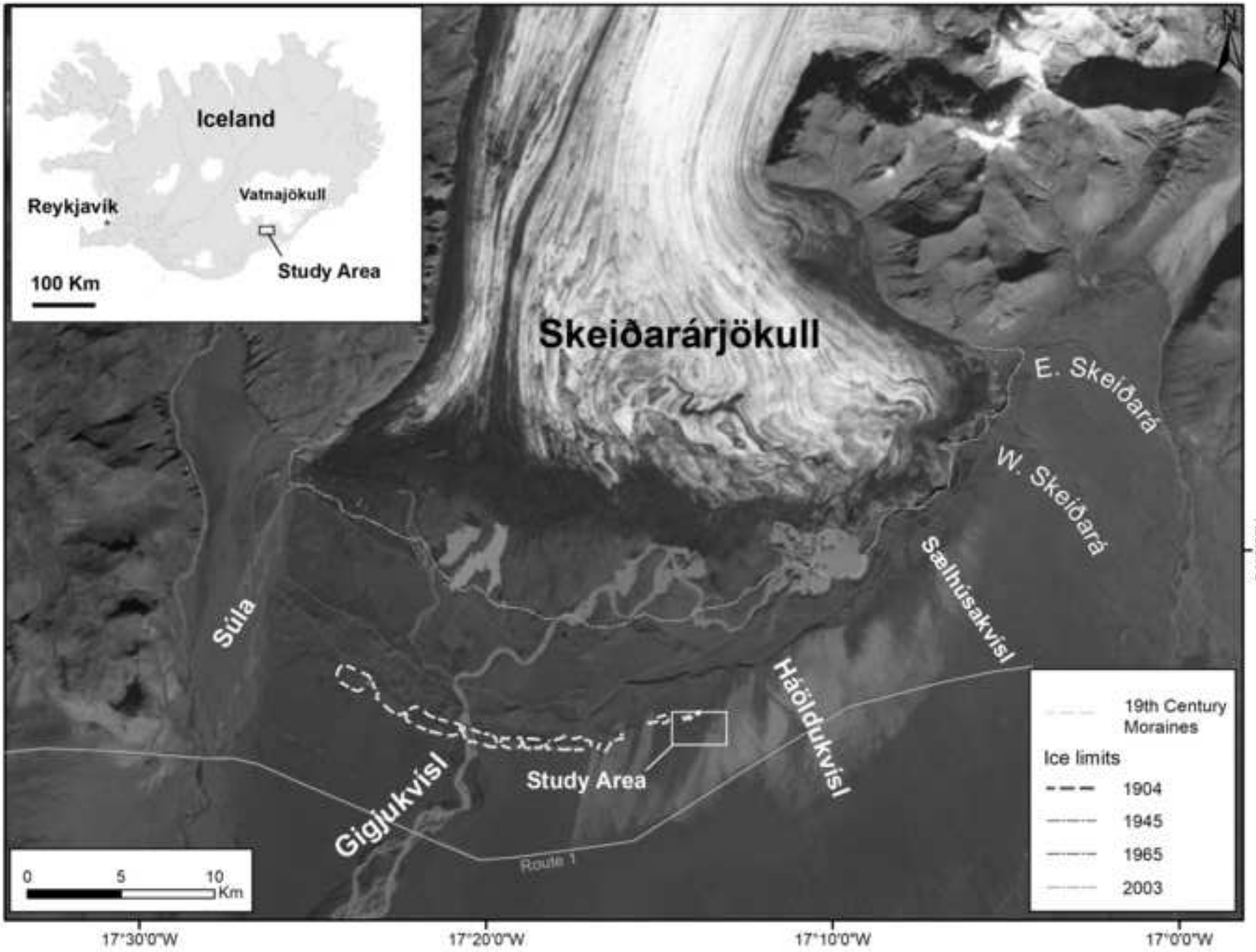

Figure (Greyscale)
Click here to download high resolution image

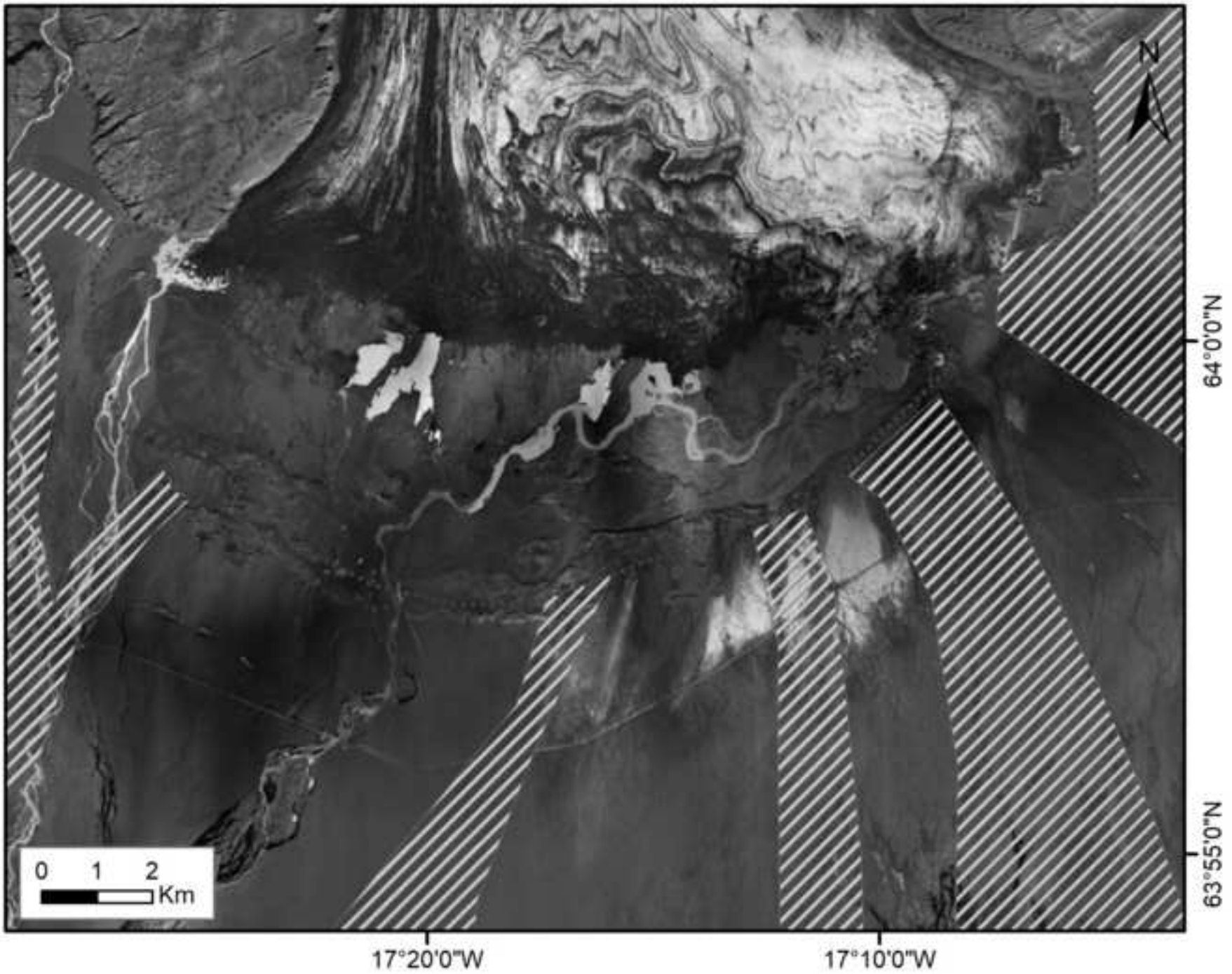

Figure (Greyscale)
Click here to download high resolution image

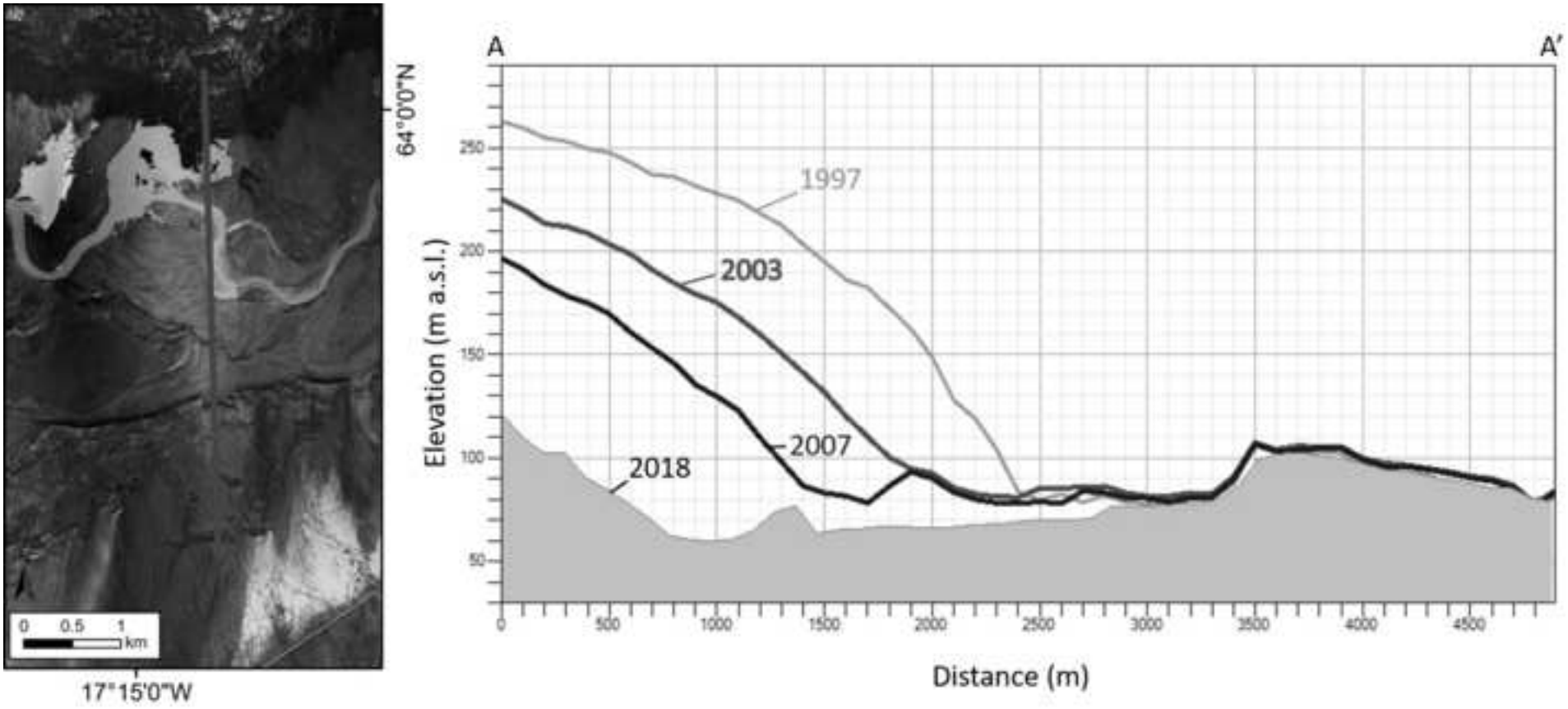

Figure (Greyscale)
Click here to download high resolution image

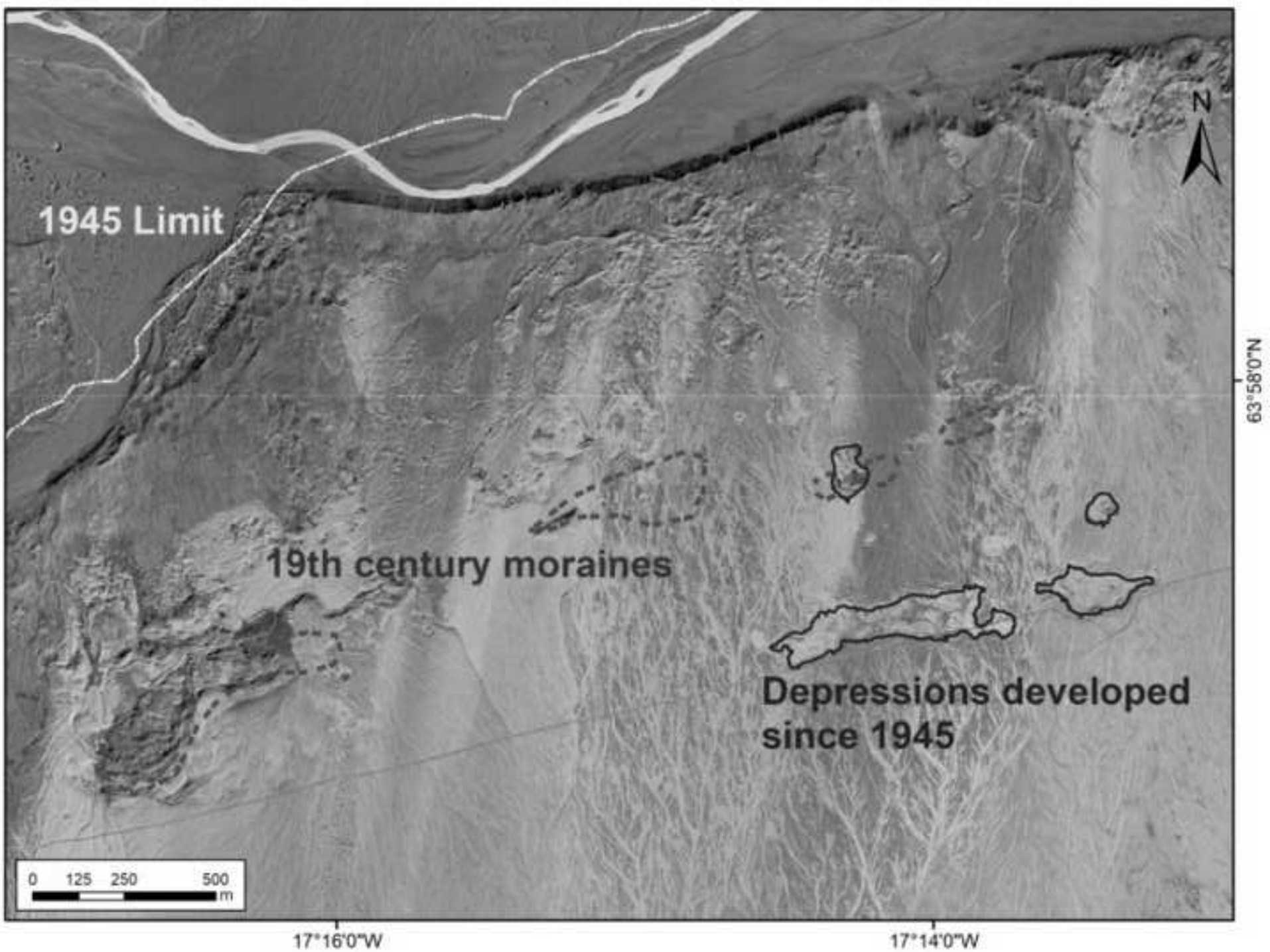

Figure (Greyscale)
Click here to download high resolution image

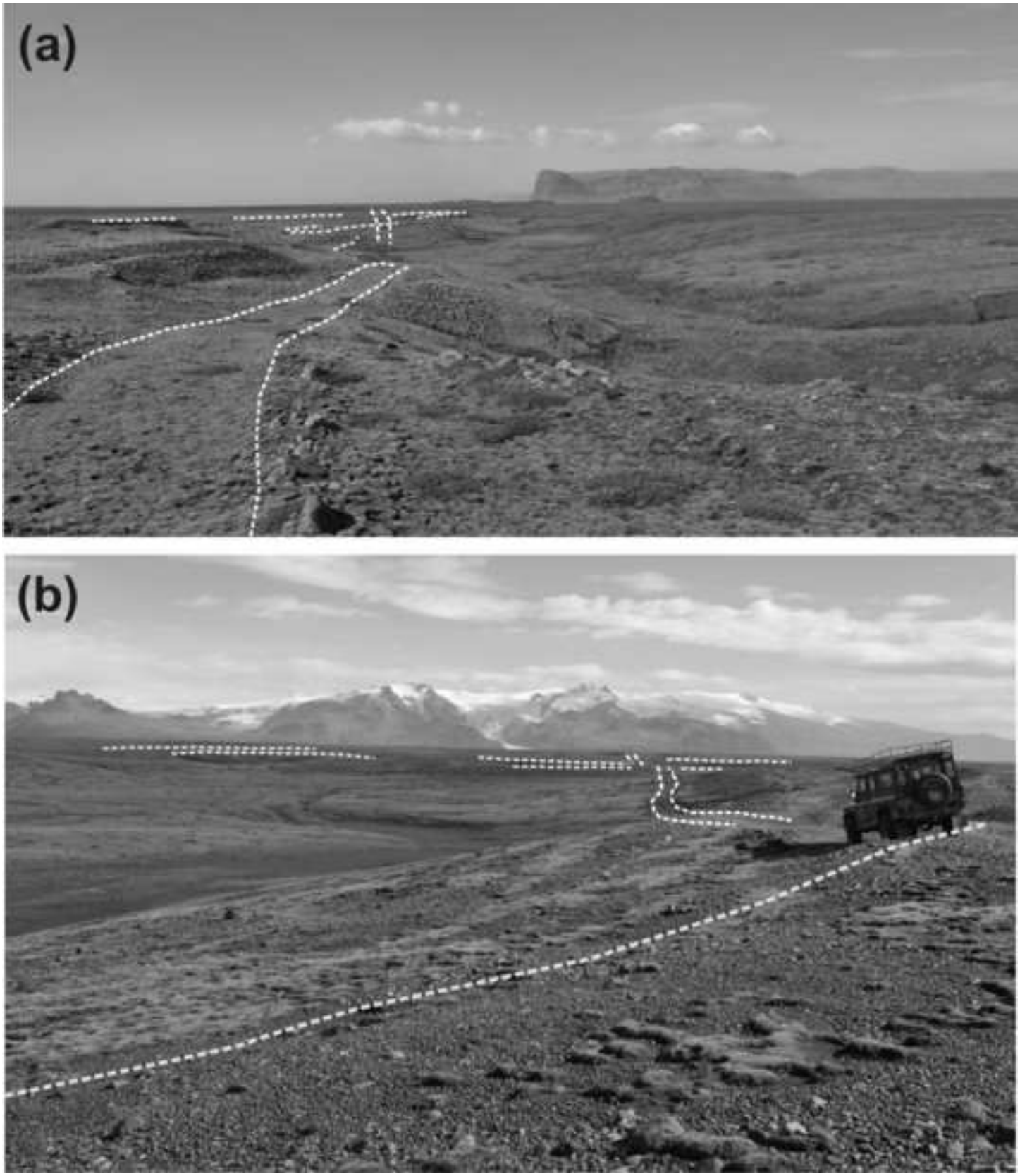

Figure (Greyscale)

Click here to download high resolution image

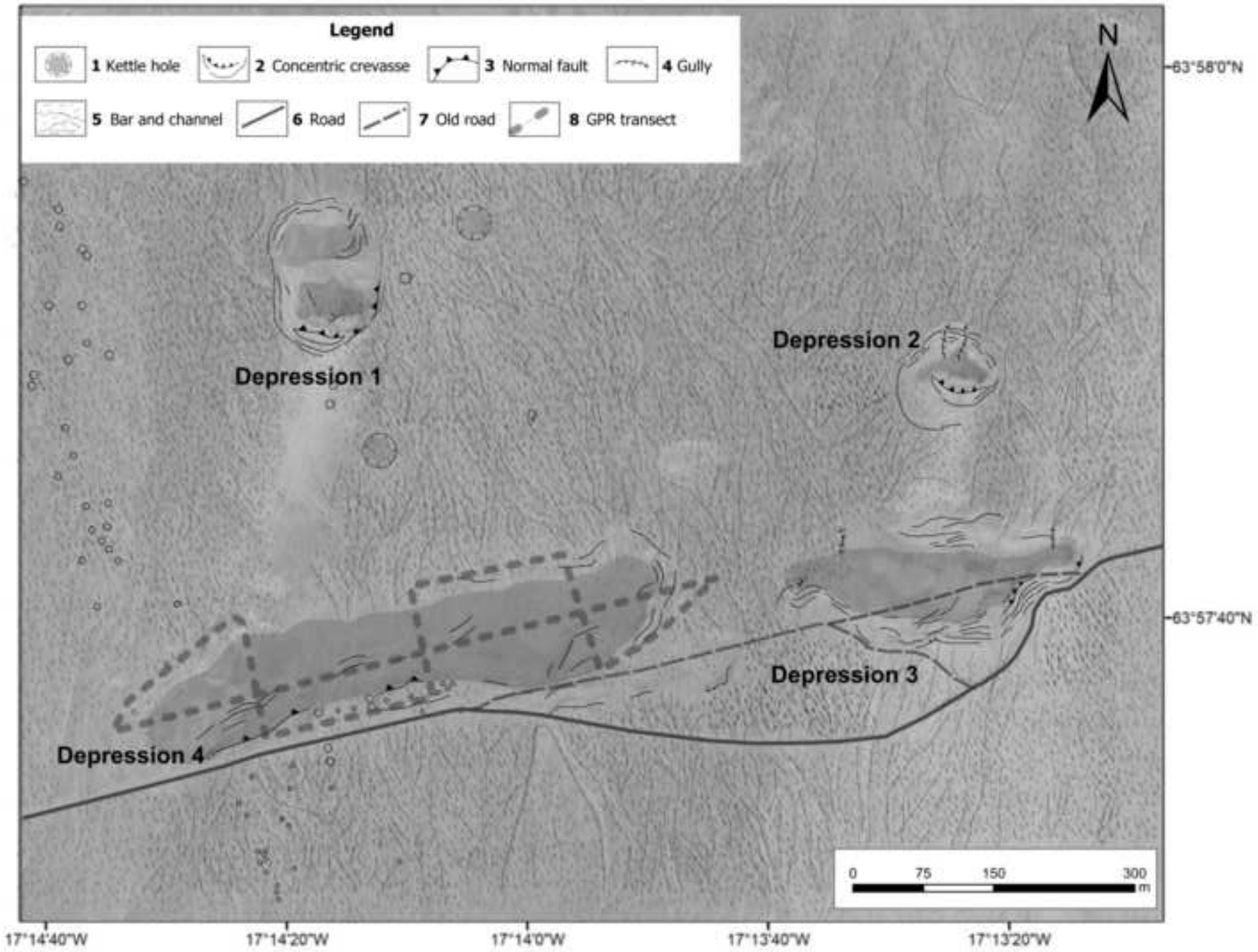

Figure (Greyscale)
Click here to download high resolution image

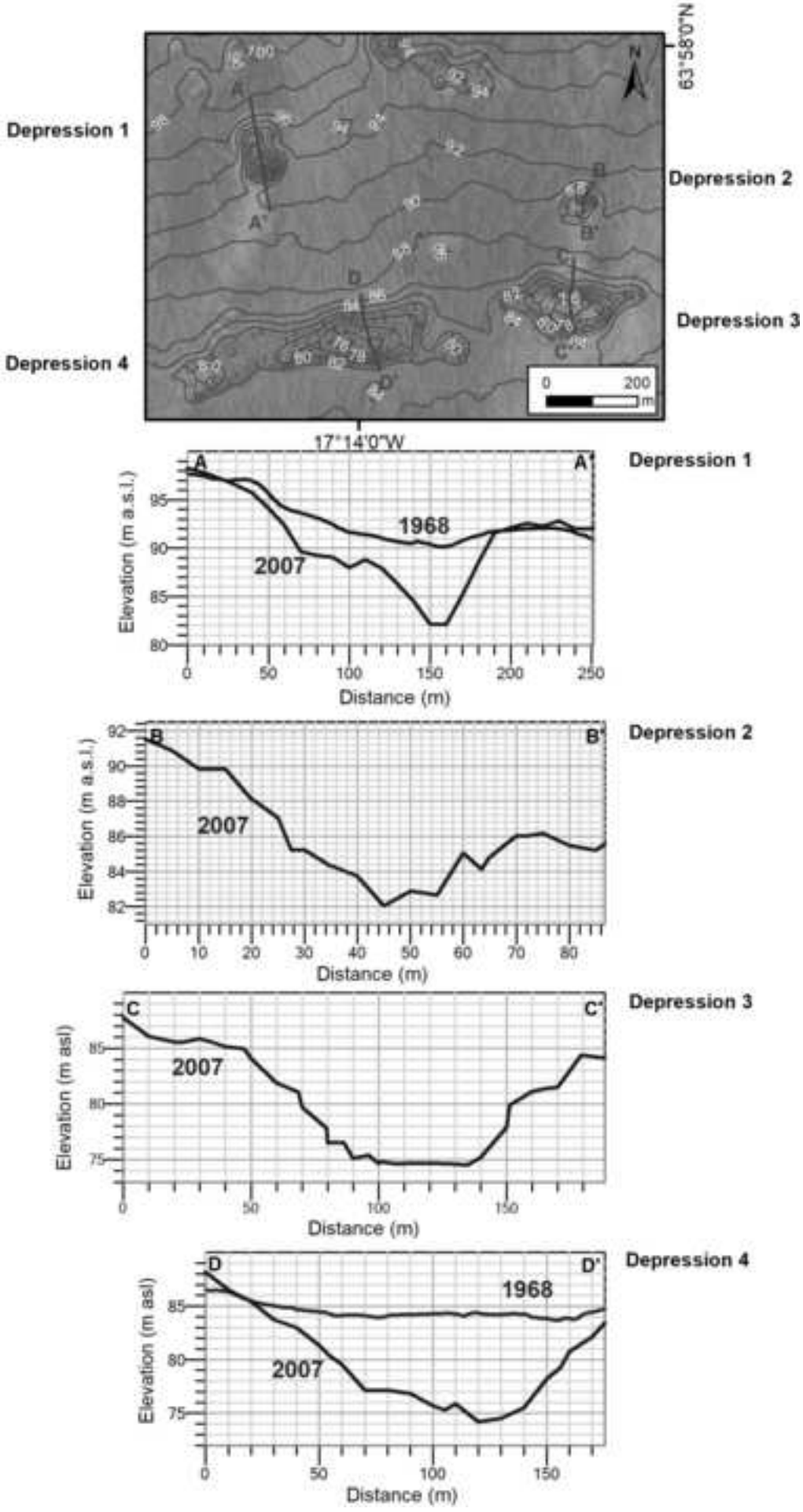

Figure (Greyscale)
Click here to download high resolution image

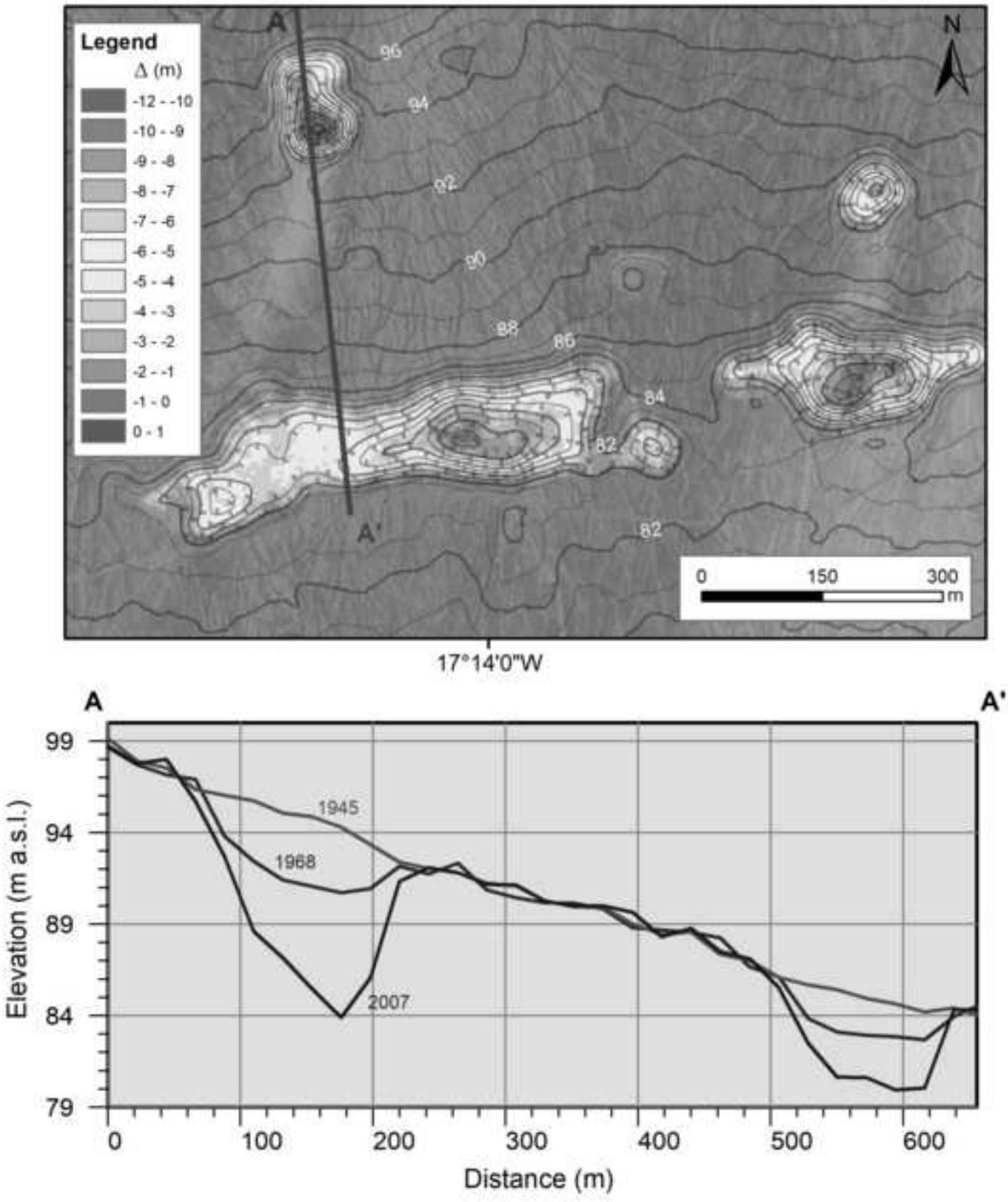

Figure (Greyscale)
Click here to download high resolution image

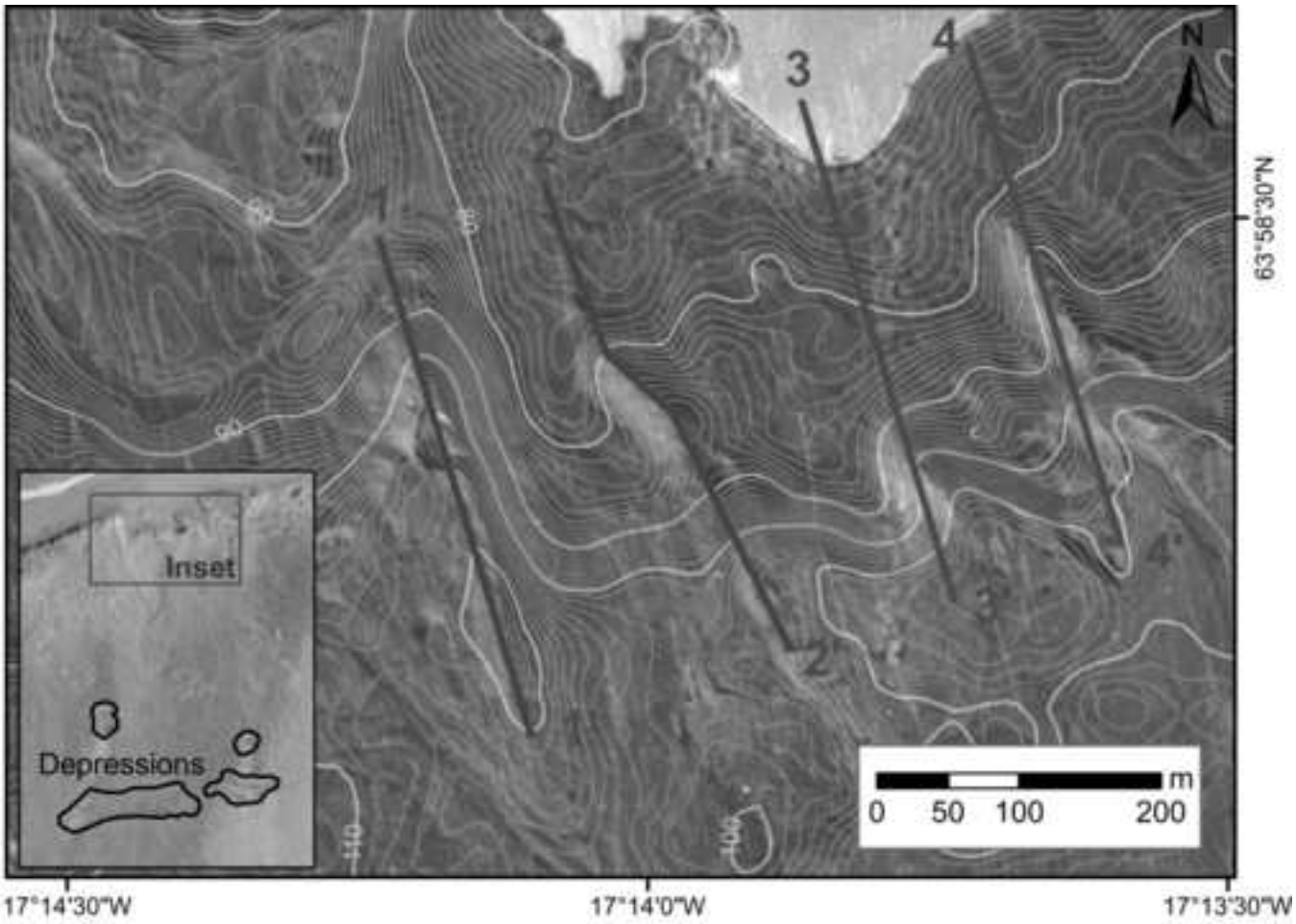

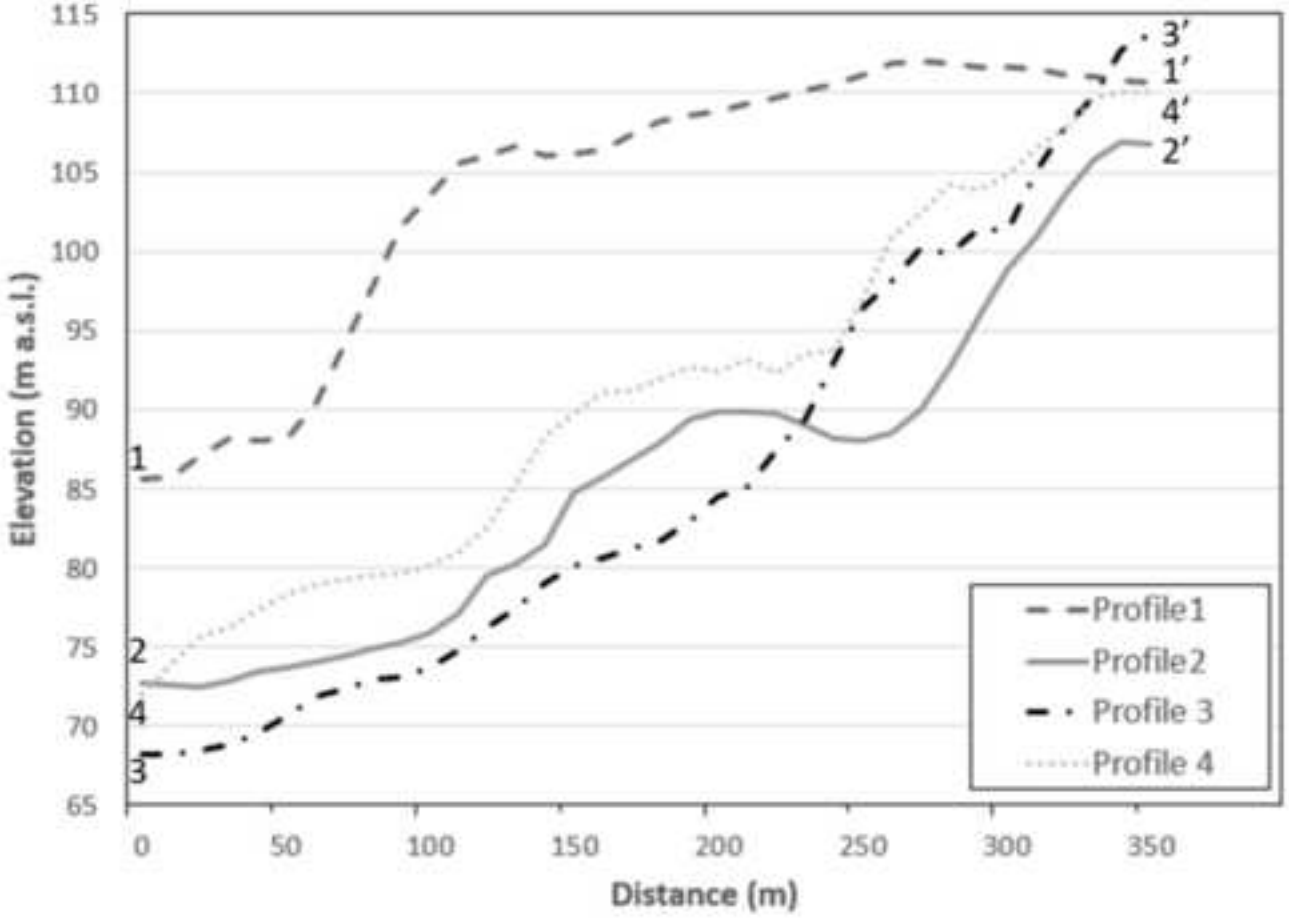

Figure (Greyscale)
Click here to download high resolution image

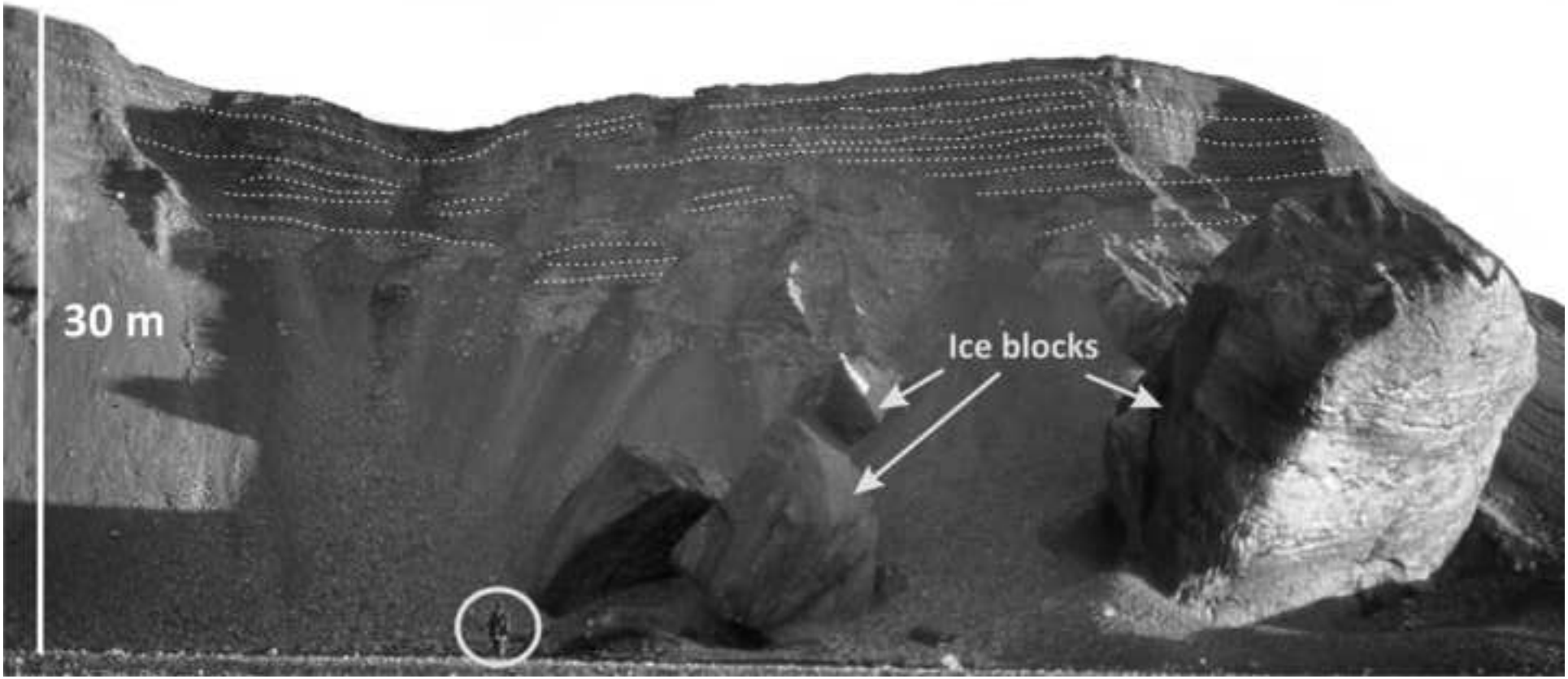

Figure (Greyscale)
Click here to download high resolution image

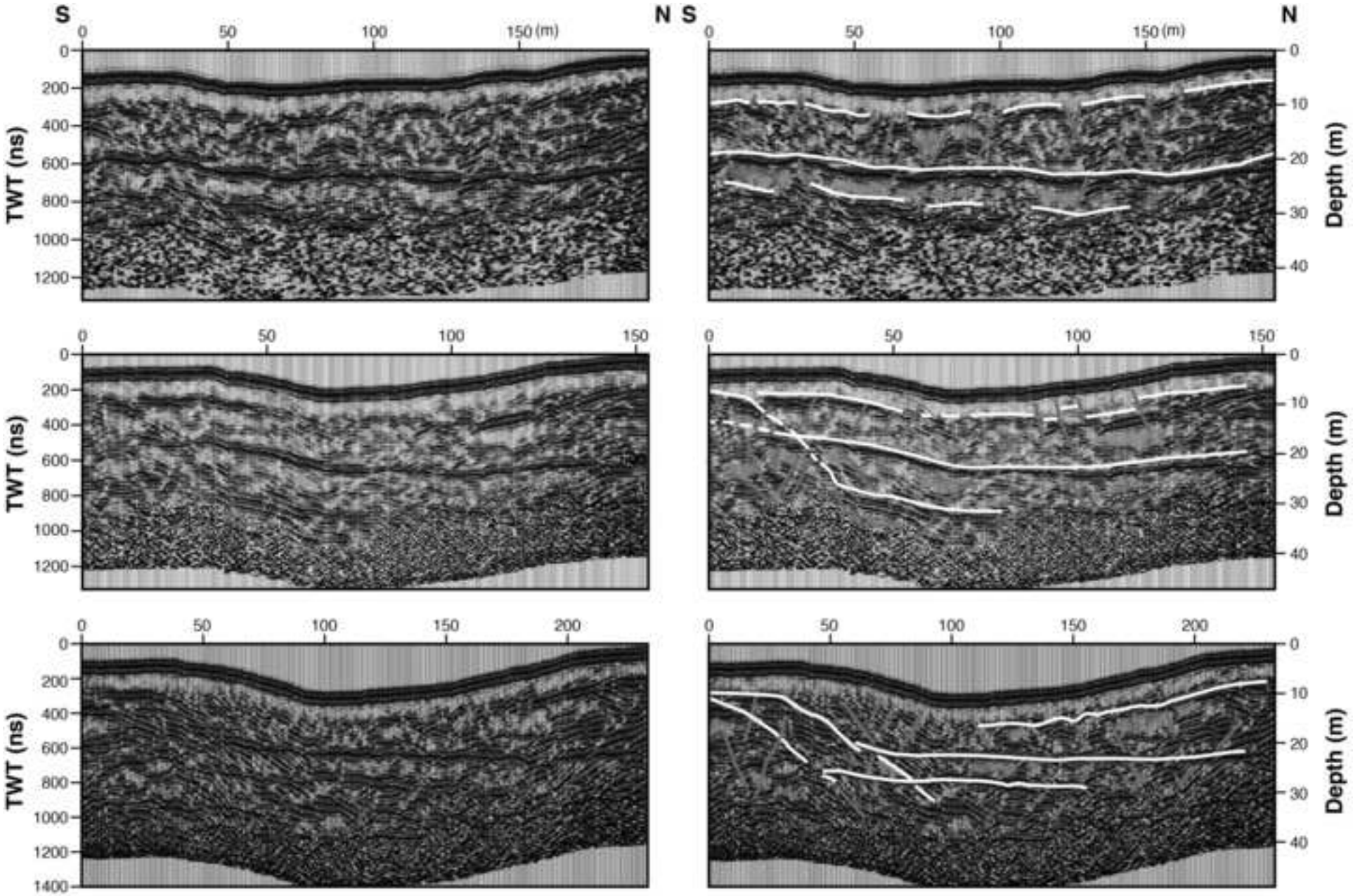

Figure (Greyscale)
Click here to download high resolution image

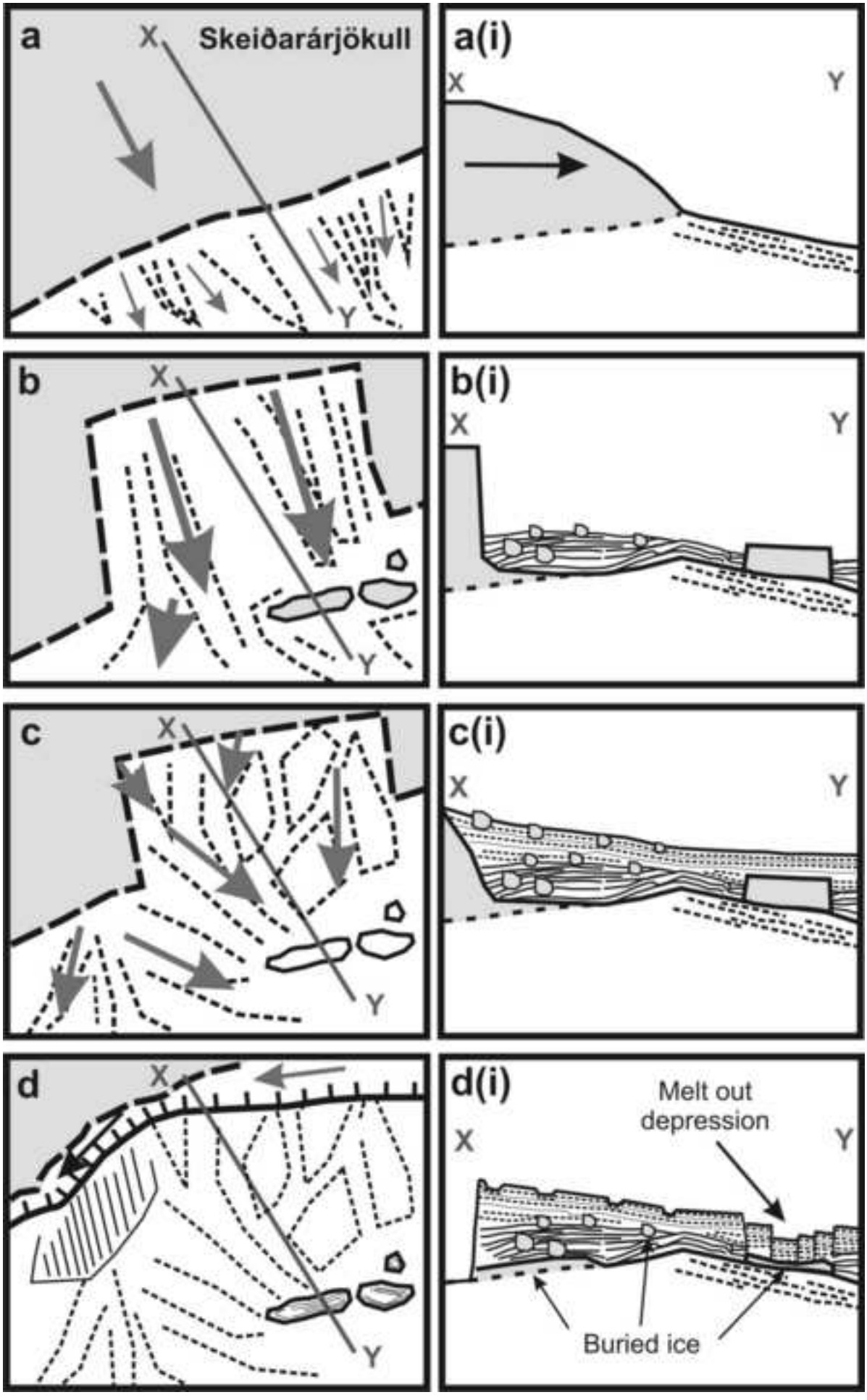

***Declaration of Interest Statement**

Declaration of interests

☒ The authors declare that they have no known competing financial interests or personal relationships that could have appeared to influence the work reported in this paper.

☐The authors declare the following financial interests/personal relationships which may be considered as potential competing interests: